AN ONCOGENIC ISOFORM SWITCH LEADS TO HNRNPA1 OVEREXPRESSION IN TRIPLE NEGATIVE BREAST CANCER

A THESIS SUBMITTED TO
THE GRADUATE SCHOOL OF NATURAL AND APPLIED SCIENCES
OF
MIDDLE EAST TECHNICAL UNIVERSITY

BY

MURAT ERDEM

IN PARTIAL FULFILLMENT OF THE REQUIREMENTS
FOR
THE DEGREE OF DOCTOR OF PHILOSOPHY
IN
BIOLOGY

AUGUST 2022

Approval of the thesis:

AN ONCOGENIC ISOFORM SWITCH LEADS TO HNRNPA1 OVEREXPRESSION IN TRIPLE NEGATIVE BREAST CANCER

submitted by **MURAT ERDEM** in partial fulfillment of the requirements for the degree of **Doctor of Philosophy** i**n Biology, Middle East Technical University** by,

Prof. Dr. Halil Kalıpçılar
Dean, Graduate School of **Natural and Applied Sciences** _____

Prof. Dr. Ayşe Gül Gözen
Head of the Department, **Biology** _____

Prof. Dr. Ayşe Elif Erson Bensan
Supervisor, **Biology, METU** _____

Examining Committee Members:

Prof. Dr. Mesut Muyan
Biology, METU _____

Prof. Dr. Ayşe Elif Erson Bensan
Supervisor, Biology, METU _____

Asst. Prof. Dr. Nihal Terzi Çizmecioğlu
Biology, METU _____

Asst. Prof. Dr. Murat Alper Cevher
Molecular Biology and Genetics, Bilkent Uni. _____

Prof. Dr. Petek Ballar Kırmızıbayrak
Biochemistry, Ege Uni. _____

Date: 05.08.2022

I hereby declare that all information in this document has been obtained and presented in accordance with academic rules and ethical conduct. I also declare that, as required by these rules and conduct, I have fully cited and referenced all material and results that are not original to this work.

Name Last name : Murat Erdem

Signature :

ABSTRACT

AN ONCOGENIC ISOFORM SWITCH LEADS TO HNRNPA1 OVEREXPRESSION IN TRIPLE NEGATIVE BREAST CANCER

Erdem, Murat
Doctor of Philosophy, Biology
Supervisor: Prof. Dr. Ayşe Elif Erson Bensan

August 2022, 93 pages

HNRNPA1 is one of the most abundant and ubiquitously expressed nuclear proteins and plays a significant role in RNA biology. It has many diverse functions in cellular nucleic acid metabolisms, including mRNA transport, miRNA maturation, and telomere maintenance. Emerging evidence suggest HNRNPA1 to be an important RNA binding protein (RBP) to regulate various RNA related processes in cancer cells. However, deregulation of *HNRNPA1* expression and its action mechanisms are unclear in breast cancers. The study aims to investigate the isoform level expression of *HNRNPA1* and the role of *HNRNPA1* in breast cancer models. Using expression data in GTEx and TCGA databases, and microarray data set, an isoform switch between the 3'UTR isoforms of *HNRNPA1* was discovered in breast cancers. It is shown that the mammary tissue has a dominantly expressed isoform with a short half-life. On the other hand, this isoform is downregulated in breast cancers, favoring a much more stable isoform. It is shown that the overexpression of this stable isoform leads to increased HNRNPA1 protein levels. In turn, high HNRNPA1 protein levels correlate with poor survival in patients. In support of this, silencing of *HNRNPA1*

causes a reversal in neoplastic phenotypes, including proliferation, clonogenic potential, migration, and invasion. In addition, silencing of *HNRNPA1* results in the downregulation of microRNAs that map to intragenic regions. Among the downregulated miRNAs, pri-miR-27b and its host gene (*C9ORF3*) expression were decreased, suggesting that pri-miR-27b and C9ORF3 expressions were co-regulated by *HNRNPA1* at the transcriptional level in MDA-MB-231 cells.

In summary, a cancer-specific isoform switch was identified for *HNRNPA1* and a novel insight was provided on the function of *HNRNPA1* in breast cancers.

Keywords: APA, *HNRNPA1*, Isoform Switch, miR-27b, Breast Cancer

ÖZ

ÜÇLÜ NEGATİF MEME KANSERİNDE ONKOJENİK İZOFORM DEĞİŞİMİ HNRNPA1'İN AŞIRI ANLATIMINA YOL AÇAR

Erdem, Murat
Doktora, Biyoloji
Tez Yöneticisi: Prof. Dr. Ayşe Elif Erson Bensan

Ağustos 2022, 93 sayfa

HNRNPA1, en fazla bulunan ve her yerde eksprese edilen nükleer proteinlerden biridir ve RNA biyolojisinde önemli bir rol oynar. mRNA taşınması, miRNA olgunlaşması ve telomer bakımı dahil olmak üzere hücresel nükleik asit metabolizmalarında birçok farklı işlevi vardır. Ortaya çıkan kanıtlar, kanser hücrelerinde HNRNPA1'in RNA ile ilgili çeşitli süreçleri düzenlenmesinde önemli bir RNA bağlayıcı protein (RBP) olduğunu göstermektedir. Bununla birlikte, meme kanserlerinde *HNRNPA1* anlatımının deregülasyonu ve bunun etki mekanizmaları belirsizdir. Bu çalışma, meme kanseri modellerinde *HNRNPA1*'in izoform düzeyinde anlatımını ve *HNRNPA1*'in rolünü araştırmayı amaçlamaktadır. GTEx ve TCGA veri tabanlarını ve mikroarray data seti kullanarak meme kanserlerinde *HNRNPA1*'in 3'UTR izoformları arasında bir izoform geçişi keşfedildi. Normal meme dokusunda kısa yarı ömre sahip olan bir izoforumun baskın olarak ifade edilmiş olduğunu gösterildi. Öte yandan, bu izoform meme kanserlerinde çok daha az ifade edilir ve çok daha stabil bir izoformun ifade edilmesini destekler. Bu kararlı izoformun aşırı ifadesinin, artan HNRNPA1 protein seviyesine yol açtığını ortaya koyuldu. Buna karşılık, yüksek HNRNPA1 protein seviyeleri, hastalarda zayıf sağkalım ile

ilişkilidir. Buna destek olarak *HNRNPA1*'in susturulması, proliferasyon, klonojenik potansiyel, göç ve istila dahil olmak üzere neoplastik fenotiplerde bir tersine dönüşe neden olur. Ek olarak, *HNRNPA1*'in susturulması, intragenik bölgelerde yer alan mikroRNA'ların aşağı regülasyonu ile sonuçlanır. Aşağı regüle edilmiş miRNA'lar arasında pri-miR-27b ve onun konakçı geninin (*C9ORF3*) ifadeleri azalmıştır. Bu da pri-miR-27b ve C9ORF3 anlatımlarının MDA-MB-231 hücrelerinde transkripsiyonel seviyede *HNRNPA1* tarafından birlikte düzenlendiğini düşündürmektedir.

Özetle, *HNRNPA1* için kansere özgü bir izoform geçişi belirlenmiş ve meme kanserlerinde *HNRNPA1* işlevine yeni bir bakış açısı sağlanmıştır.

Anahtar Kelimeler: APA, *HNRNPA1*, İzoform Geçişi, miR-27b, Meme Kanseri

To my heart

ACKNOWLEDGMENTS

Firstly, I wish to express my deepest gratitude to my supervisor Prof. Dr. A. Elif Erson Bensan, for her guidance, advice, criticism, encouragement, and insight throughout the research and for never giving up on me. Without her support, this thesis would not have been completed.

I would also like to thank all my thesis committee members; Prof. Dr. Mesut Muyan, Asst. Prof. Dr. Nihal Terzi Çizmecioğlu, Asst. Prof. Dr. Murat Alper Cevher and Prof. Dr. Tolga Can.

I am very grateful to have such a great brother Ahmet Çağlar Özketen for always being with me throughout my journey at METU, Ankara.

I would like to thank all my colleagues in the Erson lab for their friendship and for sharing their knowledge and experience.

I would also like to thank all Muyan, Banerjee and Terzi-Çizmecioğlu Lab members for their friendship and for sharing their resources whenever I needed them.

This work is partially funded by the Scientific and Technological Research Council of Turkey under grant number TUBİTAK 1002 (218Z109).

TABLE OF CONTENTS

LIST OF TABLES

TABLES

LIST OF FIGURES

FIGURES

LIST OF ABBREVIATIONS

ABBREVIATIONS

A	Adenosine
A1sh	HNRNPA1shRNA
ActD	Actinomycin D
ANOVA	Analysis of variance
APA	Alternative polyadenylation
ARE	AU-rich element
AS-NMD	Nonsense-mediated mRNA decay
BCL-XL	B -cell lymphoma extra large
bp	Base pairs
Cas9	CRISPR-associated protein 9
cDNA	Complementary deoxyribonucleic acid
CDS	Coding sequence
CFIIm	Cleavage factor IIm
CFIm	Cleavage factor Im
CHX	Cycloheximide
CLP1	Cleavage and polyadenylation factor I subunit 1
CPSF	Cleavage and polyadenylation-specific factor
Cq	Quantification Cycle
CRISPR	Clustered regularly interspaced short palindromic repeats
CSTF	Cleavage stimulation factor
DAPI	4’,6-diamidino-phenylindole
dATP	Deoxyadenosine triphosphate
DMEM	Dulbecco’s Modified Eagle Medium
DMSO	Dimethylsulfoxide
DNA	Deoxyribonucleic acid
DNA-PKcs	DNA-dependent protein kinase, catalytic subunit
DNase I	Deoxyribonuclase I
dNTP	Deoxyribonucleotide triphosphate
DSE	Downstream element
E.coli	Escherichia coli
EGF	Epithelial growth factor
EMT	Epithelial-to-mesenchymal transition
ER	Estrogen receptor
ESE	Exonic splicing enhancer
ESS	Exonic splicing silencer
EtOH	Ethyl alcohol
FBS	Fatal bovine serum
FGF-2	Fibroblast growth factor 2

G	Guanine
GAPDH	Glyceraldehyde 3-phosphate dehydrogenase
HA	Hemagglutinin
HNRNPA1	Heterogeneous nuclear ribonucleoprotein A1
HR	Hazard ratio
hTR	Complementary telomerase RNA template
IRES	Internal ribosome entry site
ITAF	IRES trans-activating factor
LB	Luria broth
MET	Mesenchymal-to-epithelial transition
miRNA	MicroRNA
mRNA	Messenger ribonucleic acid
PAP	Poly A polymerase
PCF11	Cleavage and polyadenylation factor subunit
PCR	Polymerase chain reaction
PI3KK	Phosphoinositide 3-kinase-like kinase
Poly (A)	Polyadenylation
pre-miRNA	Precursor microRNA
pre-mRNA	Precursor messenger ribonucleic acid
pri-miRNA	Primary microRNA
PTM	Post-transcriptional mechanisms
PVDF	Polyvinylidene difluoride
RACE	Rapid amplification of cDNA ends
RBP	RNA binding protein
RGG	Arg-Gly-Gly tripeptide
RNA	Ribonucleic acid
RPLP0	Ribosomal protein lateral stalk subunit P0
RRM	RNA recognition motif
RT-qPCR	Real time quantitative PCR
SDM	Site-directed mutagenesis
SDS-PAGE	Sodium dodecyl sulfate-polyacrylamide gel electrophoresis
sgRNA	Single guide RNA
shRNA	Short hairpin RNA
SRSF1	Serine and arginine rich splicing factor 1
TERRA	Telomere repeat-containing RNA
TBST	Tris buffered saline with tween
TCGA	The Cancer Genome Atlas
TNBC	Triple negative breast cancer
NT	Nontargeted shRNA
U	Uracil
USE	Upstream element
UTR	Untranslated region
XIAP	X-linked inhibitor of apoptosis

LIST OF SYMBOLS

SYMBOLS

H_2O	Dihydrogen monoxide (Water)
CO_2	Carbon dioxide

CHAPTER 1

INTRODUCTION

1.1 Heterogeneous Nuclear Ribonucleoprotein A1

Heterogeneous nuclear ribonucleoprotein A1 (HNRNPA1) is one of the most abundant and ubiquitously expressed nuclear proteins and plays a significant role in RNA biology. HNRNPA1 is a member of the RNA-binding proteins family comprising of 20 members (HNRNPA to HNRNPU) in humans (Dreyfuss, 1993; Pinol-Roma, Choi, Matunis, & Dreyfuss, 1988). *HNRNPA1* gene consists of 13 exons and has 4 poly (A) signals. There are two coding and one noncoding isoform of *HNRNPA1*. These two coding transcripts produce two isoforms; A1-B (the full-length isoform of 372 amino acids, 38 kDa), and A1-A (the shorter variant, missing residues 253 to 303, creating 320 aa protein, 34 kDa), and there are post-translational modifications on different sites of HNRNPA1 protein isoforms (Figure 1.1, A)

HNRNPA1 protein has two RNA recognition motifs (RRM1 and RRM2) responsible for binding to target RNAs (Figure 1.1, B). The flexible Glycine-rich C-terminal region consists of Arg-Gly-Gly tripeptide repeats (RGG), interspersed with aromatic (Phe, Tyr) residues that form the RGG boxes. These regions provide both protein and RNA binding capabilities to HNRNPA1. In addition, the M9 sequence localized within the Gly rich domain has a role in bidirectional transport of HNRNPA1 between the cytoplasm and nucleus in response to specific signals (Allemand et al., 2005; Piñol-Roma & Dreyfuss, 1992; Siomi & Dreyfuss, 1995). HNRNPA1 protein has many diverse functions in cellular nucleic acid metabolisms, including mRNA transport (mRNA stabilization and transcriptional regulation), alternative splicing, miRNA maturation and telomere maintenance.

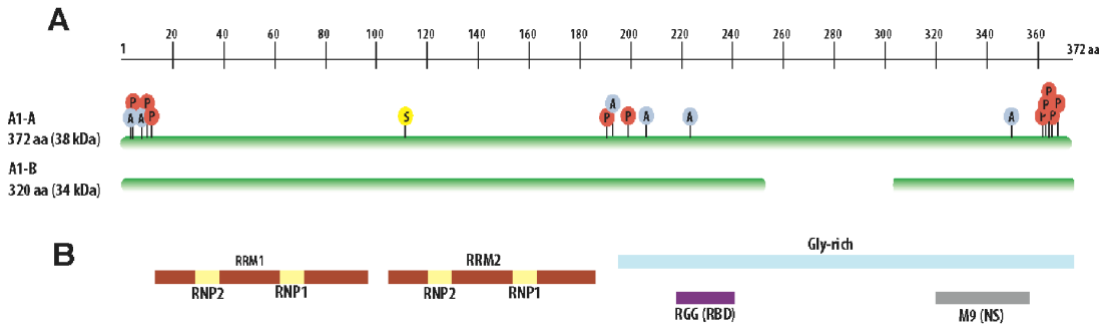

Figure 1.1. The structure and function of HNRNPA1 isoforms: A. Post-translational modifications on HNRNPA1 protein isoforms (A1-A and A1-B). These modifications are acetylation (A), phosphorylation (P) and SUMOylation (S). B. They has two RRMs on its N-terminal, the C-terminal Glycine-rich domain with an RGG box and a nuclear targeting sequence (M9). Figure taken from (Jean-Philippe, Paz, & Caputi, 2013).

1.1.1 mRNA Transport and Cell Survival

HNRNPA1 plays a role in transporting specific mRNAs from the nucleus to the cytoplasm (Figure 1.2). For example, FGF-2 induced S6K2 phosphorylates Ser4/6 sites on HNRNPA1 and increases the binding affinity of HNRNPA1 to *BCL-XL* and *XIAP* mRNAs with Internal Ribosome Entry Site (IRES) to promote their nuclear export. In the cytosol, phosphorylated HNRNPA1 detaches from these mRNAs activating their IRES-mediated translation in the cytoplasm. The phosphorylation of Ser4/6 also leads to the association of HNRNPA1 with 14-3-3σ; thus, HNRNPA1 is sumoylated on K183 and then is transported back into the nucleus. The pro-survival effects of FGF-2 occur through the phosphorylation of HNRNPA1, which increases translation of anti-apoptotic proteins (Roy et al., 2014). Since HNRNPA1 binds to IRES sequences, it acts as an IRES trans-activating factor (ITAF) for many cellular IRES containing mRNAs, including oncogenes and cell cycle regulators like MYC Cyclin D, and fibroblast growth factor 2 (FGF-2) (Martin et al., 2011) (Bonnal et al., 2005).

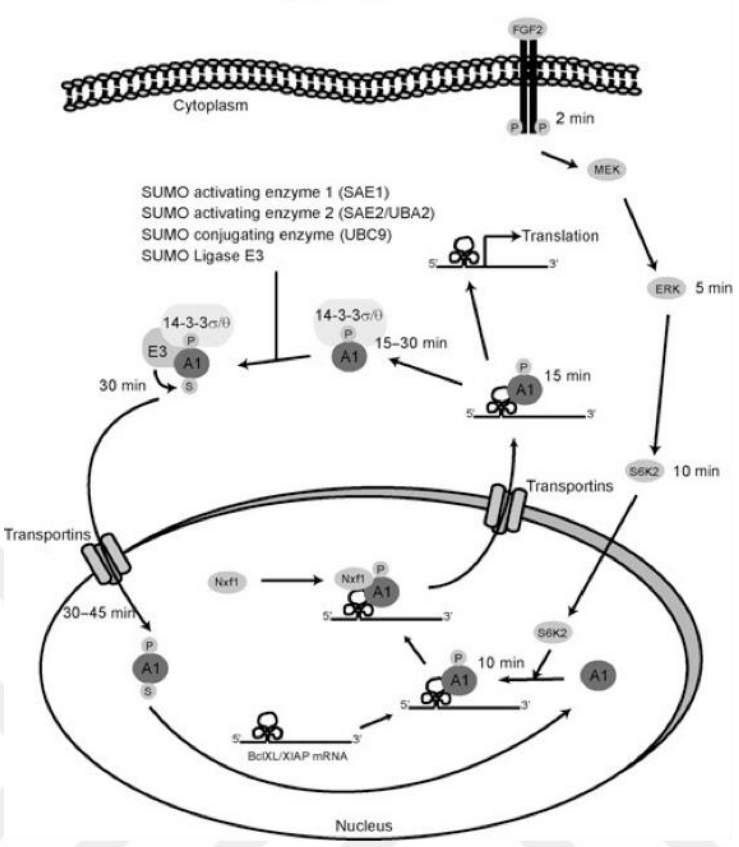

Figure 1.2. The schematic demonstration of shuttling of HNRNPA1 between nucleus and cytoplasm (Roy et al., 2014).

1.1.2 Splicing and Metastasis

One of the roles of HNRNPA1 is the regulation of RNA splicing. ΔRon, a constitutively active isoform of the Ron tyrosine kinase receptor, arises from skipping of Ron exon 11 and is connected to the activation of epithelial-to-mesenchymal transition (EMT). HNRNPA1 binds an exonic splicing silencer (ESS) in exon 11, by competing with its antagonist (SRSF1) for splicing decisions. The interaction of HNRNPA1 with the ESS sequence inhibits the binding of SRSF1 to the downstream exonic splicing enhancer (ESE), which promotes Ron exon 11 inclusion. In addition, HNRNPA1 prevents skipping of the Ron exon 11 by regulating the expression level of HNRNPA2/B1 which has a role like SRSF1 in ΔRon production (Bonomi et al., 2013). Upregulation of HNRNPA1 leads

HNRNPA2/B1 mRNA to be degraded through the nonsense-mediated mRNA decay (AS-NMD) pathway by inducing alternative splicing in the 3′UTR of HNRNPA2/B1 transcripts (Bonomi et al., 2013; Isken & Maquat, 2008). By inducing the inclusion of Ron exon 11, HNRNPA1 activates the mesenchymal-to-epithelial transition (MET) at the final stage of metastasis. (Figure 1.3) sanırım bu numaralar kaymış

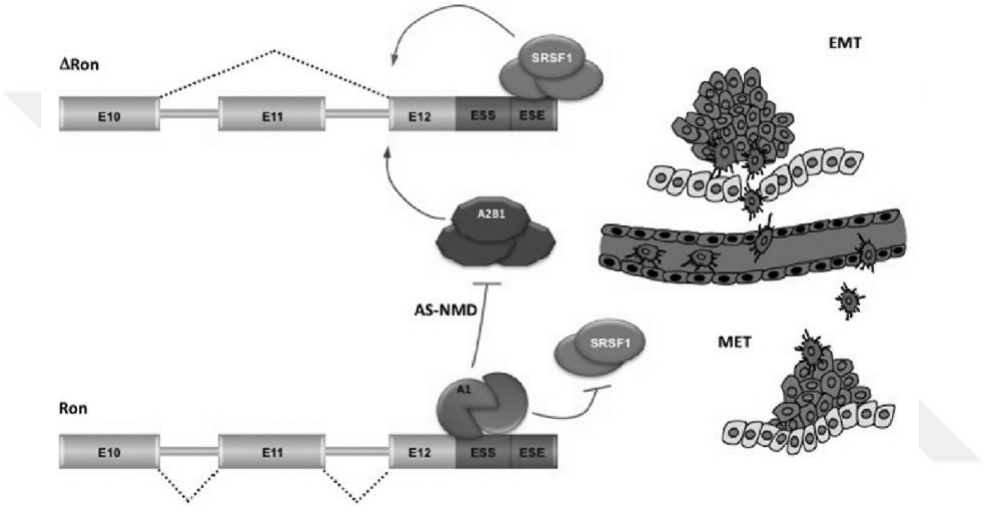

Figure 1.3. The role of HNRNPA1 (A1) in regulating delta-Ron splicing during transient EMT-MET switches (Bonomi et al., 2013).

HNRNPA1 also has a role in regulating the alternative splicing of CD44, whose gene consists of 20 exons, of which exons 1–5 (c1–c5) and 16–20 (c6– c10) are called constant exons while CD44 exons 6–15 are variable exons and typically numbered v1-v10. These variable exons are alternatively spliced to produce splice variants CD44v1-v10 depending on the inclusion of corresponding the variable exons 6–15. It was demonstrated that expression of CD44v6 and v9 variants are specific to a metastatic pancreatic carcinoma cell line, but not to the primary tumor (Li et al., 2014). The expressions of CD44v6 and v9 variants give this cell line metastatic feature (Li et al., 2014; Ringel et al., 2001). The overexpression of HNRNPA1 induces upregulating expression of CD44v6, which promotes the invasiveness of

hepatocellular carcinoma cells (Zhou et al., 2013). Invasive breast cancer cells (MDA-MB-231) express the CD44v6 variants which encode the c5v6c6, c5v6v8v9v10c6, and c5v6v7v8v9v10c6 isoforms, and downregulation of HNRNPA1 induces a significant decrease in the expression levels of c5v6v7v8v9v10c6 and c5v6v8v9v10c6 isoforms and an increase of the c5v6c6 isoform (Loh et al., 2015).

1.1.3 miRNA Maturation

HNRNPA1 also regulates the process of microRNA (miRNA) maturation. One of the HNRNPA1 specific targets is pri-miR-18a miRNA precursor, which is expressed within the miR-17-92 cluster of intronic miRNAs, which transcribes six precursor miRNAs (mir-17, mir-18a, mir-19a, mir-20a, mir-19b-1 and mir-92) on chromosome 13 (Guil & Cáceres, 2007). HNRNPA1 binds to the terminal loop and reshapes the stem-loop structure of pri-miR-18a at the nuclear step of Drosha-mediated processing; thus, HNRNPA1 increases pri-miR-18a processing by Drosha (Michlewski, Guil, & Cáceres, 2010). On the other hand, HNRNPA1 functions as a negative regulator of let-7a. HNRNPA1 interacts with the conserved terminal loop of pri-let-7a-1 and inhibits the efficiency of Drosha to cleave pri-let-7a-1. Levels of HNRNPA1 negatively correlate with mature let-7a levels in somatic cell lines (Michlewski & Cáceres, 2010).

1.1.4 Telomere Maintenance

Studies on HNRNPA1/DNA or RNA interactions have revealed that HNRNPA1 has a role in telomeric metabolism. HNRNPA1 interacts with telomeric sequences and has a critical role in telomere biogenesis (Ding et al., 1999). First of all, HNRNP A1 assists the destabilization of the G-rich extension at the 3’ telomeric end to promote the binding of telomerase to the 3’ telomeric end (Ghosh & Singh, 2018). Phosphorylation of HNRNPA1 on Ser 95 by the DDR protein DNA-PKcs, a

member of the phosphoinositide 3-kinase-like kinase (PI3KK) family (Zhang, Manche, Xu, & Krainer, 2006), and the phosphorylation of HNRNPA1 is triggered in the presence of the complementary telomerase RNA template, hTR (Ting, Pohorelic, Yu, Lees-Miller, & Beattie, 2009). Inhibition of DNA-PKC? kinase activity, or silencing of HNRNPA1, causes a significant accumulation of telomere repeat-containing RNA (TERRA) at telomeres and is related to increased frequency of fragile telomeres. Interaction of hTR/DNA-PKcs and HNRNPA1 at telomeres helps the removal of TERRA bound to chromatin, thus facilitating efficient replication of telomeres and effective end capping (Le, Maranon, Altina, Battaglia, & Bailey, 2013).

1.2 Alternative Polyadenylation

Precursor messenger RNA (pre-mRNA) are processed into mature mRNAs that can be transported to the cytosol where they are translated into proteins. These processes are 5’ capping, splicing, and 3’ polyadenylation of the precursor mRNA. Among these, polyadenylation is governed by cleavage and polyadenylation complexes at the 3’ ends of pre-mRNAs, depending on the position of polyadenylation (poly (A)) signals. Most eukaryotic genes have more than one poly(A) signal (Tian, Hu, Zhang, & Lutz, 2005; H. Zhang, 2004). Selection of alternative poly(A) (APA) signals by the cleavage and polyadenylation complex leads to multiple isoforms of the transcript with different 3′ untranslated region (UTR) lengths (Elkon, Ugalde, & Agami, 2013) (Sandberg, Neilson, Sarma, Sharp, & Burge, 2008) (Chen & Shyu, 2017). Hence, APA determines the fate of mRNAs by altering the stability, subcellular localization, and translation rate. The selection of poly(A) sites on pre-mRNA is determined by cis-acting RNA elements and trans-acting RNA elements.

1.2.1 Cis-acting RNA Elements

Poly(A) signals are usually located 10-30 nucleotides upstream of the poly(A) site

where poly(A) tail is added. Poly(A) signals are divided into two categories: canonical and noncanonical poly(A) signals. The canonical poly(A) signal (AAUAAA) is strongly enriched and conserved in all species while the noncanonical signals (AAAUAA, AUAAAA, AUUAAA, AUAAAU, AUAAAG, CAAUAA, UAAUAA, AUAAAC, AAAAUA, AAAAAA, AAAAAG) are preferred to be used at different frequencies (Derti et al., 2012).

Besides the poly(A) signal, other cis-elements have roles in directing the cleavage and polyadenylation complex to the correct position. GU/U- rich downstream element (DSE) is positioned at ~30 nucleotides downstream of the poly(A) site. The other one is U- rich upstream stimulatory element (USE) located upstream of the poly(A) signal (Chan, Choi, & Shi, 2011).

Trans-acting factors recognize the cis-elements on pre-mRNAs and regulate the poly A tail addition. Cleavage and polyadenylation complex consists of subunits of cleavage and polyadenylation stimulatory factor (CPSF), cleavage stimulatory factor (CSTF), and cleavage factor Im and IIm (CFIm, CFIIm) complexes. CPSF, CSTF, and CFIm are the core protein complexes that recruit other factors, including CFIIm, the scaffolding protein symplekin, and poly(A) polymerase (PAP) (Misra & Green, 2016) (Figure 1.4). CPSF provides the poly(A) signal AAUAAA recognition, has a role in the recruitment of the other factors of the 3' processing complex and catalyzes the cleavage reaction. CPSF complex is composed of hFip1, WDR33 (WD repeat domain 33), CPSF30, CPSF73, CPSF100, and CPSF160 subunits (Kaufmann, Martin, Friedlein, Langen, & Keller, 2004; Mandel, Bai, & Tong, 2008). Upon cooperative binding of CPSF complex to AAUAAA, CSTF complex recognizes and forms stable association with the DSE (Chan et al., 2011). CSTF complex consists of CSTF50, CSTF64 and CSTF77 subunits and its strong interaction with DSE is mediated by the CSTF64 subunit (Colgan & Manley, 1997). CFIm complex contains CFIm25, CFIm59 and CFIm68 subunits. It stabilizes the CPSF on RNA and is involved in the cleavage of pre-mRNA (Colgan & Manley, 1997). CFIIm is composed of CLP1 (cleavage and polyadenylation factor I subunit 1) and PCF11

(cleavage and polyadenylation factor subunit) and assists Pol II-mediated transcription termination (Birse, Minvielle-Sebastia, Lee, Keller, & Proudfoot, 1998; Proudfoot, 2011). PAP catalyzes the addition of adenosine residues to the 3' end of the mRNA without any template requirement (Proudfoot, 2011).

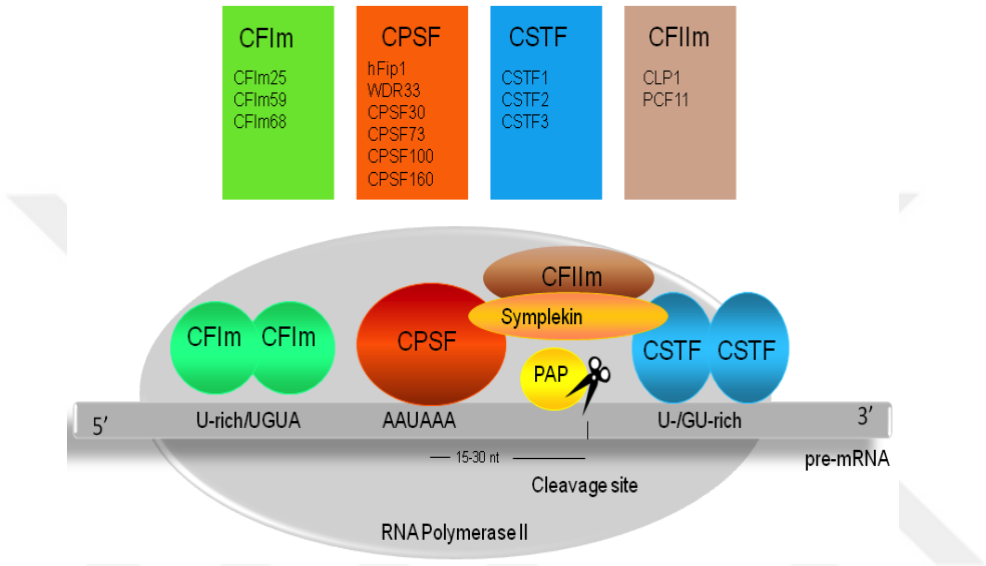

Figure 1.4. Schematic representation of the main factors involved in cleavage and polyadenylation complex. There are several proteins involved in the cleavage and polyadenylation processes in the cell. CPSF, CSTF, CFIm and CFIIm are required for cleavage. Poly(A) polymerase (PAP) and poly(A)-binding proteins (PABs) are crucial for pre-mRNA cleavage and polyadenylation. Cleavage sites are represented by the poly(A) signals (PAS). Protein complexes bind to the upstream and downstream elements (USE and DSE) to regulate the cleavage and polyadenylation processes. The figure is taken from (Erson-Bensan & Can, 2016).

1.3 Effect of Alternative Polyadenylation

Most eukaryotic genes contain more than one poly(A) signal (PAS), leading to the generation of different mRNA variants from the same gene (Figure 1.5). Selection of the proximal or distal PAS affects the length of 3'UTR of mRNA. This selection could affect the interaction of microRNAs (miRNAs) or RNA-binding proteins (RBPs) to mRNA and modulate protein synthesis. In addition, usage of intronic PAS

could affect peptide length and sequence, producing truncated proteins.

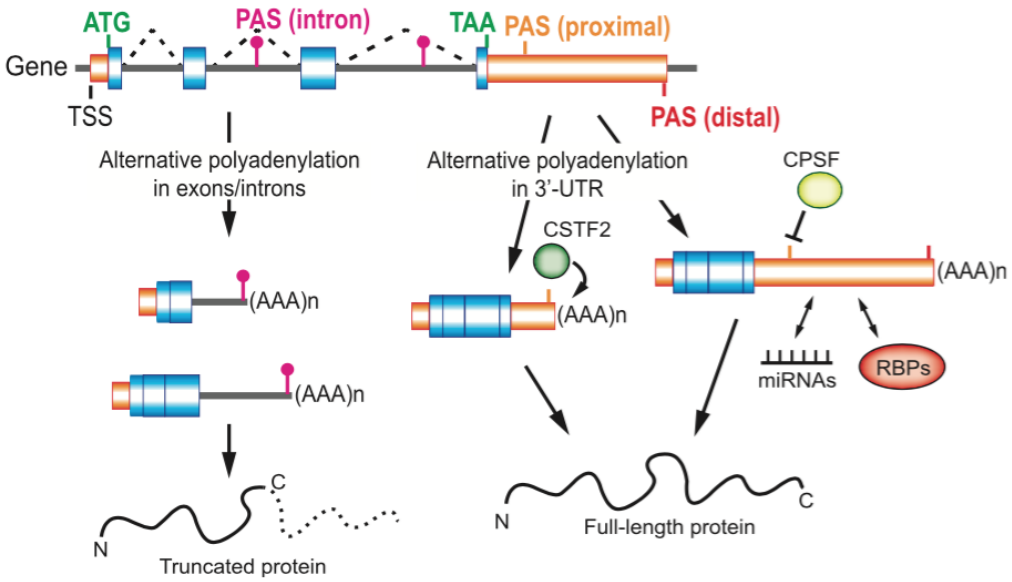

Figure 1.5. Alternative polyadenylation (APA) and its effect on protein production. The figure is taken from (Chang, Yeh, & Yong, 2017).

1.4 *HNRNPA1* and Cancer

HNRNPA1 is overexpressed in various tumor types; lung cancer (Pino et al., 2003), Burkitt lymphoma (Bommert et al., 1998), multiple myeloma (Shi et al., 2008), and leukemia (Iervolino et al., 2002) where it is thought to regulate tumorigenesis through a variety of functions that impact multiple hallmarks of cancer. These functions are controlling RNA splicing, role in telomere length maintenance, role in metastasis, miRNA maturation and mRNA transport between nucleus and cytoplasm. Hence, HNRNPA1 can affect various phases of tumor progression.

1.5 Aim of the study

- Given the oncogenic roles of *HNRNPA1*, it was interesting that the expression and potential role of *HNRNPA1* in breast cancers is found out. In silico analyses suggested that *HNRNPA1* has multiple mRNA isoforms differentially expressed in breast cancer cells. It was hypothesized that isoform level deregulation may lead to oncogenic activation of *HNRNPA1* with functional consequences in breast cancers.

CHAPTER 2

MATERIALS AND METHODS

2.1 APADetect Algorithm and APA of *HNRNPA1* in TNBC

APADetect is a probe level screen algorithm, developed by Dr. Tolga Can (Department of Computer Engineering, METU, Ankara). APADetect was used to analyze already available microarray data sets to detect expression levels of different 3'UTR isoforms (B. H. Akman, Can, & Elif Erson-Bensan, 2012; H. Akman, Erson-Bensan, B. Akman, & E. Erson-Bensan, 2014). APADetect splits probe sets into proximal and distal sub-sets based on the positions of poly(A) sites (Figure 2.1) according to the UCSC Genome Browser Database (Fujita et al., 2011). For each transcript, mean signal intensities of proximal and distal probe sets are calculated and used as indicators of short and long 3'UTR isoform abundance. Patient SLR (Short/Long Ratio) values are compared to control/normal tissue samples to detect APA based 3'UTR variants.

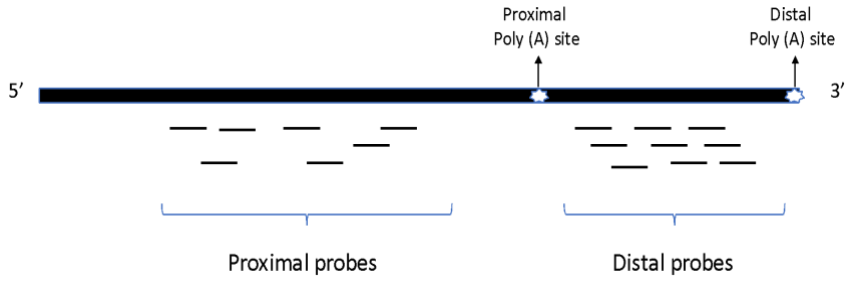

Figure 2.1. APADetect splits probe sets into proximal and distal sub-sets based on the positions of known poly (A) sites.

To investigate whether APA of *HNRNPA1* occurs in triple-negative breast cancers (TNBCs), 520 TNBC sample datasets were collected from GSE31519 (Rody et al., 2011), while histologically normal epithelium sample datasets were collected from different studies; 42 from GSE20437 (Graham et al., 2010), 15 from GSE9574 (Tripathi et al., 2008), 6 from GSE6883 (Liu et al., 2007), 6 from GSE26910 (Planche et al., 2011), 5 from GSE21422 (Kretschmer et al., 2011), 7 from GSE3744 (Richardson et al., 2006) and 1 from GSE2361 (Ge et al., 2005) for comparison.

2.2 RNA-Binding Protein and miRNA Binding Prediction

RBP (RNA-Binding Protein) binding sites on 3'UTR of HNRNPA1 isoforms were predicted via RBPDB tool (http://rbpdb.ccbr.utoronto.ca/) (Cook, Kazan, Zuberi, Morris, & Hughes, 2011a) and RBPmap web server (Paz, Kosti, Ares, Cline, & Mandel-Gutfreund, 2014). miRNAs targets on the 3'UTR of HNRNPA1 isoforms and their binding sites on the 3'UTRs were predicted via TargetScan tool (http://www.targetscan.org/vert_80/) (Agarwal, Bell, Nam, & Bartel, 2015).

2.3 Cell Lines and Culture Conditions

MCF7 and MDA-MB-231 cell line was a kind gift from Prof. Dr. Uygar Tazebay (Gebze Technical University, Kocaeli). MCF7 and MDA-MB-231 cells were grown in Dulbecco's Modified Eagle Medium (DMEM) (01-052-1A, Biological Industries) containing 10% FBS (S1810-500, Biowest), 1% penicillin/streptomycin (03-031-1B, Biological Industries), %1 Sodium Pyruvate (03-042-1B, Biological Industries). Cells were grown at 37°C with 5% CO_2, and 95% humidified air and were checked regularly for mycoplasma contamination by PCR.

2.4 Total RNA Isolation

Total RNA isolation from cells was performed with Tri Reagent (R2050-1-200, Zymo Research). For total RNA isolation from culture flask, cells were collected via trypsin (X0930-100, Biowest) and pelleted through the centrifugation. Cell pellets were washed with ice-cold PBS and pelleted once again. PBS was completely discarded and cells were lysed with 1 mL of Tri reagent. Cells were completely lysed by pipetting until viscous lysate disappeared. The cell lysates were transferred into a 1.5 ml microfuge tubes and incubated at room temperature for 5 minutes. Then, 200 µl chloroform (A3633, Applichem) was added onto the Tri reagent cell lysates and mixed by inversions for 15 seconds. Then, samples were incubated on ice for 15 minutes. The samples were centrifuged at 12000 g, 4°C for 15 minutes. After the centrifugation, approximately 500 µl of colorless aqueous phases containing RNA was transferred to 1.5 ml microfuge tubes and then, 500 µl of 2-propanol (I9516, Sigma-Aldrich) was added. The mixture was inverted for 15 seconds and tubes were incubated for 10 minutes at room temperature. After that, the tubes were centrifuged at 12000g, 4°C for 10 minutes. The supernatants were discarded and RNA pellets were washed with 1 mL of ice-cold 75% ethanol (EtOH) and centrifuged at 12000 g, 4°C for 15 minutes. The supernatant was removed and RNA pellets were air-dried. Air-dried RNA pellets were re-suspended within appropriate volume of nuclease free water and were incubated at 55°C for 10 minutes to dissolve the pellet completely. RNA samples were stored at -80°C.

2.5 DNase I Treatment

To eliminate any DNA contamination, 5 µl DNase I and 10 µl 10X DNase I buffer (04716728001, Roche Applied science) was added on the RNA sample containing tubes, and volume was completed to 100 µl by addition of nuclease-free water. Then, the tubes were incubated at 37°C for 2 hours. DNase I treatment was followed up by phenol-chloroform extraction. 100 µl of phenol-chloroform-isoamyl alcohol

(25:24:1) was added to the tubes, and the tubes were vortexed for mixing. Then, mixtures were transferred into phase lock tubes and incubated on ice 10 minutes. The tubes were centrifuged at 14000 rpm, 4°C for 20 minutes. 80 µl of the aqueous phase was transferred into a 1.5 ml tube containing 8 µl Sodium Acetate and 240 µl absolute EtOH. The tubes were incubated at -20°C overnight. The tubes were centrifuged at 14000 rpm, 4°C for 30 minutes, and supernatants were discarded. Pellets were washed with 600 µl of 75% EtOH, and the tubes were centrifuged at 14000 rpm, 4°C for 15 minutes. Supernatants were discarded, and RNA pellets were air-dried. Air-dried RNA pellets were re-suspended within the appropriate volume of nuclease-free water and were incubated at 55°C for 10 minutes to dissolve the pellet completely. After DNase I treatment, PCR using *GAPDH* (Glyceraldehyde 3-phosphate dehydrogenase) specific primers was applied to confirm that RNA samples are free of DNA contamination. Following conditions were used for the PCR reactions: incubation at 95°C for 5 minutes, 40 cycles of 95°C for 30 seconds, 56°C for 30 seconds, 72°C for 30 seconds, and final extension at 72°C for 5 minutes. RNA concentration was determined via MaestroNano Micro-Volume Spectrophotometer (Maestrogen) and stored at -80°C.

2.6 cDNA Synthesis

RNA was used for cDNA synthesis with RevertAid First Strand cDNA Synthesis Kit (K1622, Thermo Fisher Scientific). For this purpose, 1000 ng RNA and 1 µl oligo dT primer were mixed in a 200 µl tube containing an appropriate volume of water (final volume becomes 12 µl). Tubes were incubated at 65°C for 5 minutes and followed by immediate incubation on ice. 4 µl of 5X reverse transcriptase buffer, 2 µl of 10 mM dNTP mix, 1 µl of Ribolock RNase inhibitor, 1 µl RevertAid reverse transcriptase was added into each tube and mixed by pipetting. After that, the tubes were incubated at 42°C for 1 hour for synthesis and at 70°C for 10 minutes for the enzyme inactivation. Finally, cDNAs were stored at -20°C.

2.7 Cloning Experiments

2.7.1 Cloning of 3'RACE PCR Products

2.7.1.1 Rapid Amplification of cDNA Ends

Rapid amplification of cDNA ends (RACE)-specific cDNA synthesis was performed with 5 µg total RNA (DNase treated) from MCF7 and MDA-MB-231 cells using the oligo dT-anchor primer (5'-GACCACGCGTATCGATGTCGACTTTTTTTTTTT TTTTTTV-3'). The RACE-specific cDNA synthesis step took 1.5 hours at 42°C. For PCR, the following Gene Specific Primers were designed and used. 3'RACE_1: 5′-GTCGAAGTGGTTCTGGAAACT-3′, 3'RACE_2: 5'-CAGAAGCTCTGGCCCCTATG-3'. A reverse primer for the anchor sequence was used (Anchor-R: 5′-GACCACGCGTATCGATGTCGAC-3′). 3'RACE was performed using the 3′RACE_1 and Anchor-R primers via Taq DNA Polymerase (EP0402, ThermoScientific) with the following PCR. 1 µL template (cDNA), 2 µL of 2 mM dNTP, 2 µL of 10X reaction buffer, 1.6 µL $MgCl_2$ solution, 9.6 µL H_2O, and 1 µL Taq DNA polymerase (5 U/µL) were mixed in 0.2 mL tube and the reaction PCR conditions; 95°C for 3 minutes, 35 cycles of 95°C for 30 seconds, 56°C for 30 seconds and 72°C for 1 minute, and final extension at 72°C for 5 minutes. Nested 3'RACE PCR was performed using the 3'RACE_2 and Anchor-R primers with the 1/10 diluted PCR product as the template with the aforementioned PCR conditions.

2.7.1.2 Cloning of 3'RACE PCR Products into pGEMT vector

The PCR products were run on 1% agarose gels at 100 volts for 1-1.5 hours. The PCR products (bands in the gel) were gel purified by PCR clean up and gel extraction kit (740609.50, Macherey Nagel) according to the manufacturer's instructions and their concentrations were measured via MaestroNano Micro-Volume Spectrophotometer. Due to the feature of Taq DNA Polymerase, the PCR products

had A-tail at their end. Thus, they are suitable for A/T cloning. Thus, gel-purified PCR products were cloned into pGEMT easy vector (A1360, Promega) according to the manufacturer's protocol.

2.7.2 Cloning of HA-tagged HNRNPA1 Isoforms

2.7.2.1 Cloning of PCR Amplified HA-tagged HNRNPA1 Isoforms into pGEMT

First, hemagglutinin (HA) tag sequence and CDS of HNRNPA1 isoforms with or wihout their unique 3'UTRs were PCR amplified with HA-tagged HNRNPA1 primers (Table 2.1) using Phusion High-Fidelity DNA Polymerase (F530S, ThermoScientific) according to the manufacturer's instructions. The PCR products were run on agarose gels and the PCR products (bands in the gel) were gel purified by PCR clean up and gel extraction kit as was before. Taq DNA Polymerase was used to add A-tail to the gel-purified PCR products. For this, 10 µL of the gel-purified PCR products, 0.4 µL of 10 mM dATP, 2 µL of 1X reaction buffer, 6.6 µL H_2O and 1 µL Taq DNA polymerase were mixed in 0.2 mL tube and the reaction was conducted at 72°C for 30 minutes. Thus, they became suitable for A/T cloning. PCR products were cloned into the pGEMT easy vector according to the manufacturer's protocol.

Table 2.1. Primers for cloning of HA-tagged HNRNPA1 isoforms. Underlined sequences are restriction enzyme recognition sequences. CTCGAG: XhoI, AAGCTT: HindIII, GGATCC: BamHI.

Gene Accession Number	**Primer Name**	**Sequence (5'-3')**	**Annealing Temp.**
HNRNPA1 CDS	HA-HNRNPA1 Cloning F Primer	CGCATCTCGAGAAAATGTACCCA TACGATGTTCCAGATTACGCTTCT AAGTCAGAGTCTCCTAAAG	65°C
	CDS Cloning R Primer	CGCATAAGCTTTTAAAATCTTCTGC CACTGCCATAG	
HNRNPA1 (NM_002136.4)	HA-HNRNPA1 Cloning F Primer	CGCATCTCGAGAAAATGTACCCATA CGATGTTCCAGATTACGCTTCTAAGT CAGAGTCTCCTAAAG	65°C
	Isoform 2 Cloning R Primer	GGATCCTTTACACAGCACATTAAAAA AAAGAC	
	HA-HNRNPA1 Cloning F Primer	CGCATCTCGAGAAAATGTACCCA TACGATGTTCCAGATTACGCTTCT AAGTCAGAGTCTCCTAAAG	65°C
	Isoform 3 Cloning R Primer	GGATCCTTCAAGAGAATTAAATCG TTTATTGATTAC	
HNRNPA1 (NR_104427.1)	HA-HNRNPA1 Cloning F Primer	CGCATCTCGAGAAAATGTACCCA TACGATGTTCCAGATTACGCTTCT AAGTCAGAGTCTCCTAAAG	65°C
	Isoform 1 Cloning R Primer	GGATCCCTAAGTTAAATACAGTT TATTAAA	

2.7.2.2 Cloning of HA-HNRNPA1 Isoforms into pcDNA 3.1 (-)

HA-HNRNPA1 isoforms were cloned into pcDNA 3.1 (-) expression vector (V795-20, Invitrogen). For cloning, 5 μg of each pGEMT HA-HNRNPA1 isoforms and pcDNA 3.1 (-) were double digested with 1 μL of XhoI (FD0694, ThermoScientific) and 1 μL of HindIII/BamHI (FD0504/FD0054, ThermoScientific) restriction enzymes in universal FastDigest Buffer at 37°C for 1 hour to get HA-HNRNPA1 isoforms and linear pcDNA 3.1 (-). The digested vectors were run on a 1% agarose gel at 100 volts for 1-1.5 hours. The linearized pcDNA vector and HA-HNRNPA1 isoforms were gel-purified by PCR clean-up and gel extraction kit. The ligation reaction was conducted.

2.7.3 Cloning of HNRNPA1 3'UTR Isoforms

2.7.3.1 Cloning of HNRNPA1 Isoforms into pGEMT

Isoform 2 (350 bp), isoform 3 (702 bp), and isoform 1 (211 bp) 3'UTR sequences were PCR amplified with cloning primers (Table 2.2) using a Phusion High-Fidelity DNA Polymerase (F530S, ThermoScientific) and cloned into pMIR-Report (pMIR) plasmid (AM5795, Ambion). The PCR products was run on agarose gels and the PCR products (bands in the gel) were gel purified by PCR clean up and gel extraction kit as described before. A-tail reaction was applied again as described. A-tailed PCR products were cloned into pGEMT easy vector.

Table 2.2. Primers for cloning of HNRNPA1 3'UTR isoforms. Underlined sequences are restriction enzyme recognition sequences. ACTAGT: SpeI, GAGCTC: SacI, AAGCTT: HindIII.

Isoform 2 3'UTR Cloning	Forward Primer	CGCATACTAGTTTAGGAAACAAAGCTTAGCAGG
	Reverse Primer	CGCATGAGCTCTTTACACAGCACATTAAAAAAAAGAC
Isoform 3 3'UTR Cloning	Forward Primer	CGCATACTAGTTTAGGAAACAAAGCTTAGCAGG
	Reverse Primer	CGCATGAGCTCTTCAAGAGAATTAAATCGTTTATTGATTAC
Isoform 1 3'UTR Cloning	Forward Primer	GAGCTCTTAGGGAGGAGTCTGCTACT
	Reverse Primer	AAGCTTCTAAGTTAAATACAGTTTATTAAAA
Isoform 1-PartA 3'UTR Cloning	Forward Primer	GAGCTCTTAGGGAGGAGTCTGCTACT
	Reverse Primer	AAGCTTTAACGAAGTACAGTGGCTCAGATA
Isoform 1-PartB 3'UTR Cloning	Forward Primer	GAGCTCACCTTTATCTGAGCCACTGT
	Reverse Primer	AAGCTTCTAAGTTAAATACAGTTTATTAAAA

2.7.3.2 Cloning of HNRNPA1 3'UTR Isoforms into pMIR Report

HNRNPA1 3'UTR isoforms were cloned into pMIR Report vector (AM5795, Ambion). For cloning, 5 µg of each pGEMT *HNRNPA1* 3'UTR isoforms 2 and 3 and pMIR Report were double digested with 1 µL of SacI (FD1134, ThermoScientific) and 1 µL of HindIII (FD0504, ThermoScientific) restriction enzymes in universal FastDigest Buffer at 37°C for 1 hour to get 3'UTR isoforms and linear pMIR. 5 µg of each pGEMT HNRNPA1 3'UTR isoform 1 and pMIR Report were double digested with 2 µL of SacI (FD1134, ThermoScientific) and 1 µL of SpeI (ER1251, ThermoScientific) restriction enzymes in 1X Tango Buffer at 37°C for 1 hour.

The digested vectors were run on a 1% agarose gel at 100 volts for 1-1.5 hours. The linearized pMIR vector and HNRNPA1 3'UTR isoforms were gel-purified by PCR clean-up and gel extraction kit. The ligation reaction was conducted.

2.8 Site-Directed Mutagenesis: Deletion of miRNA and RBP sites

miRNA or RBP sites on HNRNPA1 3'UTR isoforms in pMIR vector were deleted via site-directed mutagenesis. For this purpose, QuikChange Primer Design-Agilent (https://www.agilent.com/store/primerDesignProgram.jsp) was used to design the primers (Appendix A, Table 4.1). 300 ng pMIR HNRNPA1 3'UTR isoform, 5 µL of each primer (10 µM), 5 µL of 2 mM dNTPs, and 0.5 µL Phusion DNA polymerase (2 U/µL) were mixed in 1X HF buffer, and reaction volume was completed to 50 µL by adding nuclease-free H_2O. Site-directed mutagenesis (SDM) PCR conditions: 98°C for 3 minutes, initial denaturation; 15 cycles (30 seconds at 98°C, 30 seconds at 65°C, and 3.5 minutes at 72°C) and 72°C for 5 minutes, final extension. 10 µL site-directed PCR was run on 0.5% agarose gel at 100 volts for 1-1.5 hour to check the PCR functioned properly.

DpnI restriction enzyme (FD1704, Thermoscientific) was used to get rid of the wild-type sequence. *DpnI* treatment was conducted by mixing 10 µL PCR product, 4 µL

of 10X FastDigest buffer, 23 µL of nuclease-free H_2O, and 3 µL *DpnI* enzyme in 0.2 mL tube and incubated overnight at 16°C. The *DpnI* treated SDM PCR products were used to transform the TOP10 competent *E.coli* bacteria. Colonies were selected via colony PCR using SDM confirmation forward and reverse primers (Appendix A, Table 4.2).

2.8.1 Cloning of HNRNPA1 shRNA into pSuper Vector

HNRNPA1 short-hairpin RNA (A1shRNA) (5'- TGAGAGATCCAAACACCAA-3') (Guil, Long, & Cáceres, 2006) was cloned into pSUPER retro.neo-GFP (OligoEngine) (a kind gift from Dr. Uygar Tazebay, Gebze Technical University, Turkey) and non-targeting (NT) shRNA (5'- CGTACGCGGAATACTTCGATT-3') was already cloned into pSUPER retro.neo-GFP in the laboratory. For shRNA oligos cloning, the sense and antisense oligos (Table 2.3) were dissolved in sterile, nuclease-free H_2O to 3 mg/ml. The annealing reaction was carried out as in the annealing of the shRNA oligos. 5 µg of pSuper vector was linearized with 1 µL Fast Digest HindIII (FD0504, ThermoScientific) and Fast Digest BglII (FD0084, ThermoScientific) restriction enzymes in universal 1X FastDigest Buffer at 37°C for 1 hour. The digested vector was run on 1% agarose gel at 100 volts for 1-1.5 hours. The linearized vector was gel purified by PCR clean-up and gel extraction kit (740609.50, Macherey Nagel) according to the manufacturer's instructions to remove any undigested circular plasmid and decrease the background in ligation and transformation. The ligation reaction was conducted as before. The colony PCR was run on 1% agarose gel at 100 volts for 1-1.5 hours. The digested vector was run on 1% agarose gel at 100 volts for 1-1.5 hours. The linearized vector was gel purified by PCR clean up and gel extraction kit (740609.50, Macherey Nagel) according to the manufacturer's instructions to remove any undigested circular plasmid and decrease the background in ligation and transformation. The ligation reaction was conducted.

Table 2.3. HNRNPA1 shRNA oligos adopted for pSuper vector.

HNRNPA1 shRNA	Sense	GATCCCCTGAGAGATCCAAACACCAATTCAAGA GATTGGTGTTTGGATCTCTCATTTTTA
	Antisense	AGCTTAAAAATGAGAGATCCAAACACCAATCTC TTGAATTGGTGTTTGGATCTCTCAGGG

2.8.2 Cloning of HNRNPA1 sgRNA into CRISPR/Cas9 Vector

To knockout *HNRNPA1*, CRISPR/Cas9 system was used. First of all, HNRNPA1 single guild RNA1 (sgRNA1) (5'- CACCGGCTATAACAACGGAGGCGG -3') and sgRNA2 (5'- CACCGAAGGGTTCCACAATCTGTA -3') (Sui et al., 2015) were cloned into pSpCas9(BB)-2A-Puro (PX459) V2.0 (62988, Addgene) (a kind gift from Prof.Dr. Mesut Muyan, Middle East Technical University, Turkey). For sgRNA cloning, the sense and antisense oligos (Table 2.4) were dissolved in sterile, nuclease-free H_2O to a concentration of 3 mg/ml. The annealing reaction was carried out as discribed before. For more extended storage, the annealed oligos were kept at -20°C until needed. 5 µg of px459 vector was linearized with 1 µL BbsI-HF restriction enzyme (R3539S, New England BioLabs) in rCutSmart buffer at 37°C for 1 hour. The digested vector was run on 1% agarose gel at 100 volts for 1-1.5 hours. The linearized vector was gel purified by PCR clean-up and gel extraction kit.

Table 2.4. HNRNPA1 sgRNA oligos (Sui et al., 2015).

sgRNA1	Sense	CACCGGCTATAACAACGGAGGCGG
	Antisense	AAACCCGCCTCCGTTGTTATAGCC
sgRNA2	Sense	CACCGAAGGGTTCCACAATCTGTA
	Antisense	AAACTACAGATTGTGGAACCCTTC

2.9 Ligation Reactions

The ligation reaction was conducted by mixing linear vector and insert at a 1:3 molar ratio. The ligation reaction was carried out at 16°C overnight by mixing 100 ng linearized vector, the calculated amount of the insert according to the formula below/ 2 µL annealed oligos, 1 µl of 10X T4 DNA ligase buffer, 0.2 µl of T4 DNA ligase (2 U/µL) (EL0011, ThermoScientific) and the appropriate amount of nuclease-free H_2O to complete reaction volume to 10 µl.

$$\frac{\text{ng of vector} \times \text{kb size of insert}}{\text{kb size of vector}} \times \text{insert:vector molar ratio} = \text{ng of insert}$$

Formula

A different protocol was followed for A/T cloning of PCR inserts into pGEMT easy vector (A1360, Promega) according to the manufacturer's protocol. In the protocol, same linear vector and insert at 1:3 molar ratio was followed, and reaction mixture was prepared by mixing 1 µl (50 ng) of linear pGEMT easy vector, calculated amount of insert, 5 µl of 2X Rapid Ligation Buffer, 1 µl of T4 DNA ligase (3 U/µL) and appropriate amount of nuclease-free H_2O to complete reaction volume to 10 µl at 4°C overnight.

2.10 Transformation of Bacteria

The ligation products//SDM applied plamids were used to transform the TOP10 competent *E. coli* bacteria. The total volume of the ligation product was mixed with the 50 µl competent bacteria in a 1.5 mL tube, and then the tube was incubated on ice for 30 minutes. After ice incubation, bacteria were heat-shocked at 42°C for 45-60 seconds. Then, the bacteria were incubated again on ice for 5 minutes. For recovery of bacteria due to the heat-shock process, 500 µl Luria broth (LB) medium was added to the bacteria, and the bacteria were incubated at 37°C for 1 hour. After

1 hour of incubation, centrifugation was applied to get rid of the excess medium at 5000 rpm for 10 minutes. The transformed bacteria pellet was dissolved within 100 µL remaining LB and spread on the agar plate. The plate was incubated at 37°C for 16 hours. Bacterium colonies with plasmid containing insert were determined with colony PCR.

For the transformation of bacteria with pGEMT contructs, during 1-hour incubation for recovery of bacteria, 10 µl of 1M IPTG and 20 µl of 50 mg/ml X-Gal were spread on ampicillin containing agar plate and the agar plates were air-dried. Only white colonies were selected for colony PCR but not the blue ones.

2.11 Colony PCR/Insert Confirmation PCR

Transformed colonies were screened by PCR using proper primer for the plasmid type (Table 2.5). 1 µL template or 1 colony taken by a micropipette tip, 2 µL of 2 mM dNTP, 2 µL of 10X reaction buffer, 1.6 µL $MgCl_2$ solution, 9.6 µL H_2O, and 0.2 µL Taq DNA polymerase (5 U/µL) were mixed in 0.2 mL tube and the reaction PCR conditions; 95°C for 5 minutes, 35 cycles of 95°C for 30 seconds, 56°C for 30 seconds and 72°C for 30-2 minutes, and final extension at 72°C for 5 minutes. The colony PCR products were run on 1% agarose gel at 100 volts for 1-1.5 hours.

Table 2.5. Vectors for cloning of inserts and primers used for confirmation of inserts in the corresponding vectors.

Vector Name	Primer Name	Sequence (5'-3')
pGMET	T7 Primer	TAATACGACTCACTATAGGG
	SP6 Primer	ATTTAGGTGACACTATAG
pcDNA 3.1	T7 Primer	TAATACGACTCACTATAGGG
	BGH Reverse primer	TAGAAGGCACAGTCGAGG
pMIR Report	pMIR Sequencing Forward	AGGCGATTAAGTTGGGTA
	pMIR Sequencing Reverse	GGAAAGTCCAAATTGCTC
pSuper	pSuper_468bp_F	AACCAGTCGGTAGATGTCAAGAA
	pSuper_468bp_R	TATTTGCATGTCGCTATGTGTTC
pX459	hU6-F	GAGGGCCTATTTCCCATGATT
	sgRNA Antisense oligo	Sequences in Table 2.4

2.12 Plasmid Isolation from Transformed E. coli

The positive (white) colonies of *E. coli* bacteria transformed with constructs were seeded in 15 mL of ampicillin containing LB medium and incubated overnight at 37°C. pGEMT plasmids were isolated from bacterial culture via GeneJET Plasmid Miniprep Kit (K0503, ThermoScientific) according to the manufacturer's protocol. Plasmid concentration was measured via MaestroNano Micro-Volume Spectrophotometer and sequenced.

2.13 Transfection Experiments

2.13.1 Transfection of MCF7 and MDA-MB-231 with pcDNA HA-HNRNPA1 Isoforms

MCF7 and MDA-MB-231 cells were seeded on 6-well plates to ~70% confluency. Media on cells were removed, and cells were washed with PBS. Fresh medium was added to cells and cells were transfected with 2 μg pcDNA HA-HNRNPA1 constructs using 4 μL TurboFect transfection reagent (R0532, ThermoScientific) according to the manufacturer's instructions. After 48 hours of transfection, cells were collected for total proteins for western blot analysis.

2.13.2 Dual-Luciferase Reporter Assay

MCF7 cells and MDA-MB-231 cells on 48-well plates (at 60-70% confluency) were co-transfected with pMIR (Firefly luciferase) (225 ng for MCF7 and 245 ng for MDA-MB-231) and phRL-TK (Renilla Luciferase) (E6241, Promega) (25 ng for MCF7 and 5 ng for MDA-MB-231) vectors 0.5 μL TurboFect transfection reagent. 24 hours after transfection, cells were collected, and dual luciferase activities were measured using the Modulus Microplate Luminometer (Turner Biosystems) with at least three technical replicates per independent biological replicate (n=3). The

luminescence intensity of Firefly luciferase (pMIR) was normalized to that of Renilla luciferase (phRL-TK).

2.13.3 Silencing of HNRNPA1 in MDA-MB-231 with pSuper RNAi System

After cloning shRNAs into pSuper vector and plasmid isolation, MDAMB231 cells were grown in 6-well plates up to ~70% confluency. The medium was discarded, cells were washed with PBS, and fresh medium was added. MDA-MB-231 cells were transfected with 2 μg pSuper A1shRNA or NTshRNA and 4 μL TurboFect. Transfected cells were selected with 1000 mg/ml G418 (Roche, 4727894001) and maintained with 500 mg/ml G418, and monoclonal cells were expanded. HNRNPA1 silencing was detected by western blotting.

2.13.4 Knockout of HNRNPA1 in MDA-MB-231 with CRISPR/Cas9

After cloning HNRNPA1 sgRNAs into p459 vector and plasmid isolation, MDA-MB-231 cells were seeded on a 6-well plate to ~70% confluency. The medium above cells were discarded, cells were washed with PBS and fresh medium was added. MDA-MB-231 cells were co-transfected with 1 μg px459 HNRNPA1 sgRNA1 and 1 μg px459 HNRNPA1 sgRNA2 vectors and 4 μL TurboFect transfection reagent. Transfected cells were selected with 0.5 μg/mL puromycin (A1113803, Gibco) and maintained with 0.25 μg/mL puromycin, and monoclonal cells were expanded. *HNRNPA1* knockout was detected by western blotting.

2.14 Actinomycin D and Cycloheximide Treatments

MCF7 cells were grown in 6-well plates up to 50% confluency before 2 μg/mL actinomycin D (ActD) (1229, Tocris Bioscience) and 100 μg/mL Cycloheximide (CHX) (0970, Tocris Bioscience) treatments. ActD was dissolved in dimethylsulfoxide (DMSO), while CHX was dissolved in EtOH. Cells were

harvested after 3 hours of ActD and CHX treatments, and RNA was isolated. Control groups received only DMSO and/or EtOH. Following DNase treatment, cDNAs were synthesized, and remaining mRNA levels were quantified using RT-qPCR. Relative mRNA levels were plotted against treatment duration and fitted to a linear regression model. Three independent treatments were performed.

2.15 RT-qPCR

Expression levels of HNRNPA1 isoforms, and pri-miR-27b were determined by RT-qPCR. SsoAdvancedTM Universal SYBR® Green Supermix (1725271, Bio-Rad Laboratories) was used. MIQE guidelines were followed throughout the PCR and RT-qPCR analyses (Bustin et al., 2009). Reactions with 10 µl volume were performed with 0.6 µl from each specific primer pair (300 nM final concentration), 5 µl SsoAdvancedTM Universal SYBR® Green Supermix, and 0.8 µl nuclease-free water. Fold change of the gene expressions were normalized against the reference gene, ribosomal protein lateral stalk subunit P0 (RPLP0) (accession: NM_001002.4 & NM_053275.3) whose expression does not change in response to any treatment or transfection. Reaction efficiency correction and the ΔΔCq method were used for quantification. Sequences of primer pairs, expected product sizes, and RT-qPCR annealing temperatures are given in Table 2.6.

Table 2.6. RT-qPCR primer list.

RNA	Primer Name	Sequence (5'-3')	Annealing Temp.
Total HNRNPA1	Hs HNRNPA1 Forward	GCTCACGGACTGTGTGGTAA	66°C
	Hs HNRNPA1 Reverse	GGCCTTGCATTCATAGCTGC	
HNRNPA1 (NM_002136.4)	HNRNPA1 Isoform 2 F	AAGTGTAAAGCATTCCAACAAAGG	60°C
	HNRNPA1 Isoform 2 R	TCAGCGTCACGATCAGACTG	
	HNRNPA1 Isoform 3 F	CAACCTGCTTGGGTGGAGAA	60°C
	HNRNPA1 Isoform 3 R	TTGCATAGGATGTGCCAACAA	
HNRNPA1 (NR_104427.1)	HNRNPA1 Isoform 1 F	CAGAAGCTCTGGCCCCTATG	64°C
	HNRNPA1 Isoform 1 R	CACAAGGACGTTCCTTTCTGC	
RPLP0 (NM_001002.4 & NM_053275.3)	RPLP0 F	GGAGAAACTGCTGCCTCATA	60°C
	RPLP0 R	GGAAAAAGGAGGTCTTCTCG	
c-MYC (NM_002467.6 & NM_001354870.1)	c-MYC F	CAGCTGCTTAGACGCTGGATT	61°C
	c-MYC R	GTAGAAATACGGCTGCACCGA	
C9ORF3	Ex2-3 Forward	GAAGACAGGGGCTCAGACAG	60°C
	Ex2-3 Reverse	GCCCTGTTGTTTATGGGAGA	
C9ORF3	Ex13-14 Forward	GCACAAGTTCACGAAAGCCT	64°C
	Ex13-14 Forward	CTCACTCACCATCAGCTCCC	
pri-miR-27b	hsa-mir-27b Forward	ACCAGCTGAGGAAGATGCTC	62°C
	hsa-mir-27b Reverse	CAGCGGCTCCAACTTAACTG	

2.16 Total Protein Isolation

Total protein isolation was performed using the M-PER Mammalian Protein Extraction Reagent (78501, Thermo Scientific). First, the medium over the cells was removed and cells were washed with 1X PBS twice. Next, the cells were treated with 250 µl of trypsin on a 6-well plate and incubated at 37°C for 5 minutes. DMEM growth medium was added to the wells to inhibit the trypsin's enzymatic activity and collect the cell suspension. Cell suspensions were transferred into 1.5 ml tubes and

centrifuged at 1500 rpm for 5 minutes to isolate the cells from medium and trypsin. The supernatants were discarded, and cells were washed with 1X PBS. The centrifugation step was repeated, and supernatants were discarded. 50 µl of M-PER, 5 µl of 10X phosSTOP (05056489001, Roche Life Science), and 10 µl of 25X protease inhibitor cocktail (4906845001, Roche Life Science) were mixed and added directly to cell pellets in 1.5 ml tubes on ice. Then, samples were incubated on ice for 30 minutes and vortexed for 30 seconds, at 10 minutes intervals. Samples were centrifuged at 14000 g, 4°C for 20 minutes. Supernatants, which contained the total protein, were then transferred into a fresh 1.5 ml tube and stored at -80°C.

2.17 Protein Concentration Measurement

Protein concentrations were determined with Pierce BCA Protein Assay Kit (23227, Thermo Fisher Scientific). The manufacturer's protocol was modified to a 96-well plate, so the reaction protocol became; 200 µl Reagent A and 4 µl Reagent were mixed, and 200 µl of the mixture was added to the wells of the 96-well plate. Then, 20 µl nuclease-free water was added and 5 µl protein sample was added. Then, the sample containing a 96-well plate was incubated at 37°C for 30 minutes. The absorbance of the samples was measured at 562 nm wavelength. The absorbance value of the blank was subtracted from those of samples and concentration of the protein samples was calculated according to the standard curve.

2.18 Western Blot

30 µg total protein extracts were denatured with 6X Loading dye at 100°C for 10 minutes. SDS-PAGE is performed using 5% stacking and 8-12% separating gels and blotting was done onto PVDF membrane (03010040001, Merck). 5% bovine serum albumin fraction V (BSA) (11943.01, Serva) in TBS-T (Tris Buffer 28 Saline-Tween) was used as a blocking reagent at room temperature for 1 hour. Blocking was followed by overnight incubation with the primary antibodies: B-actin (1:2000)

(sc-47778, Santa-Cruz), HNRNPA1 (1:2000) (4B10, sc-32301, Santa-Cruz) with a subsequent 1-hour incubation of secondary antibody (sc-2005, Santa Cruz). Membranes were visualized by WesternBright ECL Blotting Substrates (K12045-D50, Advansta) and ChemiDoc™ MP Imaging System (170-8280, Bio-Rad Laboratories) according to the manufacturer's instructions.

2.19 Immunocytochemistry

HA-HNRNPA1 isoforms with their 3'UTRs were cloned into pcDNA 3.1 (-) expression vector. Cloned vectors were transfected to MCF7 cells. Localization of HA-tagged HNRNPA1 proteins translated from isoforms 1, 2, and 3 (CDS+3'UTRs) in MCF7 cells was detected by immunocytochemistry. First, coverslips were put into ethanol and then under UV light. After that, the coverslips were placed in the wells of a 6-well plate. 2×10^5 MCF7 cells were seeded on the coverslips in the wells. The next day, HA-HNRNPA1 isoforms and 3'UTRs cloned into pcDNA 3.1 (-) were used to transfect MCF7 cells. After 48 hours of transfection, MCF7 cells were fixed with 2% paraformaldehyde, permeabilized with 0.4% Triton X-100 in PBS, blocked with 10% BSA, and incubated with rabbit anti-HA-tag monoclonal antibody (1:500; ab9110, Abcam) at RT 1 hour. Cells were stained with the Alexa fluor® 488-conjugated goat polyclonal anti-rabbit IgG secondary antibody (1:1000; ab150077, Abcam) and counterstained with fluoroshield mounting medium DAPI (ab104139, Abcam). Images of MCF7 cells were produced via Leica DMI4000 B equipped with Andor DSD2 spinning confocal microscope with 63X oil NA 1.4 objective lens.

2.20 Clonogenic Assay

Thousand MDA-MB-231/NTsh and A1sh cells were seeded as triplicates on 6-well plates and were cultured for 14 days. The medium was changed in 2 days interval. The medium was discarded, and cells were washed with PBS. Cells were fixed with 100% methanol for 20 minutes and stained with 1% crystal violet for 5 minutes.

Colonies were photographed, and visible colonies larger than three mm^2 were counted via the countPHICS tool (Brzozowska et al., 2019). The experiment was repeated three independent times with at least three technical replicates.

2.21 Wound Healing

MDA-MB-231/NTsh and A1sh cells were grown on a 6-well plate to 100% confluency. A pipette tip wounded confluent cell layers. Cells were washed with PBS three times to get rid of detached cells, and fresh medium was added. Medium change was applied every 2 days and cells were monitored for up to 48 hours for wound closure. Images were captured using an inverted microscope (Olympus Corp.), and wound width measurements were measured. ImageJ software measured the wound closure areas (Schneider, Rasband, & Eliceiri, 2012). The experiment was repeated three independent times with at least three technical replicates.

2.22 MTT Cell Proliferation Assay

7.5×10^3 stably NTsh and HNRNPA1sh transfected MDA-MB-23 cells in 100 µl of DMEM were cultured on 96-well plates for 3 days. MTT cell proliferation assay was performed at day 0 and day 3. MTT solution (10 µl) (M5655-1G, Sigma-Aldrich) was added to each well for 4 hours at 37°C with 5% CO_2 100 µl SDS was added to each well and incubated at 37°C with 5% CO_2, overnight. Absorbance was measured at 570 nm wavelength with a Multiskan GO Microplate Spectrophotometer (Thermo Fisher). The experiment was repeated three independent times with at least five technical replicates.

2.23 Migration and Invasion Assays

Migration and invasion assays were performed using a Transwell system with an 8-µm pore size (662638, Greiner Bio-One). 80% confluent MDA-MB-231/NTsh and

MDA-MB-231/A1sh cells were used. 1×10^5 cells in 100 µl of DMEM supplemented with 1% FBS were seeded in the transwell insert, and 600 µl of complete medium (DMEM supplemented with 10% FBS) was added to the wells of the 24-well plate well. Cells were incubated at 37°C and 5% CO_2 for 15 hours. The apical surface of the transwell's membrane was cleaned with cotton sticks three times. Then, the transwell was incubated in methanol for 10 min to fix the cells. It is incubated in Giemsa dye for 2 min. The membrane was placed and covered with a cover slide. The membrane was observed and photographed under the inverted microscope (Olympus Corp.). For the effects of *HNRNPA1* silencing on the invasiveness of MDA-MB-231 cells, the same protocol was applied except that membrane of the transwell was pre-coated with Matrigel (356231, Corning), and the cells were incubated for 18 hours. Both experiments were performed in triplicate.

2.24 NanoString nCounter miRNA Assay

NanoString nCounter Human miRNA V3 assay was performed according to the manufacturer's instructions (GXA-MIR3-12, NanoString Technologies) at CanSyL of METU. Human mature miRNAs (n=799), positive controls (n=6), negative controls (n=8), ligation controls (n=6), and mRNA housekeeping controls (*ACTB, B2M, GAPDH, RPL19* and *RPLP0*) were analyzed. All normalization steps were performed according to the manufacturer's instructions. Significance was calculated using an unpaired t-test for the three technical replicates. Altered miRNA expression levels were determined based on p-value ($p<0.05$) and fold change (<0.6 and >1.5). Biological pathways affected by miRNAs were determined using DIANA TOOLS mirPath v.3 (Vlachos et al., 2012).

2.25 miRNA Expression Analysis

cDNAs were synthesized from total RNA with TaqMan MicroRNA Reverse Transcription Kit (Applied Biosystems, 4427975) according to the manufacturers′

recommendations. TaqMan Universal Master Mix II (Applied Biosystems, 4440040) was used with unique miRNA probes; hsa-miR-27b (assay ID: 000409) and endogenous control RNU43 (assay ID: 001095). MIQE guidelines were followed (Bustin et al., 2009). Reaction efficiency correction and the ΔΔCq method was used for quantification.

CHAPTER 3

RESULTS

3.1 De-regulation of *HNRNPA1* expression in Breast Cancer

To determine the expression of *HNRNPA1* in normal breast tissues, The Genotype-Tissue Expression (GTEX) database was analyzed for normal tissue expression (Carithers & Moore, 2015). In normal mammary tissue, several HNRNPA1 isoforms were identified (Figure 3.1, A). The dominantly expressed isoforms are ENST00000547566.1 (isoform 1), ENST00000330752.12 (isoform 2) and ENST00000547276.5 (isoform 3) (Figure 3.1, A and B). The Human *HNRNPA1* locus seems to produce several isoforms, some alternatively spliced and others by APA (alternative polyadenylation) (Figure 3.1, A). However, when turned to TCGA (performed by Didem Naz Döken), it is clear that isoform 1 is significantly downregulated in breast cancers ($p<0.0001$) and is the least expressed one in breast cancer tissues. In contrast, isoform 2 showed the opposite pattern in normal breast and breast cancer tissues (Figure 3.1, B). These results suggested that 3'end isoforms of *HNRNPA1* existed (Figure 3.1, B), and their ratio of expression is altered in breast cancers.

A.

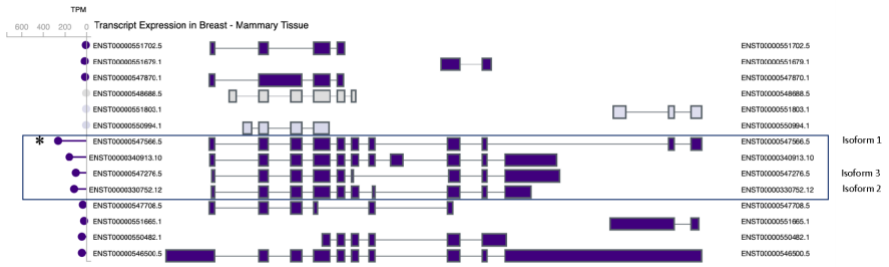
TPM
600 400 200 0
Transcript Expression in Breast - Mammary Tissue
Isoform 1
Isoform 3
Isoform 2

B.

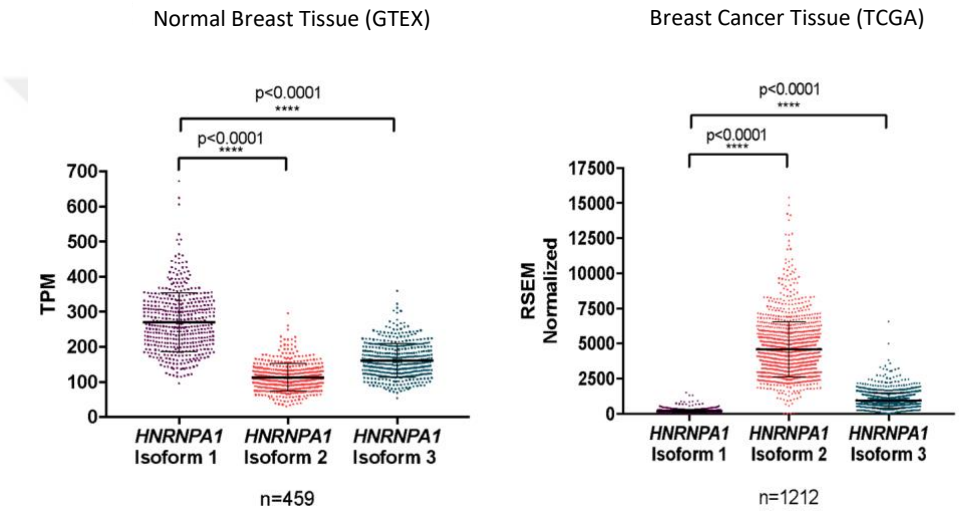
Normal Breast Tissue (GTEX)
Breast Cancer Tissue (TCGA)
p<0.0001
****
p<0.0001
****
TPM
RSEM Normalized
HNRNPA1 Isoform 1
HNRNPA1 Isoform 2
HNRNPA1 Isoform 3
n=459
n=1212

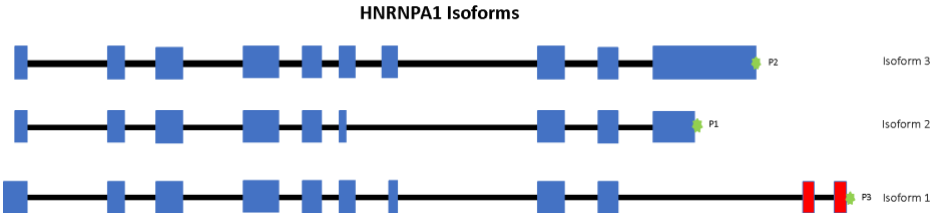
HNRNPA1 Isoforms
P2
Isoform 3
P1
Isoform 2
P3
Isoform 1

C.

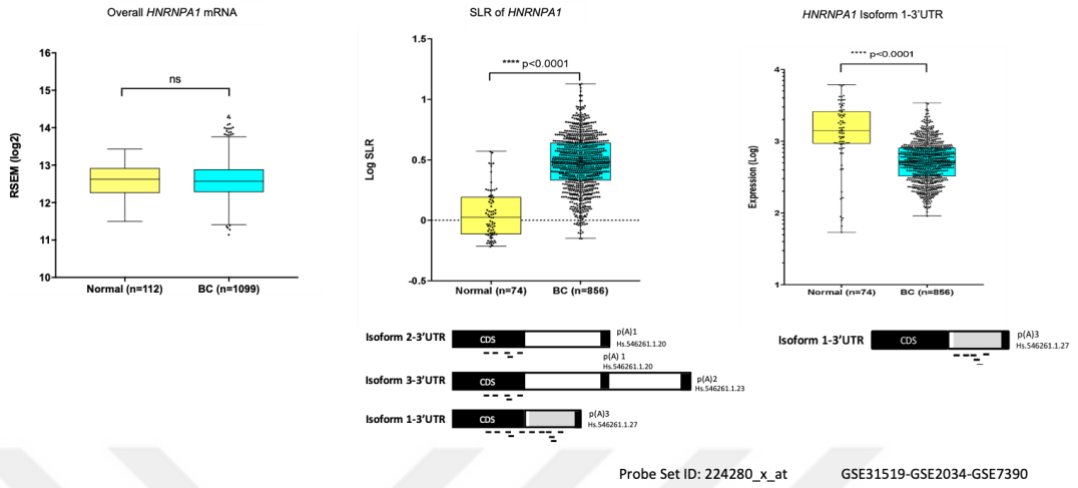

Figure 3.1. HNRNPA1 isoforms and their expression in tissues A. Existence and expression of HNRNPA1 mRNA isoforms in normal breast tissues B. Expression of HNRNPA1 isoforms (1, 2, and 3) in normal breast tissue. Expression data were obtained from the GTEx Portal (Carithers & Moore, 2015) ($p<0.000$, one-way ANOVA) on the left. Expression and schematic representation of HNRNPA1 isoforms (1, 2, and 3) in TCGA breast cancers dataset (retrieved from http://gdac.broadinstitute.org) ($p<0.0001$, one-way ANOVA) on the right. C. Overall mRNA expression of *HNRNPA1* in breast cancer patients compared with normal breast tissue shows no significant difference (Data taken from http://firebrowse.org/) (Left). Log SLR score of HNRNPA1 is significantly increased in breast cancer patients compared with normal breast tissue ($p<0.0001$) in GSE31519, GSE2034, and GSE7390 analyzing microarray dataset via APADetect (Middle). Signals from the probe set (ID: 224280_x_at) recognizes 3'UTR of isoform 1 (ENST00000547566.5). Expression of isoform 1 was low in breast cancer patients ($p<0.0001$, unpaired t-test with Welch`s Correction) (Right).

Interestingly, without considering isoforms, there was no change in the overall *HNRNPA1* expression (Figure 3.1 C, left panel). However, an altered isoform ratio was detected when breast cancer patient data were analyzed using an in-house algorithm, APADetect, to distinguish transcripts with different poly(A) ends. An increased SLR (Total isoform/isoform 1 ratio) score (Figure 3.1 C, middle panel) was due to the decrease in expression of Isoform 1 in breast cancer patient array data (GSE31519, GSE2034, and GSE7390) (Figure 3.1 C, right panel).

3.2 Confirmation of APA Events of HNRNPA1 via 3'RACE

The 3'UTR isoforms of *HNRNPA1* detected in *silico* data needed to be experimentally proven. To confirm the existence of *HNRNPA1* isoforms ending with different poly(A) sites, 3'RACE PCR was performed using 3'RACE_1 and 3'RACE_2 primers as detailly described in the Materials and Method chapter (Figure 3.2, A). Shortly, 3'RACE-specific cDNA was synthesized from MCF7 and MDA-MB-231 RNA samples using a RACE oligo dT-anchor primer. The first 3'RACE-PCR was conducted with 3'RACE_1 and Anchor-R primers. Then, the first 3'RACE-PCR product was used as a template for nested 3'RACE-PCR with a new forward (3'RACE_2) and Anchor-R primers. The nested 3'RACE-PCR products were on the agarose gel and gave the bands that would suggest the usage of P1, P2, and P3 and the existence of isoforms 2, 3, and 1 (Figure 3.2, B).

A.

B.

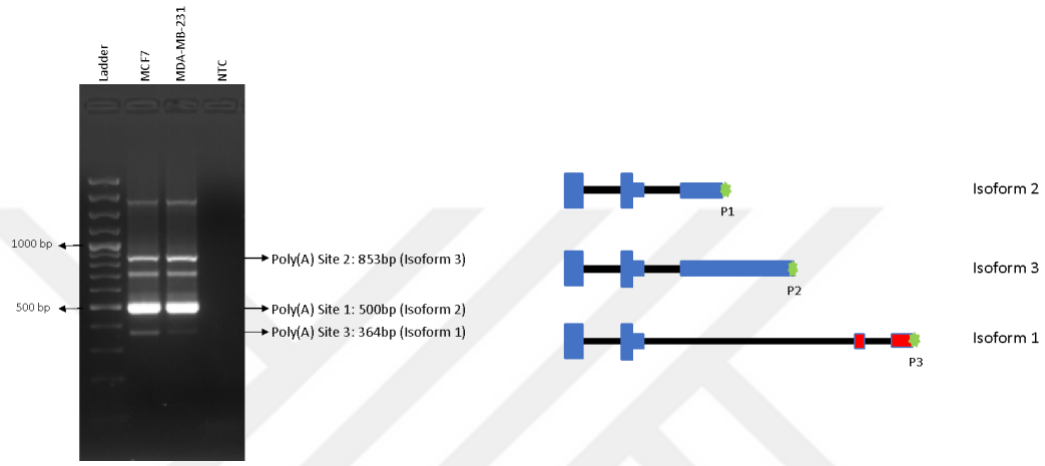

Figure 3.2. Detection of 3'UTR isoforms via 3'RACE-PCR. A. Gene structure of *HNRNPA1*, poly(A) sites and location of 3'RACE primers and CDS primers. B. Agarose gel images of 3'RACE PCR confirmed the usage of poly(A) sites 1, 2, and 3. isoform 3 uses Poly(A) site 2 (P2) with long 3'UTR, isoform 2 uses P1 with short 3'UTR, and isoform 1 uses P3 with 2 exons at the end. NTC: No template reaction.

To further verify the existence of 364bp (isoform 1), 500bp (isoform 2), and 853bp (isoform 3) products, these bands were gel extracted and inserted into the pGEMT vector by using the A/T cloning technique. Finally, these products in pGEMT vectors were sequenced for verification. Sequencing the PCR products for isoform 1, 2, and 3 verified the 3'ends of isoforms with the poly(A) site 3, 1, and 2 with Poly(A) site ID Hs.546261.1.23, Hs.546261.1.27 and Hs.546261.1.20 respectively (Figure 3.3).

A.

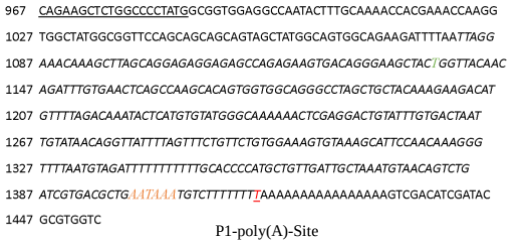

B.

C.

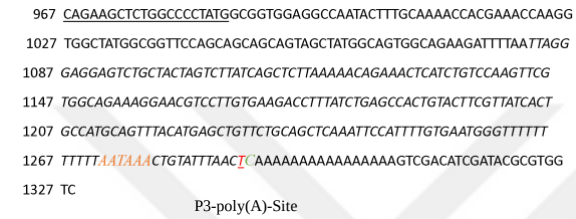

Figure 3.3. Sequencing of the 3'RACE-PCR products: A. 500bp (isoform 2 with P1-poly(A)-site), B. 853bp (isoform 3 with P2-poly(A)-site), and C. 364bp (isoform 1 with P3-poly(A)-site) products revealed the existence of the different 3'UTRs and poly(A) site usage. The Underlined Sequence is RACE_2 Primer. Italic Sequence is 3'UTR. Poly(A) Sites are red sequences. Poly(A) Signal: AATAAA. Missing Nucleotide: - (Green Dash) and Mismatch: T (Green Nucleotide).

3.3 Confirmation of CDSs of HNRNPA1 Isoforms

The CDS isoforms of *HNRNPA1* shown in GTEx data (Figure 3.1, A) was experimentally validated. PCR was performed with MCF10A cDNA using cloning primers for HNRNPA1 (Figure 3.4, A). Subsequently, cDNA was synthesized from MCF10A RNA samples using an oligo dT-primer. The PCR was conducted with the cDNA with cloning primers. Then, the PCR products were run on agarose gel and the bands were sequenced (Appendix B), showing two HNRNPA1 CDSs with/out exon 8 (Figure 3.4, B). The same agarose gel results were obtained from PCR of MDA-MB-157 cDNA and gradient PCR of MCF10A cDNA using with same cloning primers (Appendix C, Figure 4.3). Sizes of exon 8 included and excluded CDSs are 1119, and 963 nucleotides, respectively, and exon 8 excluded CDS was

the predominant one. Moreover, only these two CDSs resulting from alternative splicing were detected, and other CDS isoforms seen in GTEx data were not detected. These two coding sequences of HNRNPA1 transcripts produce two protein isoforms, HNRNPA1-B with NP_112420.1 accession number (the full-length isoform of 372 amino acids, 38 kDa) and HNRNPA1-A with NP_002127.1 accession number (the shorter variant, missing residues 253 to 303, exon 8, creating 320 aa protein, 34 kDa) (Available from: https://www.ncbi.nlm.nih.gov/gene/3178).

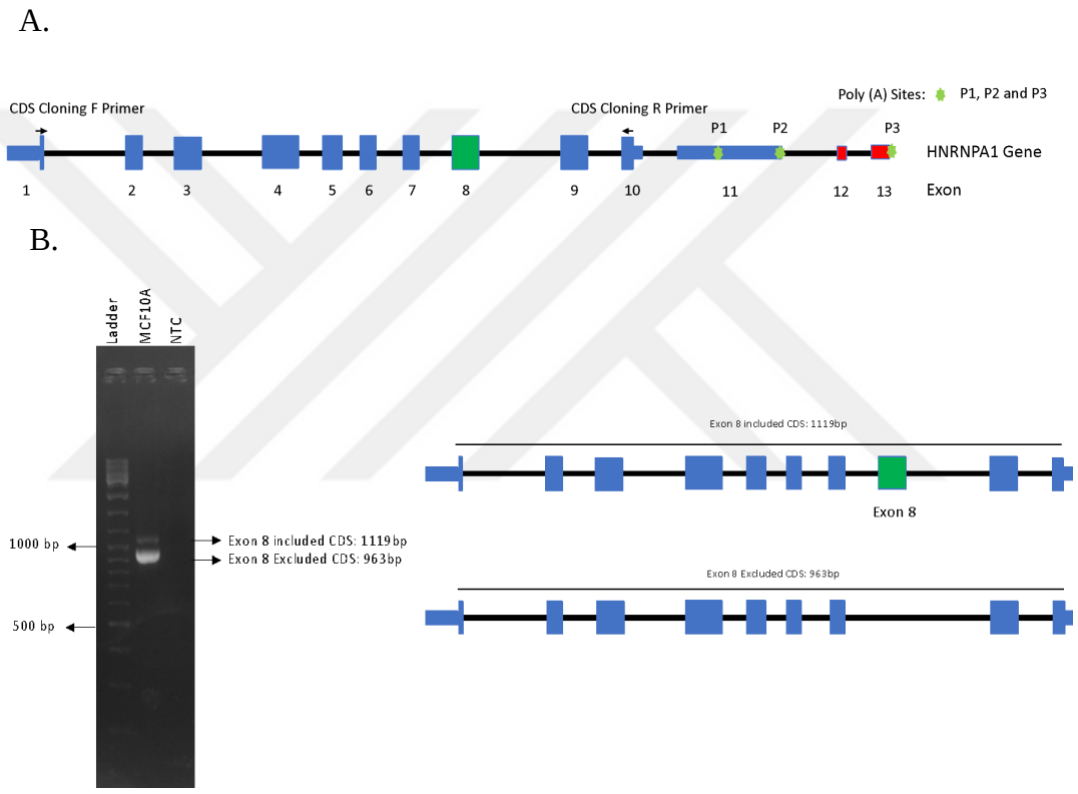

Figure 3.4. Detection of CDS isoforms via PCR. A. Gene structure of *HNRNPA1*, poly(A) sites, exon number, and location of CDS cloning primers (CDS Cloning F and R Primers). B. Agarose gel images of PCR confirmed two HNRNPA1 CDSs with/out exon 8. NTC: No template reaction.

3.4 Isoform Switch of *HNRNPA1* in Breast Cancer Cell lines and Tissues

Switch from isoform 1 to other isoforms in cancer progression (GTEx and TCGA data) was determined. This switch was also represented as an SLR value (total isoforms/isoform 1) in probe-based microarray data. After confirming 3'UTR HNRNPA1 isoforms by 3'RACE-PCR, the switch from isoform 1 to other isoforms in a panel of breast cancer patient cDNAs (n = 25) were assessed via RT-qPCR. An increased ratio of isoform 2 and 3 compared to isoform 1 was determined in approximately 90% of patient samples compared to normal (Figure 3.5).

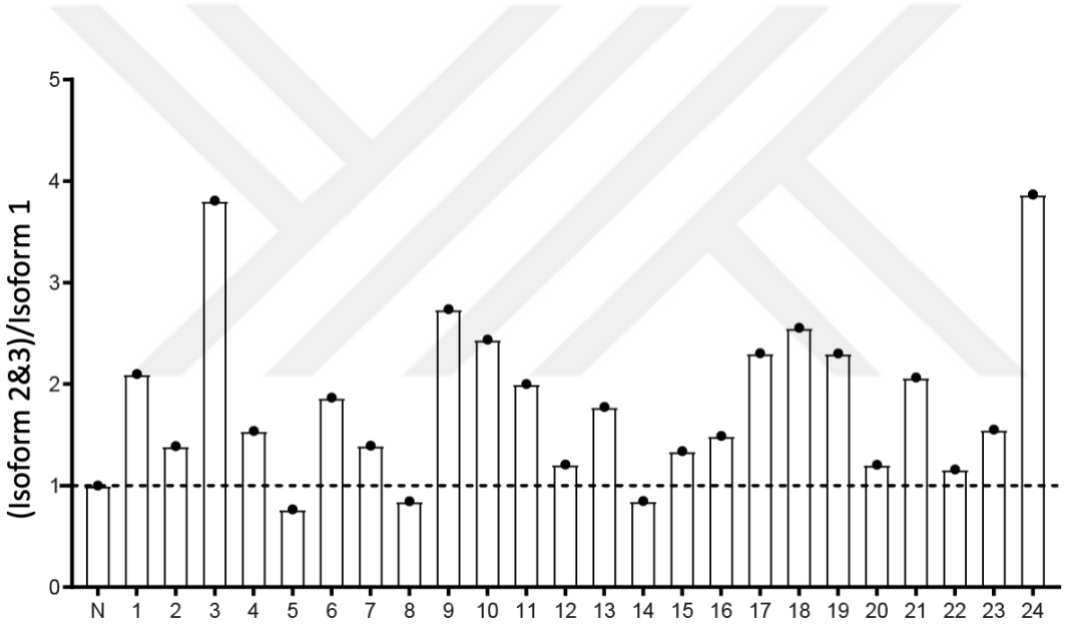

Figure 3.5. Isoform switch in breast cancer patients. The ratio of HNRNPA1 isoforms in a panel of breast cancer patient cDNAs (Origene Breast cDNA array IV). (n=1 due to limited material). The fold change for the isoforms was normalized against the reference gene, RPLP0, and normalized to normal breast tissue RNA (Thermo Fisher Scientific). The ratio was calculated as the expression of isoforms 2 and 3 to that of isoform 1.

3.5 The effects of different 3'UTRs on Protein Expression

Overall, isoform 1 is the most dominant in normal breast tissue, whereas other 3'end isoforms are also expressed. However, the ratio of these isoforms (total or other

isoforms/isoform 1) drastically shifts in breast cancer patients. After confirming the existence of these isoforms, the reason or benefit of this isoform switch needed to be clarified.

3.5.1 Coding Potentials of Isoforms

Surprisingly, isoform 1 is indicated as a non-coding variant and an NMD transcript (NR_135167). However, all isoforms share the same CDS so the Coding Potential of all three isoforms was calculated. Coding potential results show that the coding potential (~6.07) of isoform 1 has the highest value far from the coding potential (~ -0.95) of XIST, which is non-coding RNA (Table 3.1).

Table 3.1. Coding potential values of HNRNPA1 variants. XIST is a well-known non-coding RNA.

RNA	Coding Score
Isoform 1	6.06596
Isoform 2	6.04313
Isoform 3	5.91468
XIST	-0.94523

Hence, it was thought that isoform 1 may be mistakenly identified as a non-coding transcript but recorded the NMD isoform definition for this isoform.

3.5.2 Ectopic expression of HNRNPA1 Isoforms

To experimentally test the coding potential, all HNRNPA1 isoforms (isoform 1-3) were cloned into pcDNA 3.1 (-) as a fusion with hemagglutinin (HA tag) along with their 3'UTRs (Figure 3.6, A) and expressed in MCF7 and MDA-MB-231 cell lines for 48 hours (Figure 3.4, B). Western blot analysis revealed that isoform 1 is not a non-coding RNA and was translated into protein, yet isoform 1-3'UTR transfected MCF7 and MDA-MB-231 cells had lower protein levels than the other two isoforms (Figure 3.6, B).

A.

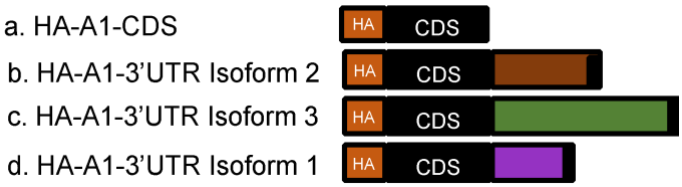

B.

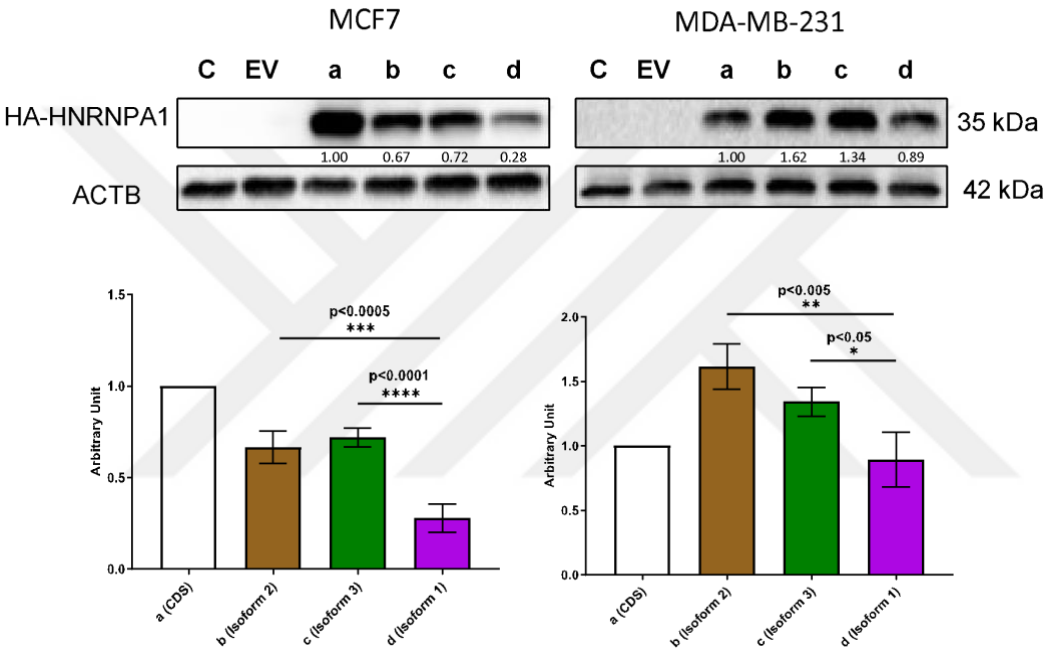

Figure 3.6. Ectopic expression of HNRNPA1 isoforms. A. Schematic representation of HA-tagged HNRNPA1 CDS with/out isoform-3'UTR sequences cloned into pcDNA3.1 (-) expression vector. B. Western blotting results indicating the ectopic expression level of HNRNPA1 in MCF7 and MDA-MB-231cell lines and densitometric analysis of the western bands are given below the blots. The construct with 3'UTR of isoform 1 had a 58% low protein level in MCF7 cells ($p<0.0005$, one-way ANOVA, n=3) and a 45% low protein level in MDA-MB-231 cells ($p<0.005$, one-way ANOVA, n=3) level compared to isoform 2. ACTB antibody was used as a protein loading control. EV: empty vector.

3.5.3 Effects of HNRNPA1 3'UTRs on Luciferase Activity

To further test whether the 3'UTR of isoform 1 has a negative effect on protein

levels, 3'UTRs of isoform 1, 2, and 3 were cloned into the firefly luciferase vector and transfected into MCF7 and MDA-MB-231 cells. The isoform 2 and 3-3'UTR constructs had a significantly higher luciferase activity than the isoform 1-3'UTR construct (Figure 3.7, A, and B). These results suggested that isoform 1 transcript compared with other isoforms may correlate with lower protein levels. (Figure 3.7, B).

A.

B.

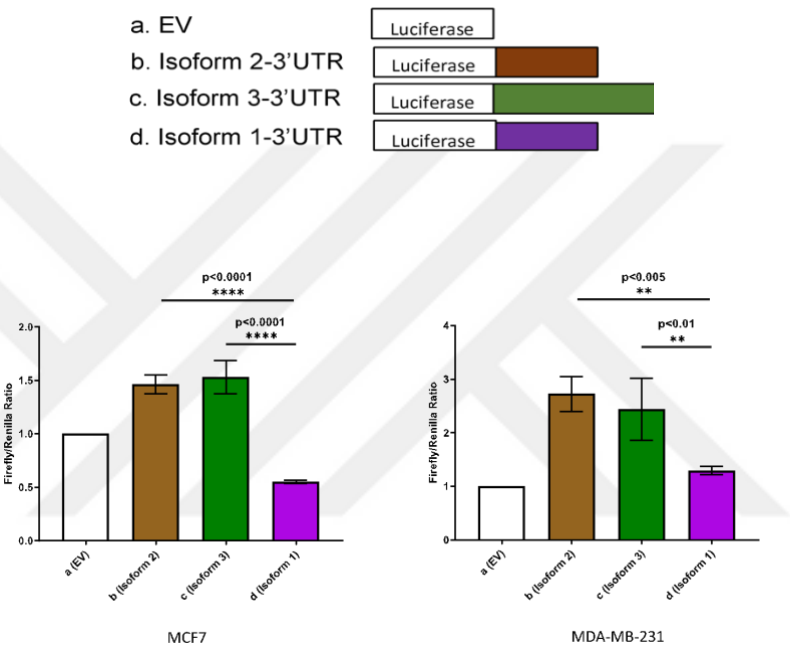

Figure 3.7. Dual-luciferase reporter assay: Effects of isoform 1, 2, and 3-3'UTRs on luciferase activity in MCF7 (A) and MDA-MB-231 (B). 3'UTR vectors or pMIR-empty vectors were co-transfected with phRL-TK. Dual-luciferase assay was performed 24 hours after transfection. Firefly/Renilla luciferase read-outs from the constructs were normalized to that of empty pMIR, which was set to 1. The construct with 3'UTR of isoform 1 had 60% low luciferase activity compared to isoform 2 ($p<0.0001$, one-way ANOVA, n=3) in MCF7 cells and MDA-MB-231 cells ($p<0.005$, one-way ANOVA, n=3).

The question was, "Why is isoform 1 translated less?". Several factors affect the translation of an mRNA. Alternative binding of miRNAs and RNA-binding proteins (RBPs) could impact protein levels because the only difference among the HNRNPA1 isoforms is the 3'UTRs.

3.6 Effects of miRNA Binding Sites on Luciferase Activity

Question is whether isoform 1 mRNA is regulated by miRNAs. TargetScan tool was used for determination of miRNA binding sites on 3'UTR of isoform 1 (Figure 3.8, A). miR-24-3p seed sequence and miR-34-5p seed sequences were individually deleted on 3'UTR of isoform 1 via SDM-PCR. Luciferase activities of deleted constructs were measured in MDA-MB-231 cells. Luciferase results showed that these miRNAs did not affect the translation of isoform 1 (Figure 3.8, B).

A.

B.

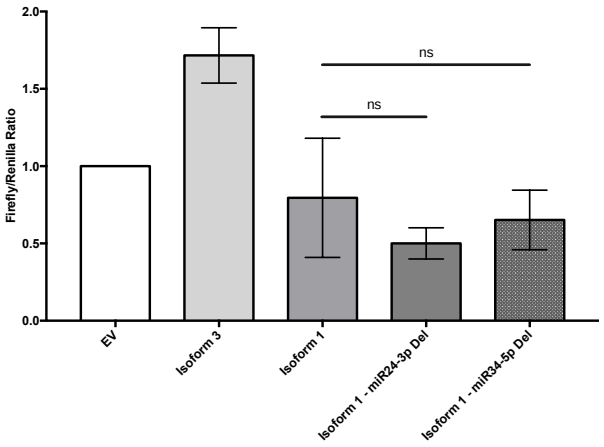

Figure 3.8. Effects of miRNA binding sites on luciferase activity A. miRNA binding sites on isoform 1-3'UTR were determined by TargetScan. B. Dual-luciferase reporter assay: Effects of deletion of miR-24-3p and miR-34-5p seed sequence on isoform 1-3'UTR on luciferase activity in MDA-MB-231 cells.

3.7 Effects of RBP Binding Sites on Luciferase Activity

Next, whether RBPs regulate the 3'UTR of isoform 1 was tested. First, 3'UTR of isoform 1 was divided into 2 parts (A and B) and then part A was further sub-cloned into 2 parts (A1 and A2) (Figure 3.9, A). These 3'UTR parts of isoform 1 were cloned into luciferase vector to figure out which part of the 3'UTR has a negative effect on translation. Part A of isoform 1-3'UTR almost diminished the luciferase activity while 2. half of isoform 1-3'UTR had the same luciferase as isoform 1-full 3'UTR (Figure 3.9, A). Thus, part A of isoform 1-3'UTR was focused on and divided into 2 parts (A1 and A2) (Figure 3.9, A). Both part A1 and A2 had recovered luciferase activity as empty vectors (EV). This result showed that part A of isoform 1-3'UTR needed to be focused on. RBPmap webserver (Paz, Kosti, Ares, Cline, & Mandel-Gutfreund, 2014) and RPBDB database (Cook, Kazan, Zuberi, Morris, & Hughes, 2011b) were used to detect RNA-binding proteins (RBPs) targeting the part A of isoform 1-3'UTR and RBPs were shown on the part A of isoform 1-3'UTR (Figure 3.9, B). These sites were deleted with site-directed mutagenesis (one site and two sites were deleted). None of these modifications caused any significant increase in luciferase activity of isoform 1-3'UTR (Figure 3.9, B).

A.

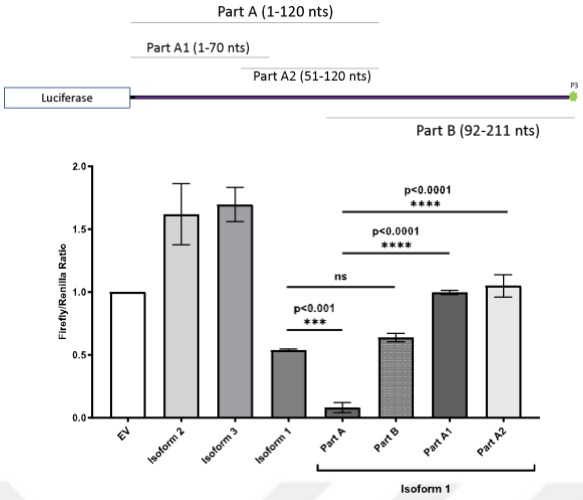

B.

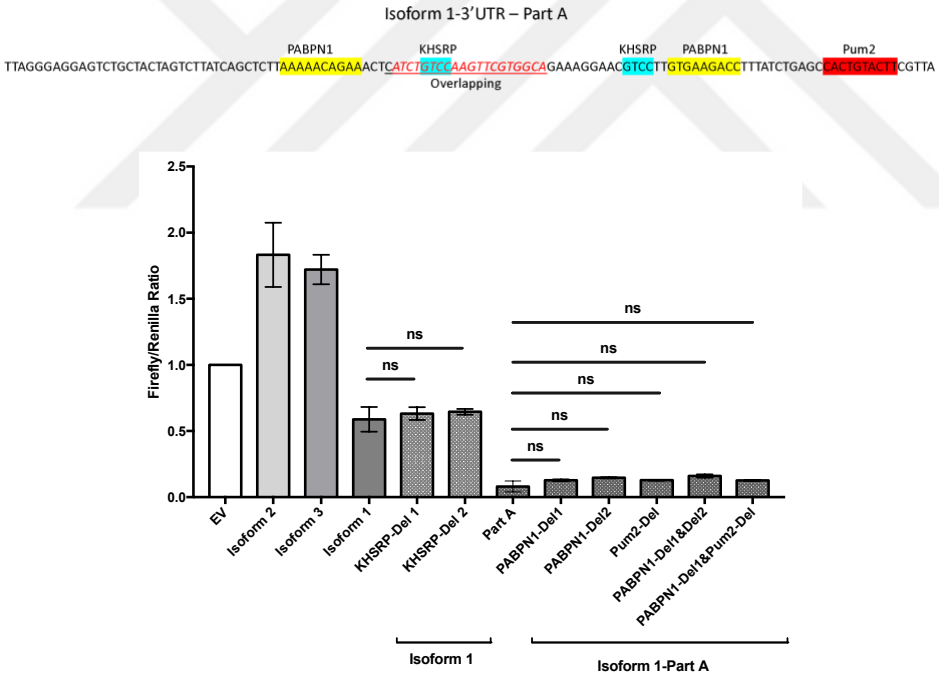

Figure 3.9. Effect of RBP binding site on luciferase activity. A. Isoform 1-3'UTR fragments that were cloned downstream of the luciferase gene. Dual luciferase reporter assay: Effects of isoform 1-3'UTR fragments on luciferase activity in MCF7. A. Isoform 1-3'UTR fragments that were cloned downstream of the luciferase gene. B. Dual-luciferase reporter assay: Effects of deletion of RBP sites on isoform 1-3'UTR and its fragments on luciferase activity in MCF7. (ns, one-way ANOVA, n=3).

3.8 Stability of HNRNPA1 3'UTR Isoforms

To understand the reason behind low protein synthesis, half-lives of mRNA isoforms were then focused on. mRNA levels of HNRNPA1 isoforms were assessed via RT-qPCR following actinomycin D (ActD) (an inhibitor of transcription (Sobell, 1985)) treatment for 12 h to prevent new transcription. The results indicated that isoform 1 is the least stable isoform like *MYC* mRNA, a well-known control used in ActD treatments due to its short half-life. the other isoforms were still stable after 12 h in both MCF7 and MDA-MB-231 cells (Figure 3.10, A). Furthermore, mRNA abundances of HNRNPA1 isoforms were determined following ActD and/or cycloheximide (an inhibitor of ribosomal elongation (Schneider-poetsch et al., 2010)) treatment of MCF7 and MDA-MB-231 for 3 h to prevent new transcription and/or translation. Interestingly, cycloheximide treatment for only 3 h had a more than 3.5 fold and 7.5 fold recovery in MCF7 and MDA-MB-231 cells respectively, only for isoform 1 but not for other isoforms (Figure 3.10, B). These results indicate that isoform 1 is degraded through its translation as cycloheximide inhibits mRNA decay (Beelman & Parker, 1994). Hence it is possible that isoform 1 is regulated through NMD despite lacking a premature stop codon.

A.

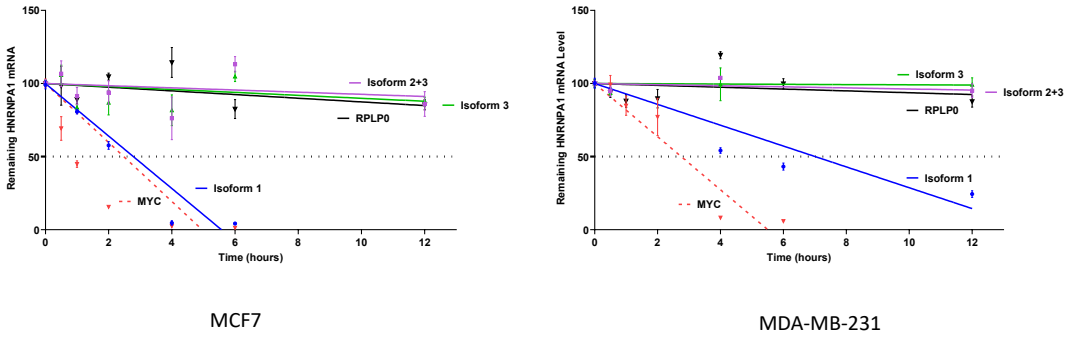

MCF7 MDA-MB-231

B.

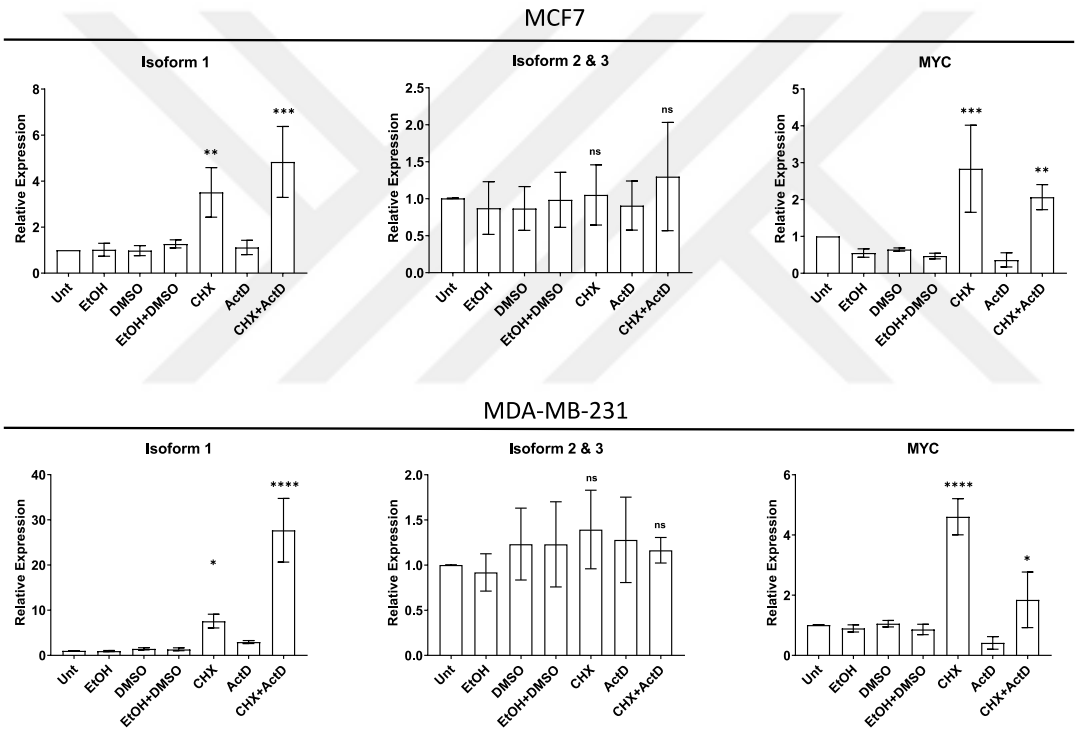

Figure 3.10. Stabilities of isoforms. The remaining HNRNPA1 transcripts were detected by RT-qPCR. *RPLP0* as a stable mRNA and MYC as an unstable mRNA were used as controls. A. Cells were treated with 10 µg/mL actinomycin D (ActD) for 12 hours to prevent transcription. (This experiment was conducted by my lab-mate İbrahim Özgül). B. Cells were treated with 2 µg/mL ActD and/or cycloheximide (CHX, 100 µg/mL) for 3 hours to prevent transcription and translation. EtOH (Ethanol) and DMSO are carrier controls. Cells were collected and RNA was isolated for RT-qPCR (*p<0.05, **p<0.01, ***p<0.001, ****p<0.0001, ns: not significant, n=3 independent experiments, student's t-test).

3.9 Effect of HNRNPA1 3'UTR Isoforms on Protein Localization

Different 3'UTR lengths and sequences provide platforms for binding and interaction of different RBPs. Moreover, these 3'UTRs may affect its protein to interacting protein partners, which affects the protein function and protein localization. The long 3'UTR of *BRIC* mRNA recruits the specific factors which determine BRIC protein functions besides its 3'UTR-independent functions (Lee & Mayr, 2019). Another example is CD47 protein localization. The long 3'UTR of CD47 provides binding sites for the RNA-binding proteins HuR and SET to the site of translation, which makes SET to interact with the newly synthesized cytoplasmic domains of CD47 and causes CD47 protein to be translocated to the cell membrane through activated RAC1 (Berkovits & Mayr, 2015). To reveal whether 3'UTRs of HNRNPA1 isoforms affect the localization of HNRNPA1 protein, immunocytochemistry (ICC) technique was used to determine protein localization. HNRNPA1 CDS as a fusion with HA tag and their different 3'UTRs were previously cloned into pcDNA 3.1 (-) (Figure 3.6, A) and these constructs were used to transfect MCF7 cells for 48 h. First, transfected MCF7 cells were incubated with rabbit anti-HA-tag monoclonal antibody and then stained with the Alexa fluor® 488-conjugated goat polyclonal anti-rabbit IgG secondary antibody. After that, cells were counterstained with a fluoroshield mounting medium with DAPI, which is a well-known nuclear staining dye. ICC images revealed that 3'UTRs of HNRNPA1 did not have any role in the localization of HNRNPA1 protein. HNRNPA1 protein was localized to the nuclei of all three constructs transfected into MCF7 cells (Figure 3.11).

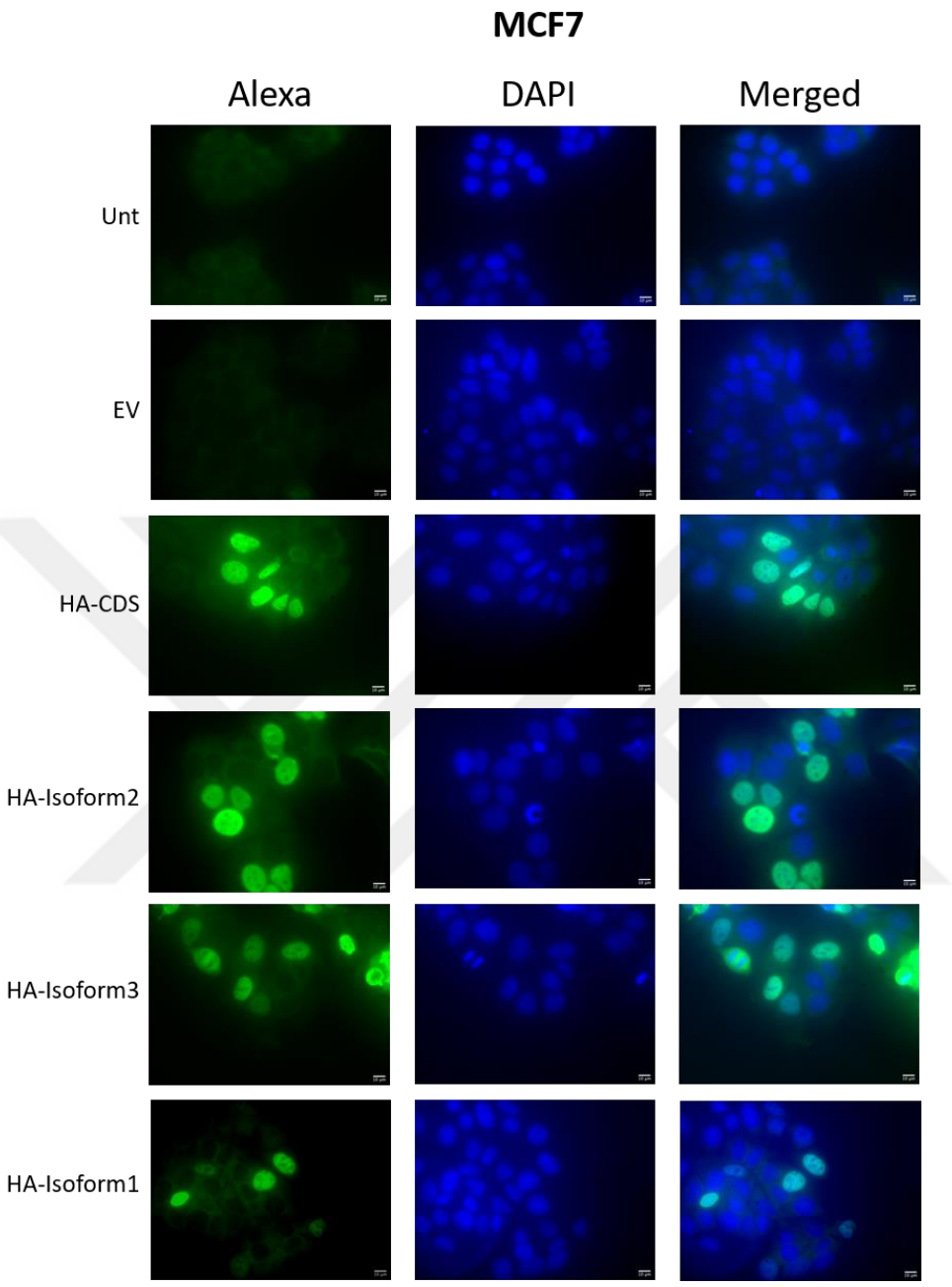

Figure 3.11. Subcellular localization of HNRNPA1 protein translated from isoforms. After 48 hours of transfection, HA-tagged HNRNPA1 translated from isoform 1, isoform 2, and isoform 3 (CDS+3'UTRs) were detected by immunocytochemistry in MCF7 cells. Alexa (HA-HNRNPA1): Green, DAPI: Blue. Scale bars: 10 μm. Unt: Untransfected MCF7 cells, EV: Empty vector (pcDNA 3.1 (-)) transfected MCF7 cells.

3.10 Effect of HNRNPA1 Protein Level on Patient Survival

These results indicated that isoform 1 is a less stable and rapidly degraded mRNA. It is thought that the dominantly expressed isoform 1 better modulates the protein level of *HNRNPA1* in cells in normal tissue. However, the unstable isoform 1 is expressed at a low level in breast cancers while isoform 2 is overexpressed. Thus, the HNRNPA1 isoform expression pattern is switched in breast cancer cells compared to normal tissue. This switch would indicate upregulation of HNRNPA1 protein. Therefore, relation between patient survival data and HNRPA1 protein levels is investigated. High and low HNRNPA1 protein expressions are indeed correlated with the poor prognosis of patients with hazard ratios of 2.8 ($p=0.019$ and 50% FDR) (Figure 3.12, A) (Lánczky & Győrffy, 2021). Hence, high HNRNPA1 protein levels in these patients correlated with decreased survival, strengthening the significance of the oncogenic role of *HNRNPA1*. However, it is needed to emphasize the importance of isoform level gene expression in such analyses. For example, the overall HNRNPA1 mRNA level detected (214280_x_at) does not correlate with relapse-free survival; however, isoform-specific re-analysis of the same dataset (GSE31519) with a different probe set (200016_x_at) targeting the highly translated isoform 2 and 3 indicates a correlation with relapse-free survival of patients (Figure 3.12, B and C).

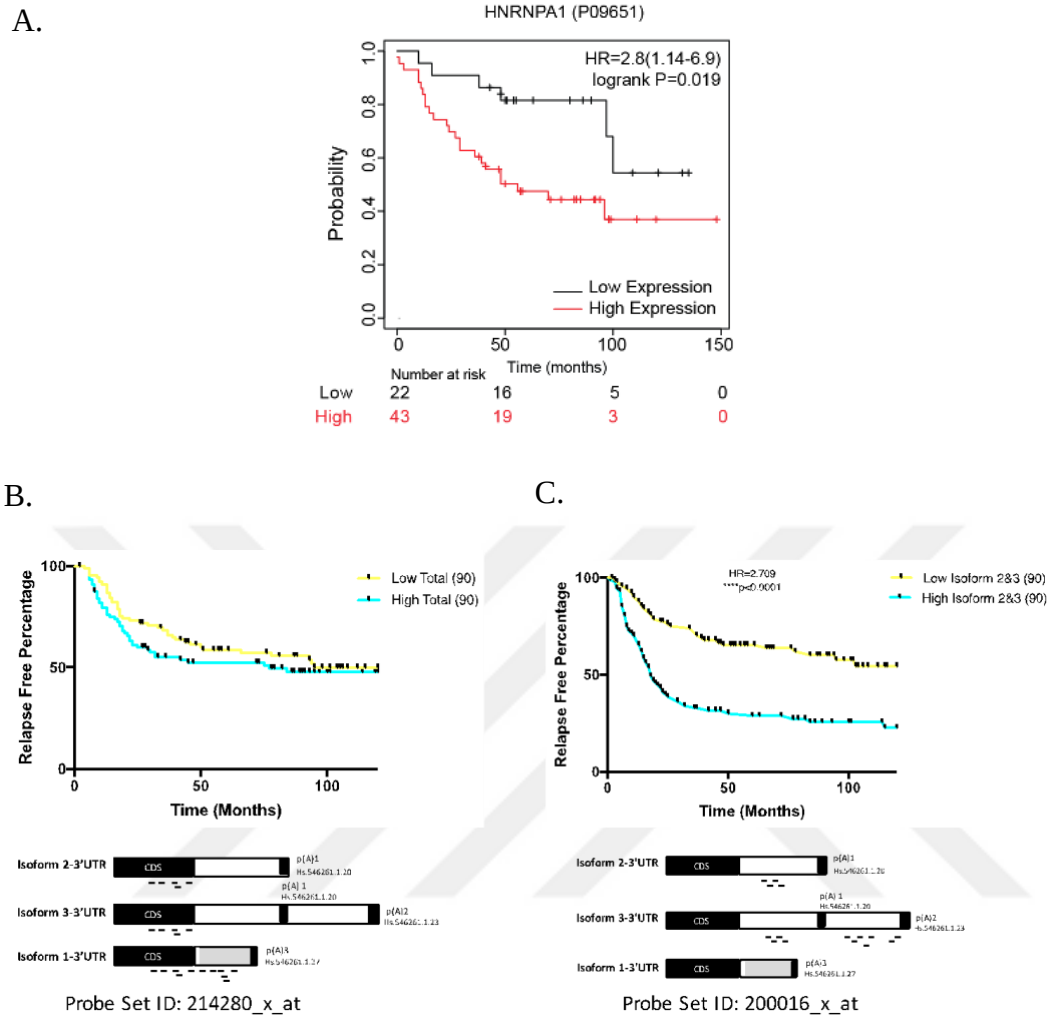

Figure 3.12. Patient survival curve upon HNRNPA1 expression. A. Kaplan-Meier plots for breast cancer patients with high (red) and low (black) HNRNPA1 protein (p=0.019, HR=2.8, and FDR=50%) retrieved from KM plotter. (Available from https://kmplot.com/). B and C. Relapse free survival rates of TNBC patients with high (highest 25%) (blue line) or low (lowest 25%) (yellow line) B. Total isoform expression of HNRNPA1 for 120 months (10 years). Total HNRNPA1 expression does not have any effect on Relapse Free Survival in the GSE31519 dataset (probe set ID 214280_x_at). C. Expression level of HNRNPA1 isoform 2&3 for a period of 120 months (10 years). Hazard ratios (95% CI) were 2.709 (p<0.0001) survival plot based on HNRNPA1 expression in the tumor tissue using data from the GSE31519 dataset with probe set ID 200016_x_at.

3.11 Phenotypic Effects of *HNRNPA1* on MDA-MB-231 Cells

After determining the negative correlation between HNRNPA1 protein levels and patient survival, it is vital to experimentally determine the phenotypic effects of *HNRNPA1* expression in MDA-MB-231 cells.

3.12 Silencing of *HNRNPA1* in MDA-MB-231 Cells

To reveal the role of *HNRNPA1* gene on phenotypic characteristics of cells, stably *HNRNPA1* silenced cells were generated. For this purpose, MDA-MB-231 cells seeded in 6-well plates were transfected with pSuper A1shRNA (A1sh 1 and A1sh 2) or NTshRNA (NT) and transfected cells were selected and maintained with G418. Monoclonal cells were expanded. *HNRNPA1* silencing was detected by western blotting in the A1sh 1 and A1sh 2 monoclonal population compared to the NT as a control (Figure 3.13).

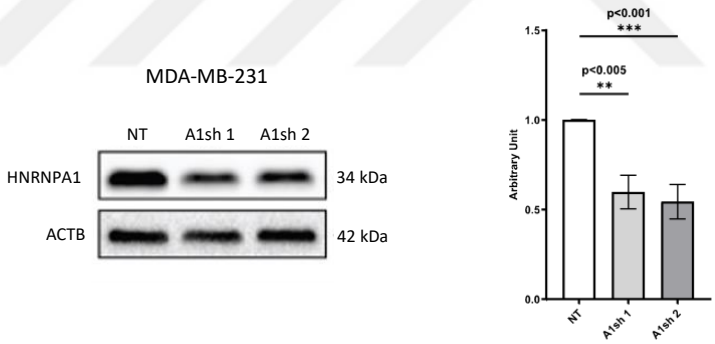

Figure 3.13. Silencing of HNRNPA1 protein levels and function in breast cancers. Two monoclonal populations (A1sh 1 and A1sh 2) are shown with decreased HNRNPA1 protein levels, and non-targeting (NT) shRNA transfected cell was used as a control. Same blots were hybridized with ACTB antibody to test sample loading. The image is representative of 3 independent experiments. Graphs show densitometric quantification of bands (**p<0.01, ***p<0.001; n=3, one-way ANOVA, Tukey's HSD).

3.13 Role of *HNRNPA1* in Clonogenicity and Motility of MDA-MB-231

After silencing of *HNRNPA1* in MDA-MB-231 cells was confirmed by western blotting, 1×10^3 MDA-MB-231/NT and A1sh (A1sh 1 and A1sh 2) cells were seeded as triplicates on 6-well plates and were cultured for 14 days to assess the colony formation capacity of the cells. Cell colonies were stained with crystal violet and photographed. The visible colonies were counted via the count and Plot HIstograms of Colony Size (countPHICS) (Brzozowska et al., 2019). *HNRNPA1* silencing significantly decreased the number of colonies formed by MDA-MB-231 cells (***$p<0.001$) (Figure 3.14, A).

The motility of MDA-MB-231 cells was assessed via wound healing assay after the *HNRNPA1* knockdown. MDA-MB-231/NTsh (NT), A1sh 1 and A1sh 2 cells were grown on a 6-well plate to 100% confluency. Confluent cell layers were wounded by a pipette tip. Cells were monitored for up to 2 days for wound closure. Images were captured and wound width measurements were measured. ImageJ software measured the wound closure areas (Schneider et al., 2012). Wound closure results showed the silencing of *HNRNPA1* decreased the motility of MDA-MB-231 cells on day 1 and day 2 (****$p<0.0001$ and ****$p<0.0001$) compared to NT cells (Figure 3.14, B).

A.

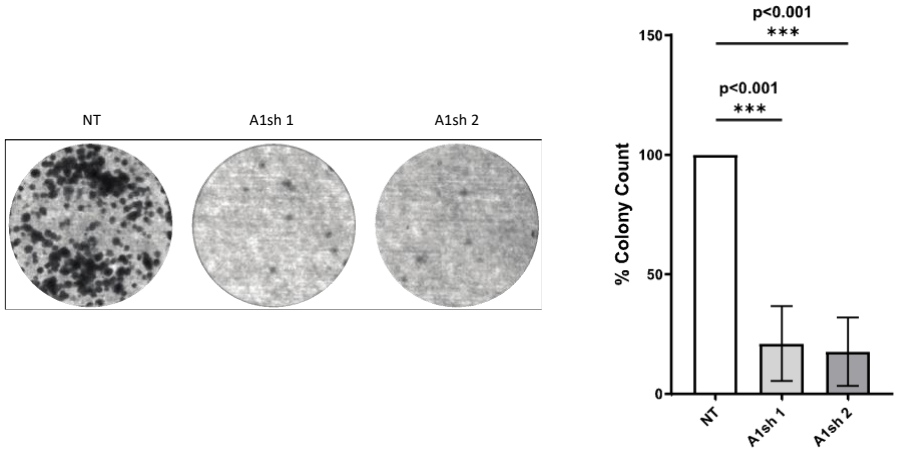

B.

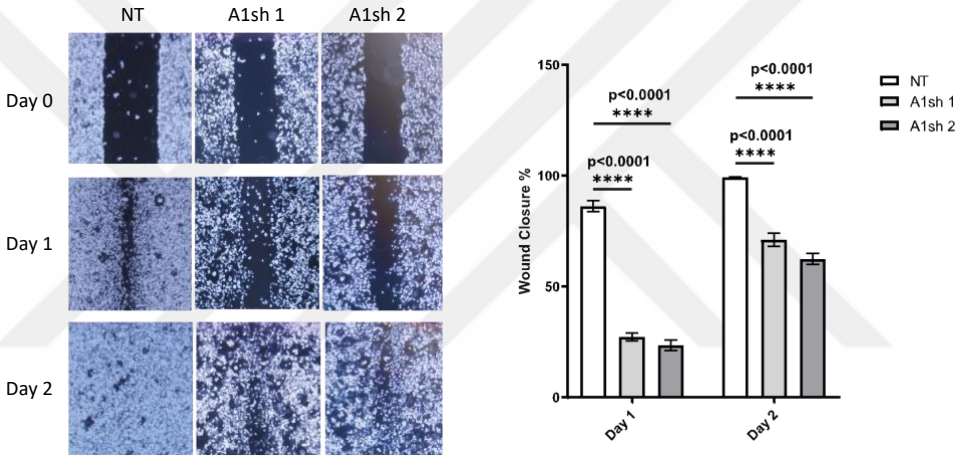

Figure 3.14. HNRNPA1 protein levels and function in breast cancers. A. Colony formation of NTsh and HNRNPA1sh cells in 14 days of seeding in MDA-MB-231 cells. Colonies were counted and analyzed using CountPHICS software (***p<0.001; n=3 independent experiments, one-way ANOVA, Tukey's HSD). B. Effect of *HNRNPA1* silencing on wound healing property of cells. A pipette tip scratched cell layers in each well. Closure of wounds in each well was examined on days 0, 1, and 2. (****p<0.0001 and ****p<0.0001; n=3, one-way ANOVA, Tukey's HSD).

3.14 Role of *HNRNPA1* in Proliferation, Migration and Invasion of MDA-MB-231

The effect of *HNRNPA1* silencing on cell proliferation was investigated via MTT cell proliferation assay. In this assay, stably (NT and A1sh) transfected MDA-MB-231 cells were cultured on 96-well plates for 3 days. MTT cell proliferation assay was performed on day 0 and day 3. Absorbance values were measured at 570 nm wavelength with a Multiskan GO Microplate Spectrophotometer (Thermo Fisher). MTT cell proliferation assay results showed that *HNRNPA1* silenced cells proliferated significantly slower than the NT transfected ones at day 3 (*$p<0.05$) (Figure 3.15, A)

Migration and invasion assays were performed using a Transwell system without and with matrigel respectively. NT and A1sh MDA-MB-231 cells in 100 µl of DMEM supplemented with 1% FBS were seeded in the transwell insert and complete medium (DMEM supplemented with 10% FBS) was added to the wells of the 24-well plate well. Cells were incubated at 37°C for 15 hours in migration and 18 hours for invasion assay. The cells on the apical surface of the transwell's membrane were removed and the membrane was stained with Giemsa dye. Then, the membrane was observed and photographed under the microscope. The cells passed through/in the membrane were counted. Both assay results indicated that *HNRNPA1* silenced MDA-MB-231 cells showed significantly less migratory and invasive characteristics compared to NT transfected cells (****$p<0.0001$ and ***$p<0.001$, respectively) (Figure 3.15, B).

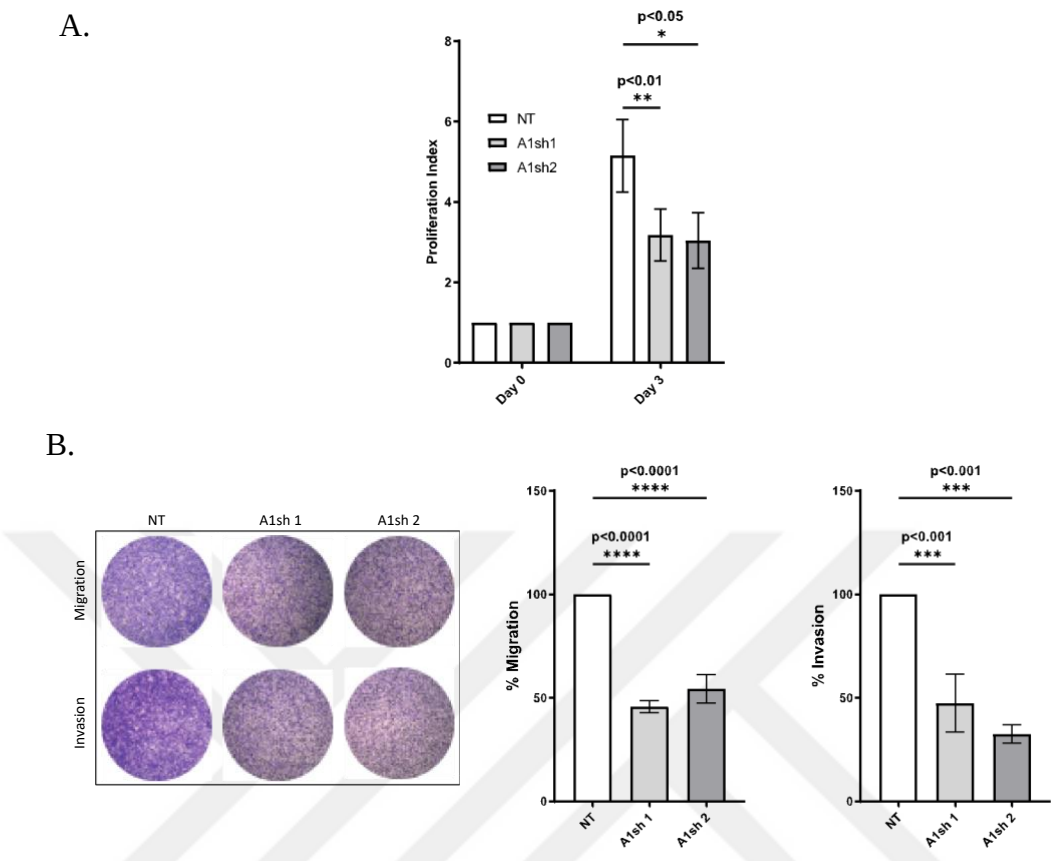

Figure 3.15. *HNRNPA1* functions in breast cancers. A. Effect of *HNRNPA1* silencing on proliferation rates detected by MTT (*p<0.05; n=3 independent experiments, one-way ANOVA, Tukey's HSD). B. Effect of *HNRNPA1* knockdown on cell migration and invasion in MDA-MB-231 cells. Cells passed through the transwell and/or Matrigel were counted (****p<0.0001 and ***p<0.001; n=3 independent experiments, one-way ANOVA, Tukey's HSD).

3.15 Effect of *HNRNPA1* Silencing on miRNAs in MDA-MB-231 Cells

The results of phenotypic experiments showed that *HNRNPA1* plays a role in wound healing, motility, proliferation, migration and invasion features of MDA-MB-231. Also, HNRNPA1 is a member of RNA-binding protein family and has a major role in mRNA biogenesis (Dreyfuss, 1993; Pinol-Roma et al., 1988). To investigate the effect of *HNRNPA1* on phenotypic properties of MDA-MB-231 through the miRNA biogenesis, miRNA levels in NT and A1sh MDA-MB-231 cells were determined via NanoString nCounter miRNA panel. The expression levels of 34 out of 798 miRNAs in the NanoString panel changed (> 1.5-fold or < 0.67-fold) upon silencing of

HNRNPA1 in MDA-MB231 cells (Figure 3.16, A). Among these 34 miRNAs, whose expressions were altered upon the silencing of *HNRNPA1*, 32 miRNAs were downregulated, and 2 of them were upregulated (Figure 3.16, A and B). 19 of these miRNAs were intergenic, 12 were intronic and 2 were exonic, and 1 miRNA was in the 3'UTR region of a host gene (Figure 3.16, B).

To determine which cellular pathways are affected by these 34 miRNAs whose expressions were changed by *HNRNPA1* silencing in MDA-MB-231 cells, DIANA mirPath v.3 pathway analyzer tool (available at http://snf-515788.vm.okeanos.grnet.gr/) was used. Pathways in cancer, proteoglycans in cancer, focal adhesion, regulation of actin cytoskeleton, endocytosis, PI3K-Akt, Ras, MAPK1, Rap and cAMP signaling pathways (Figure 3.16, C) were enriched.

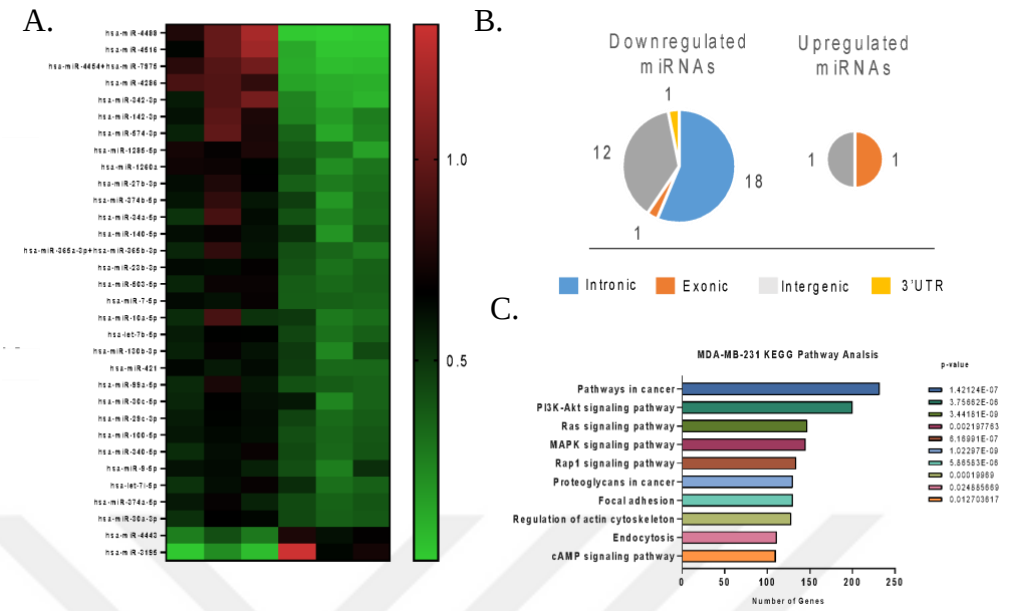

Figure 3.16. Effect of *HNRNPA1* silencing on miRNAs. (A) RNA isolated from *HNRNPA1*-silenced, and control cells were detected by the NanoString miRNA panel. Heatmap shows miRNA expression fold changes (< 0.6 and > 1.5) in HNRNPA1sh (A1sh) MDA-MB-231 cells. (B) Pie charts visualize the proportion of differentially expressed miRNAs grouped according to their genomic features in HNRNPA1sh (A1sh) MDA-MB-231 cells (blue color for the intronic miRNAs, orange for exonic miRNAs, gray for intergenic, and yellow for miRNAs located in 3'UTRs of host genes). (C) Biological pathways affected by miRNAs whose expression levels were changed upon long-term *HNRNPA1* silencing in MDA-MB-231 were determined by DIANA-mirPath.

3.16 Regulation of miR-27b Expression by HNRNPA1 in Breast Cancer

miR-27b-3p was one of the interesting miRNAs with decreased expression by *HNRNPA1* silencing in MDA-MB-231 cells (Figure 3.16, A). Results of analysis of 99 TNBC patients' data, in vitro and in vivo experiments indicate that miR-27b-3p favors TNBC progression and metastasis by inhibiting peroxisome proliferator-activated receptor gamma (PPARG); thus, miR-27b-3p could be a potential prognostic marker of TNBC (Shen et al., 2020). In addition, the inhibition of miR-27b by stable expression of anti-miR-27b construct shows reduced cell proliferative, anchorage-independent growth, migrative, and invasive characteristics of highly invasive and metastatic breast cancer cell lines (MDA-MB-231) and decreases tumor

growth and metastases in vivo (Jin et al., 2013). Similarly, in another study, over-expression of the miR-23b-miR-27b-miR-24 cluster in poorly metastatic 4TO7 cells promotes metastatic lung lesions (Jin et al., 2013). Likewise, another study indicates that the inhibition of miR-27b by antagomirs in MDA-MB-231 decreases the cell invasion by upregulating ST14 (suppressor of tumorigenicity 14) whereas miR-27b overexpression promotes invasiveness of ZR-75-1 (moderately invasive breast cancer cells) (Wang, Rathinam, Walch, & Alahari, 2009). Those studies show that miR-27b has an oncogenic function in breast cancer.

3.17 Expression Level of miR-27b-3p in *HNRNPA1* Silenced MDA-MB-231 Cells

Nanostring results indicated that the mature miR-27b-3p level was decreased to 0.46 fold in *HNRNPA1*-silenced cells compared to control (Figure 3.17, A) (read counts dropped from 654.17 to 296.5 after silencing of *HNRNPA1*). To confirm the NanoString results, TaqMan miRNA PCR was applied to A1sh and NT MDA-MB-231 clones. TaqMan miRNA PCR revealed significant decrease in miRNA-27b-3p levels in A1sh MDA-MB-231 cells (*$p<0.05$, ****$p<0.0001$compared to NT MDA-MB-231 one (Figure 3.13, B).

A. B.

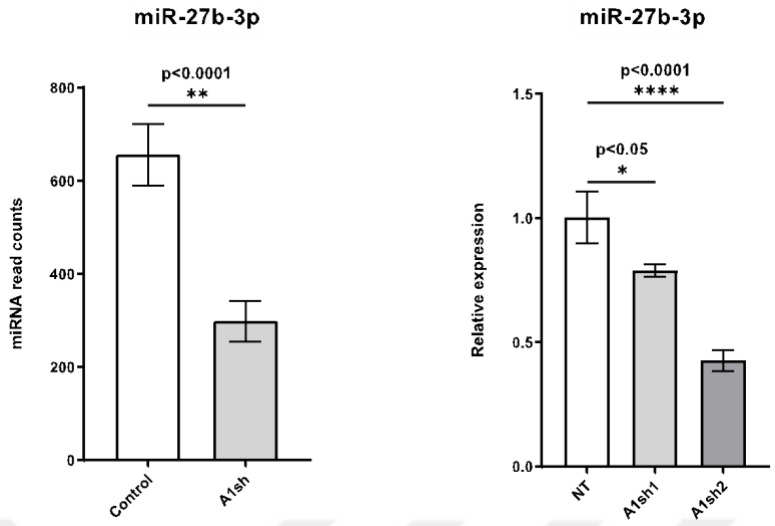

Figure 3.17. Mature miR-27b-3p levels in *HNRNPA1* silenced cells. A. miR-27b-3p count reads were decreased in *HNRNPA1* silenced MDA-MB-231 cells on the NanoString miRNA panel. B. Mature miRNA levels in *HNRNPA1* silenced MDA-MB-231 cells were detected by TaqMan miRNA PCR (*p<0.05, **p<0.01, ****p<0.0001; n=3 biological replicates, one-way ANOVA, Tukey's HSD).

3.18 Effect of *HNRNPA1* Silencing on pri-miR-27b and Its Host Gene (C9ORF3)

Human miR-27b is an intronic miRNA, and its gene is located in intron 14 of the C9ORF3 gene (Figure 3.18 C). To decipher at which stage (transcription or maturation) HNRNPA1 protein affects miR-27b-3p expression level, pri-miR-27b level was determined by RT-qPCR using primers targeting the flanking regions of miR-27b locus (Figure 3.18, C). RT-qPCR results revealed that *HNRNPA1* knockdown decreased the pri-miR-27b (primary miRNA) level (Figure 3.18, A) (Figure 3.17). Therefore, HNRNPA1 affected the level of miR-27b-3p at transcription but not during the maturation steps of miRNAs.

As *MIR27b* gene resides in *C9ORF3*, the next question was whether MIR27b and *C9ORF3* gene expressions are co-regulated by HNRNPA1 protein. For this purpose, expressions of *C9ORF3* gene at RNA level were tested by RT-qPCR by using primers targeting the exons 2 and 3, respectively (Figure 3.18, C). RT-qPCR results

indicated that *HNRNPA1* knockdown lowered C9ORF3 mRNA expression level (Figure 3.18, B).

In agreement with these results, *HNRNPA1* knockout via CRISPR/Cas9 in MDA-MB-231 cells gave similar results (Appendix A, Table 4.11). *MIR27b* and *C9ORF3* genes are possibly transcriptionally co-regulated by HNRNPA1.

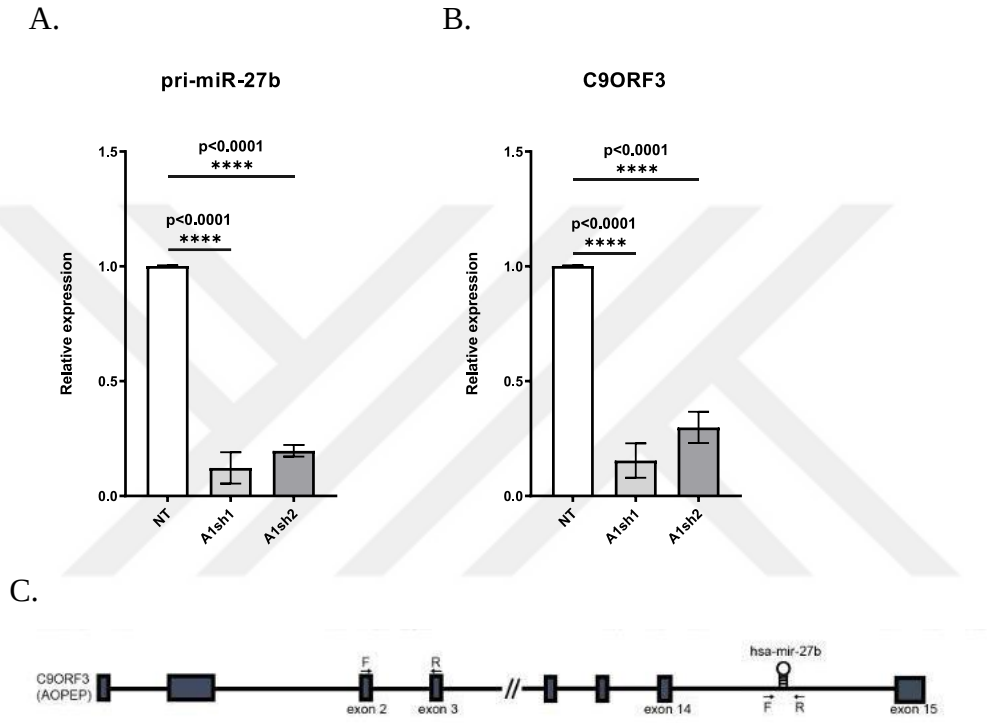

Figure 3.18. pri-miR-27b and C9ORF3 levels in *HNRNPA1* silenced cells. A. pri-miR-27b and B. Host gene *C9ORF3* expression levels were quantified by RT-qPCR (****p<0.0001; n=3 biological replicates, one-way ANOVA, Tukey's HSD). C. Gene structure of host gene, miR-27b and primer positions are shown below the graphs. F: Forward primer and R: Reverse Primer.

3.19 Effect of miR-27b Level on Patient Survival

miR-27b-3p expression level was upregulated by HNRNPA1 protein in MDA-MB-231 which is triple-negative breast cancer cell line, so the relation between miR-27b level and ER-positive and negative patient survival were investigated. High miR-27

expression is correlated with the poor prognosis of ER-negative patients with hazard ratios of 1.7 (p=0.012 and 50% FDR) (Figure 3.19, A), but not with that of ER-positive patients (Figure 3.19, B) (Lánczky & Győrffy, 2021). These results could suggest that correlation between high *HNRNPA1* expression and the poor prognosis of ER-negative patients may be regulated in one way via the effect of HNRNPA1 on the miR-27b level.

A. B.

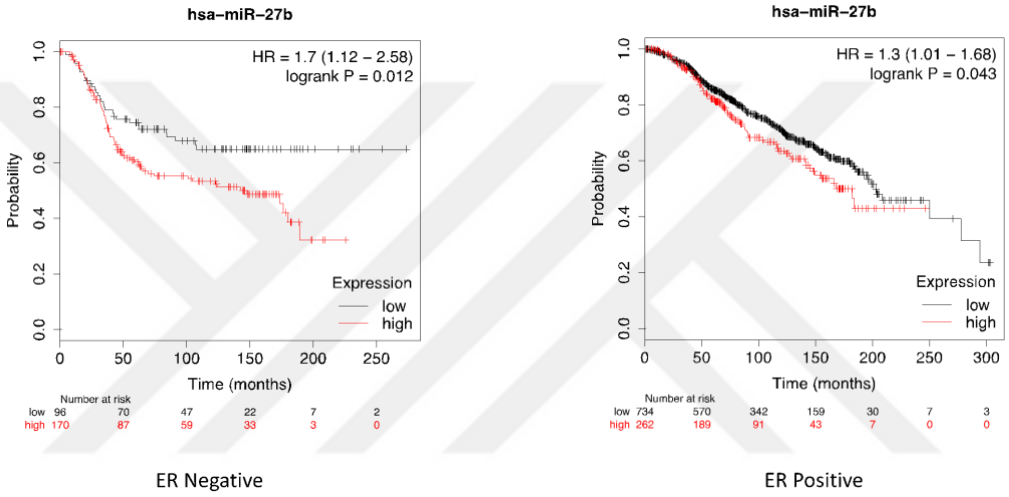

Figure 3.19. Kaplan-Meier survival curve upon miR-27b expression. A. Kaplan-Meier plots for ER-negative breast cancer patients with high (red) and low (black) miR-27b level (p=0.012, HR=1.7, and FDR over 50%), retrieved from KM plotter. B. Kaplan-Meier plots for ER-positive breast cancer patients with high (red) and low (black) miR-27b levels. Data retrieved from KM plotter. (Available from https://kmplot.com/).

Overall, *HNRNPA1* is described as a potent oncogene candidate in triple negative breast cancers. Given its oncogenic roles, it was not clear how *HNRNPA1* expression is deregulated in breast cancers. It is shown for the first time that an isoform switch leads to oncogenic activation of *HNRNPA1* in breast cancers.

CHAPTER 4

CONCLUSION

There is mounting evidence suggesting that alternative polyadenylation (APA) and alternative splicing are involved in cancer progression in addition to well-known mutations. APA and alternative splicing events can affect the protein expression, function and profile via changing the 3'UTR sequence and length or coding sequence of mRNA. These events may not have any influence on a gene expression but may lead to a change in the isoform expression profile of the gene through switching one isoform to another one of the same genes. Thus, understanding isoform switches could put light on the unknown regulation mechanisms of cancer-related genes and open new doors for diagnostic and therapeutic approaches.

Analysis of the GTEx database for normal tissue expression (Carithers & Moore, 2015) showed that many different mRNA isoforms of the *HNRNPA1* gene exist due to the alternative splicing and/or APA. When the TCGA data were analyzed, these isoforms existed, but the expression pattern of these isoforms differs in tumors. isoform 1 is the dominantly expressed isoform in normal tissue, while the expression of isoform 2 is favored in breast cancer. All expressed HNRNPA1 isoforms mainly have different 3'UTRs. The 3'ends of HNRNPA1 isoforms produced as a result of APA were confirmed by 3'RACE PCR and sequencing. Our experimental and *in-silico* approach confirmed an isoform switch for *HNRNPA1* in breast cancers.

To understand the reason why this isoform switch occurs in cancer progression, the effect of these different 3'UTRs on gene expression at protein level was investigated. These isoforms tagged with HA sequence were ectopically expressed in MCF7 and MDA-MB-231 cells and HNRNPA1 protein levels were assessed via western blotting using anti-HA antibody. Furthermore, 3'UTRs of isoforms were cloned upstream of luciferase and the effect of 3'UTRs on luciferase activity was

investigated. Both western blot and luciferase assay showed that isoform 1 was leading to lower protein levels compared to the other two isoforms due to its distinct 3'UTR sequence.

The stabilities of the isoforms were compared in ActD treated MCF7 and MDA-MB-231 via RT-qPCR. It was found that isoform 1 was the least stable one, and its 3'UTR makes the isoform less stable. Also, CHX was used to treat the cells to halt the protein expression. Inhibition of translation by CHX treatment led to the elevated isoform 1 level, suggesting that isoform 1 is degraded by translation. The expression of the *HNRNPA1* gene at the protein level is seen to be regulated via APA, favoring the more stable isoforms (2 and 3) in breast cancer.

The localization of HNRNPA1 protein translated from isoforms with different 3'UTRs in MCF7 cells was determined via ICC technique. ICC images revealed that HNRNPA1 protein was localized to the nuclei of all three constructs transfected into MCF7 cells. However, there is also a possibility that the 3'UTRs of HNRNPA1 may affect the interacting protein partners and the functions of the HNRNPA1. For this purpose, HA-tagged HNRNPA1 proteins translated from isoforms (CDS+3'UTRs) in MCF7 cells should be immunoprecipitated by anti-HA-tag monoclonal antibody and the interacting proteins can be detected by mass-spectrometry.

Survival analysis also revealed the overexpression of HNRNPA1 protein is correlated with poor survival in breast cancer patients. Highly translated isoforms (2 and 3), of which the expressions were only detected by 200016_x_at probes, are also correlated with poor patient survival. Similarly, *in vitro* silencing of *HNRNPA1* had a negative effect on neoplastic phenotypes of MDA-MB-231 cells. Thus, more stable and more translated HNRNPA1 isoforms are present in breast tumors.

HNRNPA1 is an RNA binding protein and has roles in RNA biology. To reveal the mechanism of *HNRNPA1* oncogenic function, the *HNRNPA1* silencing cell model was developed, and upon this silencing, affected miRNAs were determined via NanoString nCounter miRNA panel. The expression of 34 different miRNAs was altered by *HNRNPA1* silencing in MDA-MB-231 cells. Among these miRNAs, miR-

27b-3p was selected to investigate further the effect of *HNRNPA1* silencing in MDA-MB-231 cells. Parallel with NanoString results, TaqMan miRNA PCR showed a significant decrease in miRNA-27b-3p levels in *HNRNPA1* silenced MDA-MB-231 cells.

Overall, this thesis work highlights that isoform switches are part of the cancer transcriptome. This perspective explains how oncogenes can be activated where overall mRNA levels may not change. Therefore, isoform switch discovery in cancer cells is a promising approach for discovering new cancer genes with biological impact. The isoform switch described here for *HNRNPA1* may have further implications for breast cancer and possibly other malignancies

.

REFERENCES

Agarwal, V., Bell, G. W., Nam, J. W., & Bartel, D. P. (2015). Predicting effective microRNA target sites in mammalian mRNAs. ELife, 4(AUGUST 2015). https://doi.org/10.7554/eLife.05005

Akman, B. H., Can, T., & Elif Erson-Bensan, A. (2012). Estrogen-induced upregulation and 3′-UTR shortening of CDC6. Nucleic Acids Research, 40(21), 10679–10688. https://doi.org/10.1093/nar/gks855

Akman, H., Erson-Bensan, A., B. Akman, H., & E. Erson-Bensan, A. (2014). Alternative Polyadenylation and Its Impact on Cellular Processes. MicroRNA, 3(1), 2–9. https://doi.org/10.2174/2211536602666131210001152

Allemand, E., Guil, S., Myers, M., Moscat, J., Cáceres, J. F., & Krainer, A. R. (2005). Regulation of heterogenous nuclear ribonucleoprotein A1 transport by phosphorylation in cells stressed by osmotic shock. Proceedings of the National Academy of Sciences of the United States of America, 102(10), 3605–3610. https://doi.org/10.1073/pnas.0409889102

Beelman, C. A., & Parker, R. (1994). Differential effects of translational inhibition in cis and in trans on the decay of the unstable yeast MFA2 mRNA. Journal of Biological Chemistry, 269(13), 9687–9692. https://doi.org/10.1016/s0021-9258(17)36937-5

Berkovits, B. D., & Mayr, C. (2015). Alternative 3'UTRs act as scaffolds to regulate membrane protein localization. Nature, 522(7556), 363. https://doi.org/10.1038/NATURE14321

Birse, C. E., Minvielle-Sebastia, L., Lee, B. A., Keller, W., & Proudfoot, N. J. (1998). Coupling termination of transcription to messenger RNA maturation in yeast. Science, 280(5361), 298–301. https://doi.org/10.1126/science.280.5361.298

Bommert, K., Brockstedt, E., Rickers, A., Kostka, S., Laubersheimer, A., Wittmann-liebold, B., … Otto, A. (1998). Identification of apoptosis-associated proteins in a human Burkitt lymphoma cell line - Cleavage of heterogeneous nuclear ... Identification of Apoptosis-associated Proteins in a Human Burkitt, 273(November 2015), 28057–28064. https://doi.org/10.1074/jbc.273.43.28057

Bonnal, S., Pileur, F., Orsini, C., Parker, F., Pujol, F., Prats, A. C., & Vagner, S. (2005). Heterogeneous nuclear ribonucleoprotein A1 is a novel internal ribosome entry site trans-acting factor that modulates alternative initiation of translation of the fibroblast growth factor 2 mRNA. Journal of Biological Chemistry, 280(6), 4144–4153. https://doi.org/10.1074/jbc.M411492200

Bonomi, S., Di Matteo, A., Buratti, E., Cabianca, D. S., Baralle, F. E., Ghigna, C., & Biamonti, G. (2013). HnRNP A1 controls a splicing regulatory circuit promoting mesenchymal-to-epithelial transition. Nucleic Acids Research, 41(18), 8665–8679. https://doi.org/10.1093/nar/gkt579

Brzozowska, B., Gałecki, M., Tartas, A., Ginter, J., Kaźmierczak, U., & Lundholm, L. (2019). Freeware tool for analysing numbers and sizes of cell colonies. Radiation and Environmental Biophysics, 58(1), 109–117. https://doi.org/10.1007/s00411-018-00772-z

Bustin, S. A., Benes, V., Garson, J. A., Hellemans, J., Huggett, J., Kubista, M., … Wittwer, C. T. (2009). The MIQE guidelines: Minimum information for publication of quantitative real-time PCR experiments. Clinical Chemistry, 55(4), 611–622. https://doi.org/10.1373/clinchem.2008.112797

Carithers, L. J., & Moore, H. M. (2015, October 1). The Genotype-Tissue Expression (GTEx) Project. Biopreservation and Biobanking. Mary Ann Liebert Inc. https://doi.org/10.1089/bio.2015.29031.hmm

Chan, S., Choi, E.-A., & Shi, Y. (2011). Pre-mRNA 3' -end processing complex assembly and function. Wiley Interdisciplinary Reviews: RNA, 2(3), 321–335. https://doi.org/10.1002/wrna.54.Pre-mRNA

Chang, J., Yeh, H., & Yong, J. (2017). Alternative Polyadenylation in Human Diseases. Endocrinology and Metabolism, 32(4), 413. https://doi.org/10.3803/EnM.2017.32.4.413

Chen, C.-Y. A., & Shyu, A.-B. (2017). Emerging Themes in Regulation of Global mRNA Turnover in cis. Trends in Biochemical Sciences, 42(1), 16–27. https://doi.org/10.1016/j.tibs.2016.08.014

Colgan, D. F., & Manley, J. L. (1997). Mechanism and regulation of mRNA polyadenylation. Genes & Development, 11(21), 2755–2766. https://doi.org/10.1101/gad.11.21.2755

Cook, K. B., Kazan, H., Zuberi, K., Morris, Q., & Hughes, T. R. (2011a). RBPDB: A database of RNA-binding specificities. Nucleic Acids Research, 39(SUPPL. 1). https://doi.org/10.1093/nar/gkq1069

Cook, K. B., Kazan, H., Zuberi, K., Morris, Q., & Hughes, T. R. (2011b). RBPDB: A database of RNA-binding specificities. Nucleic Acids Research, 39(SUPPL. 1), 301–308. https://doi.org/10.1093/nar/gkq1069

Derti, A., Garrett-engele, P., Macisaac, K. D., Stevens, R. C., Sriram, S., Chen, R., … Babak, T. (2012). A quantitative atlas of polyadenylation in five mammals, 1173–1183. https://doi.org/10.1101/gr.132563.111.Freely

Ding, J., Hayashi, M. K., Zhang, Y., Manche, L., Krainer, A. R., & Xu, R. M. (1999). Crystal structure of the two-RRM domain of hnRNP A1 (UP1) complexed with single-stranded telomeric DNA. Genes and Development, 13(9), 1102–1115. https://doi.org/10.1101/gad.13.9.1102

Dreyfuss, G. (1993). hnRNP Proteins and the Biogenesis of mRNA. Annual Review of Biochemistry, 62(1), 289–321. https://doi.org/10.1146/annurev.biochem.62.1.289

Elkon, R., Ugalde, A. P., & Agami, R. (2013). Alternative cleavage and polyadenylation: Extent, regulation and function. Nature Reviews Genetics, 14(7), 496–506. https://doi.org/10.1038/nrg3482

Erson-Bensan, A. E., & Can, T. (2016). Alternative Polyadenylation: Another Foe in Cancer. Molecular Cancer Research, 14(6), 507–517. https://doi.org/10.1158/1541-7786.MCR-15-0489

Fujita, P. A., Rhead, B., Zweig, A. S., Hinrichs, A. S., Karolchik, D., Cline, M. S., … Kent, W. J. (2011). The UCSC genome browser database: Update 2011. Nucleic Acids Research, 39(SUPPL. 1), 876–882. https://doi.org/10.1093/nar/gkq963

Ge, X., Yamamoto, S., Tsutsumi, S., Midorikawa, Y., Ihara, S., Wang, S. M., & Aburatani, H. (2005). Interpreting expression profiles of cancers by genome-wide survey of breadth of expression in normal tissues. Genomics, 86(2), 127–141. https://doi.org/10.1016/j.ygeno.2005.04.008

Ghosh, M., & Singh, M. (2018). RGG-box in hnRNPA1 specifically recognizes the telomere G-quadruplex DNA and enhances the G-quadruplex unfolding ability of UP1 domain. Nucleic Acids Research, 46(19), 10246–10261. https://doi.org/10.1093/nar/gky854

Graham, K., De Las Morenas, A., Tripathi, A., King, C., Kavanah, M., Mendez, J., … Rosenberg, C. L. (2010). Gene expression in histologically normal epithelium from breast cancer patients and from cancer-free prophylactic mastectomy patients shares a similar profile. British Journal of Cancer, 102(8), 1284–1293. https://doi.org/10.1038/sj.bjc.6605576

Guil, S., & Cáceres, J. F. (2007). The multifunctional RNA-binding protein hnRNP A1 is required for processing of miR-18a. Nature Structural and Molecular Biology, 14(7), 591–596. https://doi.org/10.1038/nsmb1250

Guil, S., Long, J. C., & Cáceres, J. F. (2006). hnRNP A1 Relocalization to the Stress Granules Reflects a Role in the Stress Response. Molecular and Cellular Biology, 26(15), 5744–5758. https://doi.org/10.1128/mcb.00224-06

Iervolino, A., Santilli, G., Trotta, R., Guerzoni, C., Cesi, V., Bergamaschi, A., … Perrotti, D. (2002). hnRNP A1 Nucleocytoplasmic Shuttling Activity Is

Required for Normal Myelopoiesis and BCR / ABL Leukemogenesis, 22(7), 2255–2266. https://doi.org/10.1128/MCB.22.7.2255–2266.2002

Isken, O., & Maquat, L. E. (2008). The multiple lives of NMD factors: Balancing roles in gene and genome regulation. Nature Reviews Genetics, 9(9), 699–712. https://doi.org/10.1038/nrg2402

Jean-Philippe, J., Paz, S., & Caputi, M. (2013). hnRNP A1: The Swiss Army Knife of gene expression. International Journal of Molecular Sciences, 14(9), 18999–19024. https://doi.org/10.3390/ijms140918999

Jin, L., Wessely, O., Marcusson, E. G., Ivan, C., Calin, G. A., & Alahari, S. K. (2013). Prooncogenic Factors miR-23b and miR-27b Are Regulated by Her2/Neu, EGF, and TNF-α in Breast Cancer. Cancer Research, 73(9), 2884–2896. https://doi.org/10.1158/0008-5472.CAN-12-2162

Kaufmann, I., Martin, G., Friedlein, A., Langen, H., & Keller, W. (2004). Human Fip1 is a subunit of CPSF that binds to U-rich RNA elements and stimulates poly(A) polymerase. The EMBO Journal, 23(3), 616–626. https://doi.org/10.1038/sj.emboj.7600070

Kretschmer, C., Sterner-Kock, A., Siedentopf, F., Schoenegg, W., Schlag, P. M., & Kemmner, W. (2011). Identification of early molecular markers for breast cancer. Molecular Cancer, 10(1), 15. https://doi.org/10.1186/1476-4598-10-15

Lánczky, A., & Győrffy, B. (2021). Web-based survival analysis tool tailored for medical research (KMplot): Development and implementation. Journal of Medical Internet Research, 23(7), 1–7. https://doi.org/10.2196/27633

Le, P. N., Maranon, D. G., Altina, N. H., Battaglia, C. L. R., & Bailey, S. M. (2013). TERRA, hnRNP A1, and DNA-PKcs Interactions at Human Telomeres. Frontiers in Oncology, 3(April), 1–14. https://doi.org/10.3389/fonc.2013.00091

Lee, S. H., & Mayr, C. (2019). Gain of Additional BIRC3 Protein Functions through 3′-UTR-Mediated Protein Complex Formation. Molecular Cell, 74(4), 701-712.e9. https://doi.org/10.1016/J.MOLCEL.2019.03.006

Li, Z., Chen, K., Jiang, P., Zhang, X., Li, X., & Li, Z. (2014). CD44v/CD44s expression patterns are associated with the survival of pancreatic carcinoma patients. Diagnostic Pathology, 9(1), 1–11. https://doi.org/10.1186/1746-1596-9-79

Liu, R., Wang, X., Chen, G. Y., Dalerba, P., Gurney, A., Hoey, T., … Clarke, M. F. (2007). The Prognostic Role of a Gene Signature from Tumorigenic Breast-Cancer Cells. New England Journal of Medicine, 356(3), 217–226. https://doi.org/10.1056/NEJMoa063994

Loh, T. J., Moon, H., Cho, S., Jang, H., Liu, Y. C., Tai, H., … Shen, H. (2015). CD44 alternative splicing and hnRNP A1 expression are associated with the metastasis of breast cancer. Oncology Reports, 34(3), 1231–1238. https://doi.org/10.3892/or.2015.4110

Mandel, C. R., Bai, Y., & Tong, L. (2008). Protein factors in pre-mRNA 3′-end processing. Cellular and Molecular Life Sciences, 65(7–8), 1099–1122. https://doi.org/10.1007/s00018-007-7474-3

Martin, J., Masri, J., Cloninger, C., Holmes, B., Artinian, N., Funk, A., … Gera, J. (2011). Phosphomimetic substitution of heterogeneous nuclear ribonucleoprotein A1 at serine 199 abolishes AKT-dependent internal ribosome entry site-transacting factor (ITAF) function via effects on strand annealing and results in mammalian target of rapamycin co. Journal of Biological Chemistry, 286(18), 16402–16413. https://doi.org/10.1074/jbc.M110.205096

Michlewski, G., & Cáceres, J. F. (2010). Antagonistic role of hnRNP A1 and KSRP in the regulation of let-7a biogenesis. Nature Structural and Molecular Biology, 17(8), 1011–1018. https://doi.org/10.1038/nsmb.1874

Michlewski, G., Guil, S., & Cáceres, J. F. (2010). Stimulation of pri-miR-18a Processing by hnRNP A1 (pp. 28–35). https://doi.org/10.1007/978-1-4419-7823-3_3

Misra, A., & Green, M. R. (2016). From polyadenylation to splicing: Dual role for mRNA 3’ end formation factors. RNA Biology, 13(3), 259–264. https://doi.org/10.1080/15476286.2015.1112490

Paz, I., Kosti, I., Ares, M., Cline, M., & Mandel-Gutfreund, Y. (2014). RBPmap: A web server for mapping binding sites of RNA-binding proteins. Nucleic Acids Research, 42(W1). https://doi.org/10.1093/nar/gku406

Pino, I., Pío, R., Toledo, G., Zabalegui, N., Vicent, S., Rey, N., … Montuenga, L. M. (2003). Altered patterns of expression of members of the heterogeneous nuclear ribonucleoprotein (hnRNP) family in lung cancer. Lung Cancer, 41(2), 131–143. https://doi.org/10.1016/S0169-5002(03)00193-4

Pinol-Roma, S., Choi, Y. D., Matunis, M. J., & Dreyfuss, G. (1988). Immunopurification of heterogeneous nuclear ribonucleoprotein particles reveals an assortment of RNA-binding proteins [published erratum appears in Genes Dev 1988 Apr;2(4):490]. Genes Dev, 2(2), 215–227. https://doi.org/10.1101/gad.2.2.215

Piñol-Roma, S., & Dreyfuss, G. (1992). Shuttling of pre-mRNA binding proteins between nucleus and cytoplasm. Nature, 355, 730–732. https://doi.org/10.1038/355730a0

Planche, A., Bacac, M., Provero, P., Fusco, C., Delorenzi, M., Stehle, J. C., & Stamenkovic, I. (2011). Identification of prognostic molecular features in the reactive stroma of human breast and prostate cancer. PLoS ONE, 6(5). https://doi.org/10.1371/journal.pone.0018640

Proudfoot, N. J. (2011). Ending the message: poly (A) signals then and now. Genes & Development, 25, 1770–1782. https://doi.org/10.1101/gad.17268411.Freely

Richardson, A. L., Wang, Z. C., De Nicolo, A., Lu, X., Brown, M., Miron, A., … Ganesan, S. (2006). X chromosomal abnormalities in basal-like human breast cancer. Cancer Cell, 9(2), 121–132. https://doi.org/10.1016/j.ccr.2006.01.013

Ringel, J., Jesnowski, R., Schmidt, C., Köhler, H. J., Rychly, J., Batra, S. K., & Löhr, M. (2001). CD44 in normal human pancreas and pancreatic carcinoma cell lines. Teratogenesis, Carcinogenesis, and Mutagenesis, 21(1), 97–106. https://doi.org/10.1002/1520-6866(2001)21:1<97::AID-TCM9>3.0.CO;2-O

Rody, A., Karn, T., Liedtke, C., Pusztai, L., Ruckhaeberle, E., Hanker, L., … Kaufmann, M. (2011). A clinically relevant gene signature in triple negative and basal-like breast cancer. Breast Cancer Research, 13(5), R97. https://doi.org/10.1186/bcr3035

Roy, R., Durie, D., Li, H., Liu, B. Q., Skehel, J. M. ar., Mauri, F., … Pardo, O. E. (2014). hnRNPA1 couples nuclear export and translation of specific mRNAs downstream of FGF-2/S6K2 signalling. Nucleic Acids Research, 42(20), 12483–12497. https://doi.org/10.1093/nar/gku953

Sandberg, R., Neilson, J. R., Sarma, A., Sharp, P. A., & Burge, C. B. (2008). Proliferating cells express mRNAs with shortened 3′ untranslated regions and fewer microRNA target sites. Science, 320(5883), 1643–1647. https://doi.org/10.1126/science.1155390

Schneider-poetsch, T., Ju, J., Eyler, D. E., Dang, Y., Bhat, S., Merrick, W. C., … Liu, J. O. (2010). Cycloheximide mechanism. NNature Chemical Biology, 6(3), 209–217. https://doi.org/10.1038/nchembio.304.Inhibition

Schneider, C. A., Rasband, W. S., & Eliceiri, K. W. (2012). NIH Image to ImageJ: 25 years of image analysis. Nature Methods, 9(7), 671–675. https://doi.org/10.1038/nmeth.2089

Shen, S. J., Song, Y., Ren, X. Y., Xu, Y. L., Zhou, Y. D., Liang, Z. Y., & Sun, Q. (2020). MicroRNA-27b-3p Promotes Tumor Progression and Metastasis by Inhibiting Peroxisome Proliferator-Activated Receptor Gamma in Triple-Negative Breast Cancer. Frontiers in Oncology, 10(August), 1–11. https://doi.org/10.3389/fonc.2020.01371

Shi, Y., Frost, P. J., Hoang, B. Q., Benavides, A., Sharma, S., Gera, J. F., & Lichtenstein, A. K. (2008). IL-6-Induced Stimulation of c-Myc Translation in Multiple Myeloma Cells Is Mediated by Myc Internal Ribosome Entry Site Function and the RNA-Binding Protein, hnRNP A1. Cancer Research, 68(24), 10215–10222. https://doi.org/10.1158/0008-5472.CAN-08-1066

Siomi, H., & Dreyfuss, G. (1995). A nuclear localization domain in the hnRMP A1 protein. J. Cell Bio., 129(3), 551–560. https://doi.org/10.1083/jcb.129.3.551

Sobell, H. M. (1985). Actinomycin and DNA transcription. Proceedings of the National Academy of Sciences of the United States of America, 82(16), 5328–5331. https://doi.org/10.1073/pnas.82.16.5328

Sui, J., Lin, Y. F., Xu, K., Lee, K. J., Wang, D., & Chen, B. P. C. (2015). DNA-PKcs phosphorylates hnRNP-A1 to facilitate the RPA-to-POT1 switch and telomere capping after replication. Nucleic Acids Research, 43(12), 5971–5983. https://doi.org/10.1093/nar/gkv539

Tian, B., Hu, J., Zhang, H., & Lutz, C. S. (2005). A large-scale analysis of mRNA polyadenylation of human and mouse genes. Nucleic Acids Research, 33(1), 201–212. https://doi.org/10.1093/nar/gki158

Ting, N. S. Y., Pohorelic, B., Yu, Y., Lees-Miller, S. P., & Beattie, T. L. (2009). The human telomerase RNA component, hTR, activates the DNA-dependent protein kinase to phosphorylate heterogeneous nuclear ribonucleoprotein A1. Nucleic Acids Research, 37(18), 6105–6115. https://doi.org/10.1093/nar/gkp636

Tripathi, A., King, C., De La Morenas, A., Perry, V. K., Burke, B., Antoine, G. A., … Rosenberg, C. L. (2008). Gene expression abnormalities in histologically normal breast epithelium of breast cancer patients. International Journal of Cancer, 122(7), 1557–1566. https://doi.org/10.1002/ijc.23267

Vlachos, I. S., Kostoulas, N., Vergoulis, T., Georgakilas, G., Reczko, M., Maragkakis, M., … Hatzigeorgiou, A. G. (2012). DIANA miRPath v.2.0: Investigating the combinatorial effect of microRNAs in pathways. Nucleic Acids Research, 40(W1), 498–504. https://doi.org/10.1093/nar/gks494

Wang, Y., Rathinam, R., Walch, A., & Alahari, S. K. (2009). ST14 (suppression of tumorigenicity 14) gene is a target for miR-27b, and the inhibitory effect of ST14 on cell growth is independent of miR-27b regulation. Journal of Biological Chemistry, 284(34), 23094–23106. https://doi.org/10.1074/jbc.M109.012617

Zhang, H. (2004). PolyA_DB: a database for mammalian mRNA polyadenylation. Nucleic Acids Research, 33(Database issue), D116–D120. https://doi.org/10.1093/nar/gki055

Zhang, Q., Manche, L., Xu, R., & Krainer, A. R. (2006). hnRNP A1 associates with telomere ends and stimulates telomerase activity hnRNP A1 associates with telomere ends and stimulates telomerase activity, 1116–1128. https://doi.org/10.1261/rna.58806.proteinaceous

Zhou, Z. J., Dai, Z., Zhou, S. L., Fu, X. T., Zhao, Y. M., Shi, Y. H., … Fan, J. (2013). Overexpression of HnRNP A1 promotes tumor invasion through regulating CD44v6 and indicates poor prognosis for hepatocellular carcinoma. International Journal of Cancer, 132(5), 1080–1089. https://doi.org/10.1002/ijc.27742

APPENDICES

A. Primer lists

Table 4.1. SDM-PCR primers.

Primer Name	Sequence (5'-3')
KHSRP 55-58 F Primer	CTTAAAAACAGAAACTCATCTAAGTTCGTGGCAGAAAGGAAC
KHSRP 55-58 R Primer	GTTCCTTTCTGCCACGAACTTAGATGAGTTTCTGTTTTTAAG
KHSRP 80-83 F Primer	GTTCGTGGCAGAAAGGAACTTGTGAAGACCTTTATCTG
KHSRP 80-83 F Primer	CAGATAAAGGTCTTCACAAGTTCCTTTCTGCCACGAAC
PABPN1 37-46 F Primer	CGAACTTGGACAGATGAGTAAGAGCTGATAAGACTAGTAG
PABPN1 37-46 R Primer	CTACTAGTCTTATCAGCTCTTACTCATCTGTCCAAGTTCG
PABPN1 85-94 F Primer	GGCAGAAAGGAACGTCCTTTTATCTGAGCCACTGTA
PABPN1 85-94 R Primer	TACAGTGGCTCAGATAAAAGGACGTTCCTTTCTGCC
Pum2 106-115 F Primer	CTTGTGAAGACCTTTATCTGAGCCGTTAAAGCTTAATAAAGGATCTT
Pum2 106-115 R Primer	AAGATCCTTTATTAAGCTTTAACGGCTCAGATAAAGGTCTTCACAAG
miR24-3p Del F Primer	GGAACGTCCTTGTGAAGACCTTTATACTGTACTTCGTT
miR24-3p Del R Primer	AACGAAGTACAGTATAAAGGTCTTCACAAGGACGTTCC
miR34-5p Del F Primer	ATCTGAGCCACTGTACTTCGTTATATGCAGTTTACATGAG
miR34-5p Del R Primer	CTCATGTAAACTGCATATAACGAAGTACAGTGGCTCAGAT

Table 4.2. Confirmation Primers for SDMs.

Primer Name	Sequence (5'-3')	Product Size	
		Wildtype	Mutant
KHSRP Del Conf F Primer	GCTCTTAAAAACAGAAACTCATC	76 bp	72 bp
KHSRP Del Conf R Primer	GGCTCAGATAAAGGTCTTCAC		
PABPN1 Del Conf F Primer	GCTACTAGTCTTATCAGCTC	103 bp	93 bp
PABPN1 Del Conf R Primer	CGAAGTACAGTGGCTCAGAT		
Pum2 Del Conf F Primer	GTGAAGACCTTTATCTGAGC	81 bp	71 bp
Pum2 Del Conf R Primer	ACCAACACACAGATCCAATG		
miR24-34 Del Conf F Primer	GAACGTCCTTGTGAAGACC	76 bp	65 bp
miR24-34 Del Conf R Primer	CAGCTCATGTAAACTGCATGG		

B. Sequencing Results

A.

```
Query: Homo sapiens heterogeneous nuclear ribonucleoprotein A1 (HNRNPA1),
transcript variant 1, mRNA Query ID: NM_002136.4 Length: 963


>Isoform_A_963bp BGH_Primer
Sequence ID: Query_105524 Length: 1181
Range 1: 11 to 971

Score:1760 bits(953), Expect:0.0,
Identities:960/963(99%),  Gaps:2/963(0%), Strand: Plus/Minus

Query  83    ATGTCTAAGTCAGAGTCTCCTAAAGAGCCCGAACAGCTGAGGAAGCTCTTCATTGGAGGG  142
             ||||||||||||||||||| ||||||||||||||||||||||||||||||||||||||||
Sbjct  971   ATGTCTAAGTCAGAGTCTC-TAAAGAGCCCGAACAGCTGAGGAAGCTCTTCATTGGAGGG  913

Query  143   TTGAGCTTTGAAACAACTGATGAGAGCCTGAGGAGCCATTTTGAGCAATGGGGAACGCTC  202
             |||||||||||||||||||||||||| ||||||||||||||||||||||||||||||||
Sbjct  912   TTGAGCTTTGAAACAACTGATGAGAGC-TGAGGAGCCATTTTGAGCAATGGGGAACGCTC  854

Query  203   ACGGACTGTGTGGTAATGAGAGATCCAAACACCAAGCGCTCCAGGGGCTTTGGGTTTGTC  262
             ||||||||||||||||||||||||||||||||||||||||||||||||||||||||||||
Sbjct  853   ACGGACTGTGTGGTAATGAGAGATCCAAACACCAAGCGCTCCAGGGGCTTTGGGTTTGTC  794

Query  263   ACATATGCCACTGTGGAGGAGGTGGATGCAGCTATGAATGCAAGGCCACACAAGGTGGAT  322
             ||||||||||||||||||||||||||||||||||||||||||||||||||||||||||||
Sbjct  793   ACATATGCCACTGTGGAGGAGGTGGATGCAGCTATGAATGCAAGGCCACACAAGGTGGAT  734

Query  323   GGAAGAGTTGTGGAACCAAAGAGAGCTGTCTCCAGAGAAGATTCTCAAAGACCAGGTGCC  382
             ||||||||||||||||||||||||||||||||||||||||||||||||||||||||||||
Sbjct  733   GGAAGAGTTGTGGAACCAAAGAGAGCTGTCTCCAGAGAAGATTCTCAAAGACCAGGTGCC  674

Query  383   CACTTAACTGTGAAAAAGATATTTGTTGGTGGCATTAAAGAAGACACTGAAGAACATCAC  442
             ||||||||||||||||||||||||||||||||||||||||||||||||||||||||||||
Sbjct  673   CACTTAACTGTGAAAAAGATATTTGTTGGTGGCATTAAAGAAGACACTGAAGAACATCAC  614

Query  443   CTAAGAGATTATTTTGAACAGTATGGAAAAATTGAAGTGATTGAAATCATGACTGACCGA  502
             ||||||||||||||||||||||||||||||||||||||||||||||||||||||||||||
Sbjct  613   CTAAGAGATTATTTTGAACAGTATGGAAAAATTGAAGTGATTGAAATCATGACTGACCGA  554

Query  503   GGCAGTGGCAAGAAAAGGGGCTTTGCCTTTGTAACCTTTGACGACCATGACTCCGTGGAT  562
             ||||||||||||||||||||||||||||||||||||||||||||||||||||||||||||
Sbjct  553   GGCAGTGGCAAGAAAAGGGGCTTTGCCTTTGTAACCTTTGACGACCATGACTCCGTGGAT  494

Query  563   AAGATTGTCATTCAGAAATACCATACTGTGAATGGCCACAACTGTGAAGTTAGAAAAGCC  622
             ||||||||||||||||||||||||||||||||||||||||||||||||||||||||||||
Sbjct  493   AAGATTGTCATTCAGAAATACCATACTGTGAATGGCCACAACTGTGAAGTTAGAAAAGCC  434

Query  623   CTGTCAAAGCAAGAGATGGCTAGTGCTTCATCCAGCCAAAGAGGTCGAAGTGGTTCTGGA  682
             ||||||||||||||||||||||||||||||||||||||||||||||||||||||||||||
Sbjct  433   CTGTCAAAGCAAGAGATGGCTAGTGCTTCATCCAGCCAAAGAGGTCGAAGTGGTTCTGGA  374

Query  683   AACTTTGGTGGTGGTCGTGGAGGTGGTTTCGGTGGGAATGACAACTTCGGTCGTGGAGGA  742
             ||||||||||||||||||||||||||||||||||||||||||||||||||||||||||||
Sbjct  373   AACTTTGGTGGTGGTCGTGGAGGTGGTTTCGGTGGGAATGACAACTTCGGTCGTGGAGGA  314

Query  743   AACTTCAgtggtcgtggtggctttggtggcagccgtggtggtggtggatatggtggcagt  802
             ||||||||||||||||||||||||||||||||||||||||||||||||||||||||||||
Sbjct  313   AACTTCAGTGGTCGTGGTGGCTTTGGTGGCAGCCGTGGTGGTGGTGGATATGGTGGCAGT  254

Query  803   ggggatggctataatggatttggtAATGATGGAAGCAATTTTGGAGGTGGTGGAAGCTAC  862
             ||||||||||||||||||||||||||||||||||||||||||||||||||||||||||||
Sbjct  253   GGGGATGGCTATAATGGATTTGGTAATGATGGAAGCAATTTTGGAGGTGGTGGAAGCTAC  194

Query  863   AATGATTTTGGGAATTACAACAATCAGTCTTCAAATTTTGGACCCATGAAGGGAGGAAAT  922
             ||||||||||||||||||||||||||||||||||||||||||||||||||||||||||||
Sbjct  193   AATGATTTTGGGAATTACAACAATCAGTCTTCAAATTTTGGACCCATGAAGGGAGGAAAT  134

Query  923   TTTGGAGGCAGAAGCTCTGGCCCCTATGGCGGTGGAGGCCAATACTTTGCAAAACCACGA  982
             ||||||||||||||||||||||||||||||||||||||||||||||||||||||||||||
Sbjct  133   TTTGGAGGCAGAAGCTCTGGCCCCTATGGCGGTGGAGGCCAATACTTTGCAAAACCACGA  74

Query  983   AACCAAGGTGGCTATGGCGGTTCCAGCAGCAGCAGTAGCTATGGCAGTGGCAGAAGATTT  1042
             ||||||||||||||||||||||||||||||||||||||||||||||||||||||||||||
Sbjct  73    AACCAAGGTGGCTATGGCGGTTCCAGCAGCAGCAGTAGCTATGGCAGTGGCAGAAGATTT  14

Query  1043  TAA  1045
              ||
Sbjct  13    AAA  11
```

B.

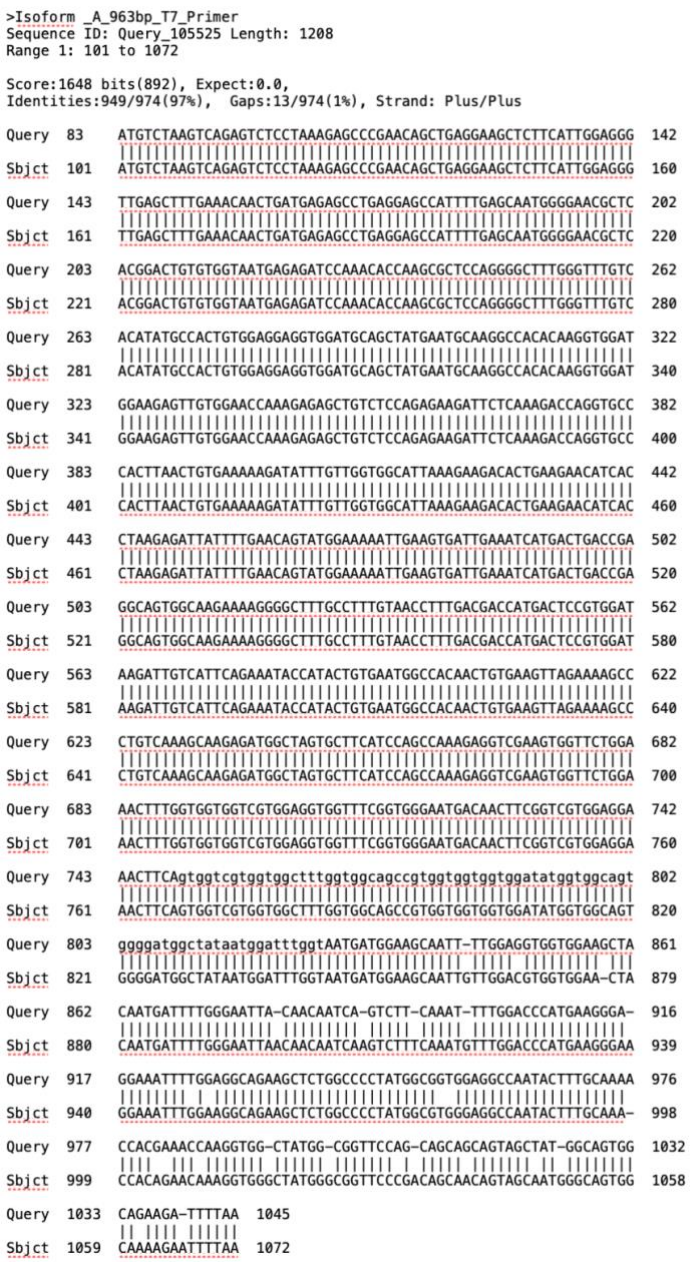

Figure 4.1. Sequencing results of HNRNPA1 CDSs with 963 bp size (exon 8 excluded) cloned in pcDNA3.1 (-) and alignment of HNRNPA1 mRNA sequence with NP_002127.1 accession number against sequencing results obtained with BGH primer (A) and T7 primer (B).

A.

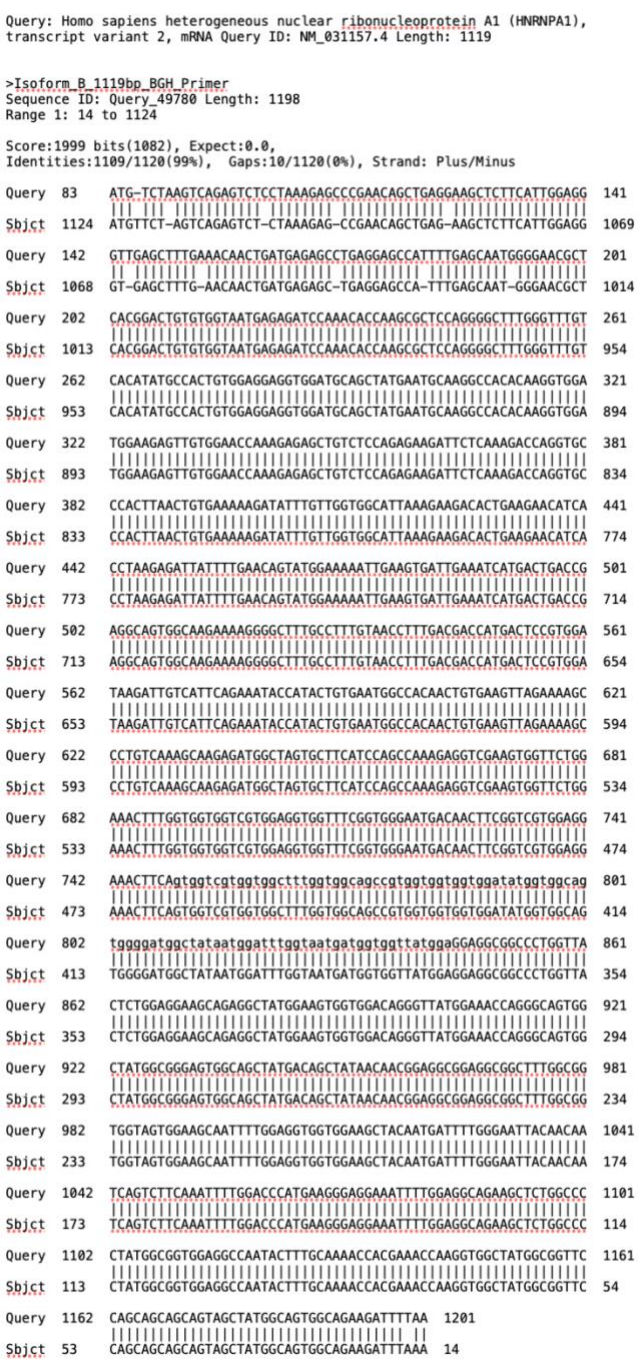

```
Query: Homo sapiens heterogeneous nuclear ribonucleoprotein A1 (HNRNPA1),
transcript variant 2, mRNA Query ID: NM_031157.4 Length: 1119


>Isoform_B_1119bp_BGH_Primer
Sequence ID: Query_49780 Length: 1198
Range 1: 14 to 1124

Score:1999 bits(1082), Expect:0.0,
Identities:1109/1120(99%),  Gaps:10/1120(0%), Strand: Plus/Minus

Query  83    ATG-TCTAAGTCAGAGTCTCCTAAAGAGCCCGAACAGCTGAGGAAGCTCTTCATTGGAGG  141
             ||| ||| |||||||||||| |||||||| |||||||||||||| ||||||||||||||||
Sbjct  1124  ATGTTCT-AGTCAGAGTCT-CTAAAGAG-CCGAACAGCTGAG-AAGCTCTTCATTGGAGG  1069

Query  142   GTTGAGCTTTGAAACAACTGATGAGAGCCTGAGGAGCCATTTTGAGCAATGGGGAACGCT  201
             || |||||||| |||||||||||||||| |||||||||| |||||||||| |||||||||
Sbjct  1068  GT-GAGCTTTG-AACAACTGATGAGAGC-TGAGGAGCCA-TTTGAGCAAT-GGGAACGCT  1014

Query  202   CACGGACTGTGTGGTAATGAGAGATCCAAACACCAAGCGCTCCAGGGGCTTTGGGTTTGT  261
             ||||||||||||||||||||||||||||||||||||||||||||||||||||||||||||
Sbjct  1013  CACGGACTGTGTGGTAATGAGAGATCCAAACACCAAGCGCTCCAGGGGCTTTGGGTTTGT  954

Query  262   CACATATGCCACTGTGGAGGAGGTGGATGCAGCTATGAATGCAAGGCCACACAAGGTGGA  321
             ||||||||||||||||||||||||||||||||||||||||||||||||||||||||||||
Sbjct  953   CACATATGCCACTGTGGAGGAGGTGGATGCAGCTATGAATGCAAGGCCACACAAGGTGGA  894

Query  322   TGGAAGAGTTGTGGAACCAAAGAGAGCTGTCTCCAGAGAAGATTCTCAAAGACCAGGTGC  381
             ||||||||||||||||||||||||||||||||||||||||||||||||||||||||||||
Sbjct  893   TGGAAGAGTTGTGGAACCAAAGAGAGCTGTCTCCAGAGAAGATTCTCAAAGACCAGGTGC  834

Query  382   CCACTTAACTGTGAAAAAGATATTTGTTGGTGGCATTAAAGAAGACACTGAAGAACATCA  441
             ||||||||||||||||||||||||||||||||||||||||||||||||||||||||||||
Sbjct  833   CCACTTAACTGTGAAAAAGATATTTGTTGGTGGCATTAAAGAAGACACTGAAGAACATCA  774

Query  442   CCTAAGAGATTATTTTGAACAGTATGGAAAAATTGAAGTGATTGAAATCATGACTGACCG  501
             ||||||||||||||||||||||||||||||||||||||||||||||||||||||||||||
Sbjct  773   CCTAAGAGATTATTTTGAACAGTATGGAAAAATTGAAGTGATTGAAATCATGACTGACCG  714

Query  502   AGGCAGTGGCAAGAAAAGGGGCTTTGCCTTTGTAACCTTTGACGACCATGACTCCGTGGA  561
             ||||||||||||||||||||||||||||||||||||||||||||||||||||||||||||
Sbjct  713   AGGCAGTGGCAAGAAAAGGGGCTTTGCCTTTGTAACCTTTGACGACCATGACTCCGTGGA  654

Query  562   TAAGATTGTCATTCAGAAATACCATACTGTGAATGGCCACAACTGTGAAGTTAGAAAAGC  621
             ||||||||||||||||||||||||||||||||||||||||||||||||||||||||||||
Sbjct  653   TAAGATTGTCATTCAGAAATACCATACTGTGAATGGCCACAACTGTGAAGTTAGAAAAGC  594

Query  622   CCTGTCAAAGCAAGAGATGGCTAGTGCTTCATCCAGCCAAAGAGGTCGAAGTGGTTCTGG  681
             ||||||||||||||||||||||||||||||||||||||||||||||||||||||||||||
Sbjct  593   CCTGTCAAAGCAAGAGATGGCTAGTGCTTCATCCAGCCAAAGAGGTCGAAGTGGTTCTGG  534

Query  682   AAACTTTGGTGGTGGTCGTGGAGGTGGTTTCGGTGGGAATGACAACTTCGGTCGTGGAGG  741
             ||||||||||||||||||||||||||||||||||||||||||||||||||||||||||||
Sbjct  533   AAACTTTGGTGGTGGTCGTGGAGGTGGTTTCGGTGGGAATGACAACTTCGGTCGTGGAGG  474

Query  742   AAACTTCAgtggtcgtggtggctttggtggcagccgtggtggtggtggatatggtggcag  801
             ||||||||||||||||||||||||||||||||||||||||||||||||||||||||||||
Sbjct  473   AAACTTCAGTGGTCGTGGTGGCTTTGGTGGCAGCCGTGGTGGTGGTGGATATGGTGGCAG  414

Query  802   tggggatggctataatggatttggtaatgatggtggttatggaGGAGGCGGCCCTGGTTA  861
             ||||||||||||||||||||||||||||||||||||||||||||||||||||||||||||
Sbjct  413   TGGGGATGGCTATAATGGATTTGGTAATGATGGTGGTTATGGAGGAGGCGGCCCTGGTTA  354

Query  862   CTCTGGAGGAAGCAGAGGCTATGGAAGTGGTGGACAGGGTTATGGAAACCAGGGCAGTGG  921
             ||||||||||||||||||||||||||||||||||||||||||||||||||||||||||||
Sbjct  353   CTCTGGAGGAAGCAGAGGCTATGGAAGTGGTGGACAGGGTTATGGAAACCAGGGCAGTGG  294

Query  922   CTATGGCGGGAGTGGCAGCTATGACAGCTATAACAACGGAGGCGGAGGCGGCTTTGGCGG  981
             ||||||||||||||||||||||||||||||||||||||||||||||||||||||||||||
Sbjct  293   CTATGGCGGGAGTGGCAGCTATGACAGCTATAACAACGGAGGCGGAGGCGGCTTTGGCGG  234

Query  982   TGGTAGTGGAAGCAATTTTGGAGGTGGTGGAAGCTACAATGATTTTGGGAATTACAACAA  1041
             ||||||||||||||||||||||||||||||||||||||||||||||||||||||||||||
Sbjct  233   TGGTAGTGGAAGCAATTTTGGAGGTGGTGGAAGCTACAATGATTTTGGGAATTACAACAA  174

Query  1042  TCAGTCTTCAAATTTTGGACCCATGAAGGGAGGAAATTTTGGAGGCAGAAGCTCTGGCCC  1101
             ||||||||||||||||||||||||||||||||||||||||||||||||||||||||||||
Sbjct  173   TCAGTCTTCAAATTTTGGACCCATGAAGGGAGGAAATTTTGGAGGCAGAAGCTCTGGCCC  114

Query  1102  CTATGGCGGTGGAGGCCAATACTTTGCAAAACCACGAAACCAAGGTGGCTATGGCGGTTC  1161
             ||||||||||||||||||||||||||||||||||||||||||||||||||||||||||||
Sbjct  113   CTATGGCGGTGGAGGCCAATACTTTGCAAAACCACGAAACCAAGGTGGCTATGGCGGTTC  54

Query  1162  CAGCAGCAGCAGTAGCTATGGCAGTGGCAGAAGATTTTAA  1201
             |||||||||||||||||||||||||||||||||| ||
Sbjct  53    CAGCAGCAGCAGTAGCTATGGCAGTGGCAGAAGATTTAAA  14
```

B.

```
Query: Homo sapiens heterogeneous nuclear ribonucleoprotein A1 (HNRNPA1),
transcript variant 2, mRNA Query ID: NM_031157.4 Length: 1119


>Isoform_B_1119bp_T7_Primer
Sequence ID: Query_49781 Length: 799
Range 1: 94 to 799

Score:1258 bits(681), Expect:0.0,
Identities:699/707(99%),  Gaps:3/707(0%), Strand: Plus/Plus

Query  83   ATGTCTAAGTCAGAGTCTCCTAAAGAGCCCGAACAGCTGAGGAAGCTCTTCATTGGAGGG  142
            ||||||||||||||||||||||||||||||||||||||||||||||||||||||||||||
Sbjct  94   ATGTCTAAGTCAGAGTCTCCTAAAGAGCCCGAACAGCTGAGGAAGCTCTTCATTGGAGGG  153

Query  143  TTGAGCTTTGAAACAACTGATGAGAGCCTGAGGAGCCATTTTGAGCAATGGGGAACGCTC  202
            ||||||||||||||||||||||||||||||||||||||||||||||||||||||||||||
Sbjct  154  TTGAGCTTTGAAACAACTGATGAGAGCCTGAGGAGCCATTTTGAGCAATGGGGAACGCTC  213

Query  203  ACGGACTGTGTGGTAATGAGAGATCCAAACACCAAGCGCTCCAGGGGCTTTGGGTTTGTC  262
            ||||||||||||||||||||||||||||||||||||||||||||||||||||||||||||
Sbjct  214  ACGGACTGTGTGGTAATGAGAGATCCAAACACCAAGCGCTCCAGGGGCTTTGGGTTTGTC  273

Query  263  ACATATGCCACTGTGGAGGAGGTGGATGCAGCTATGAATGCAAGGCCACACAAGGTGGAT  322
            ||||||||||||||||||||||||||||||||||||||||||||||||||||||||||||
Sbjct  274  ACATATGCCACTGTGGAGGAGGTGGATGCAGCTATGAATGCAAGGCCACACAAGGTGGAT  333

Query  323  GGAAGAGTTGTGGAACCAAAGAGAGCTGTCTCCAGAGAAGATTCTCAAAGACCAGGTGCC  382
            ||||||||||||||||||||||||||||||||||||||||||||||||||||||||||||
Sbjct  334  GGAAGAGTTGTGGAACCAAAGAGAGCTGTCTCCAGAGAAGATTCTCAAAGACCAGGTGCC  393

Query  383  CACTTAACTGTGAAAAAGATATTTGTTGGTGGCATTAAAGAAGACACTGAAGAACATCAC  442
            ||||||||||||||||||||||||||||||||||||||||||||||||||||||||||||
Sbjct  394  CACTTAACTGTGAAAAAGATATTTGTTGGTGGCATTAAAGAAGACACTGAAGAACATCAC  453

Query  443  CTAAGAGATTATTTTGAACAGTATGGAAAAATTGAAGTGATTGAAATCATGACTGACCGA  502
            ||||||||||||||||||||||||||||||||||||||||||||||||||||||||||||
Sbjct  454  CTAAGAGATTATTTTGAACAGTATGGAAAAATTGAAGTGATTGAAATCATGACTGACCGA  513

Query  503  GGCAGTGGCAAGAAAAGGGGCTTTGCCTTTGTAACCTTTGACGACCATGACTCCGTGGAT  562
            ||||||||||||||||||||||||||||||||||||||||||||||||||||||||||||
Sbjct  514  GGCAGTGGCAAGAAAAGGGGCTTTGCCTTTGTAACCTTTGACGACCATGACTCCGTGGAT  573

Query  563  AAGATTGTCATTCAGAAATACCATACTGTGAATGGCCACAACTGTGAAGTTAGAAAAGCC  622
            ||||||||||||||||||||||||||||||||||||||||||||||||||||||||||||
Sbjct  574  AAGATTGTCATTCAGAAATACCATACTGTGAATGGCCACAACTGTGAAGTTAGAAAAGCC  633

Query  623  CTGTCAAAGCAAGAGATGGCTAGTGCTTCATCCAGCCAAAGAGGTCGAAGTGGTTCTGGA  682
            ||||||||||||||||||||||||||||||||||||||||||||||||||||||||||||
Sbjct  634  CTGTCAAAGCAAGAGATGGCTAGTGCTTCATCCAGCCAAAGAGGTCGAAGTGGTTCTGGA  693

Query  683  AACTTTGGTGGTGGTCGTGGAGGTGGTTTCGGTGGGAATGACAACTTC-GGTCGTGGAGG  741
            |||||||||||||||||||||||||||||||||| ||||||||||||| ||||||||||||
Sbjct  694  AACTTTGGTGGTGGTCGTGGAGGTGGTTTCGGTGGAAATGACAACTTCGGGTCGTGGAGG  753

Query  742  AAACTTCAgtggtc-gtggtggctttggtggcagccgtggtggtggt  787
            ||||||| | |||| || |||||||||| |||| ||||||||||||
Sbjct  754  AAACTTCGGGGGTCCGT-GTGGCTTTGGGGGCAACCGTGGTGGTGGT  799
```

Figure 4.2. Sequencing results of HNRNPA1 CDSs with 1119 bp size (exon 8 included) cloned in pcDNA3.1 (-) and alignment of HNRNPA1 mRNA sequence with NP_112420.1 accession number against sequencing results obtained with BGH primer (A) and T7 primer (B).

C. Agarose gel results

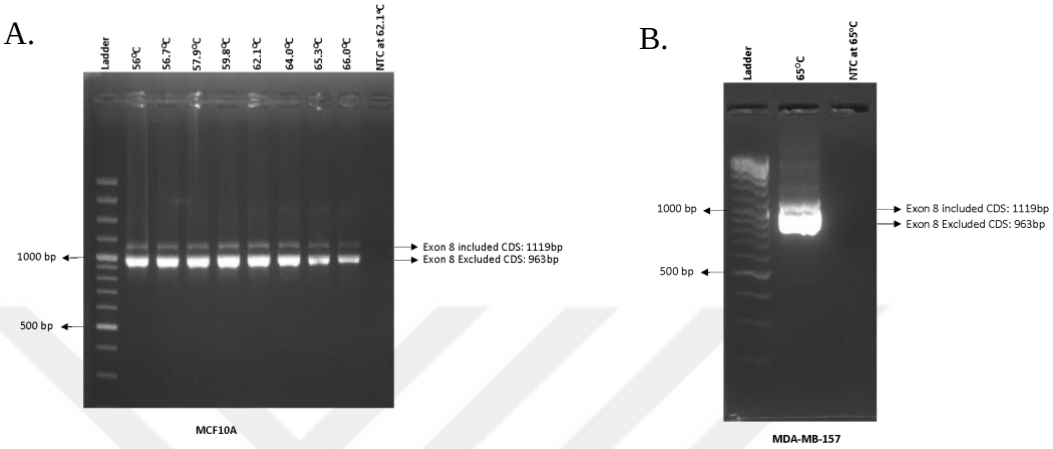

Figure 4.3. Agarose gel of PCR for detection of CDS isoforms via PCR by using CDS Cloning F and R Primers in MCF10A (A) and MDA-MB-157 (B) cells. Agarose gel images of PCR confirmed two HNRNPA1 CDSs with/out exon 8. NTC: No template reaction.

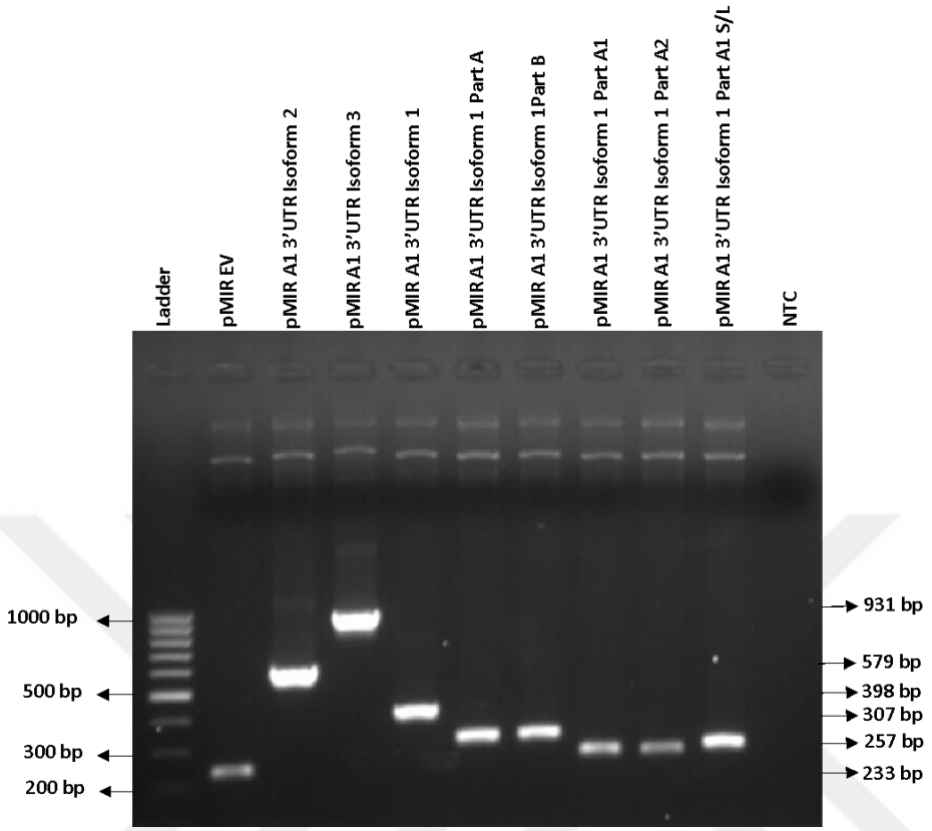

Figure 4.4. Agarose gel of PCR for confirmations of HNRNPA1 3'UTRs and isoform 1-3'UTR fragments in pMIR report vector.

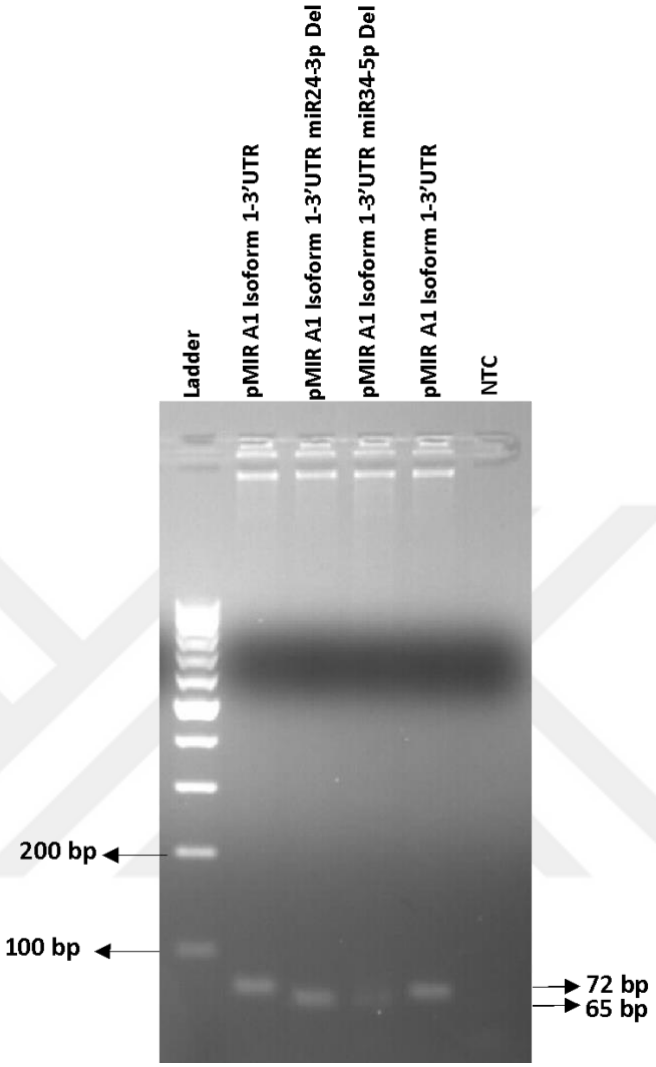

Figure 4.5. Agarose gel of PCR for SDMs of HNRNPA1 3'UTRs and isoform 1-3'UTR fragments in pMIR report vector. Wildtype: 72 bp and mutant (deleted miRNA seed binding site): 65 bp.

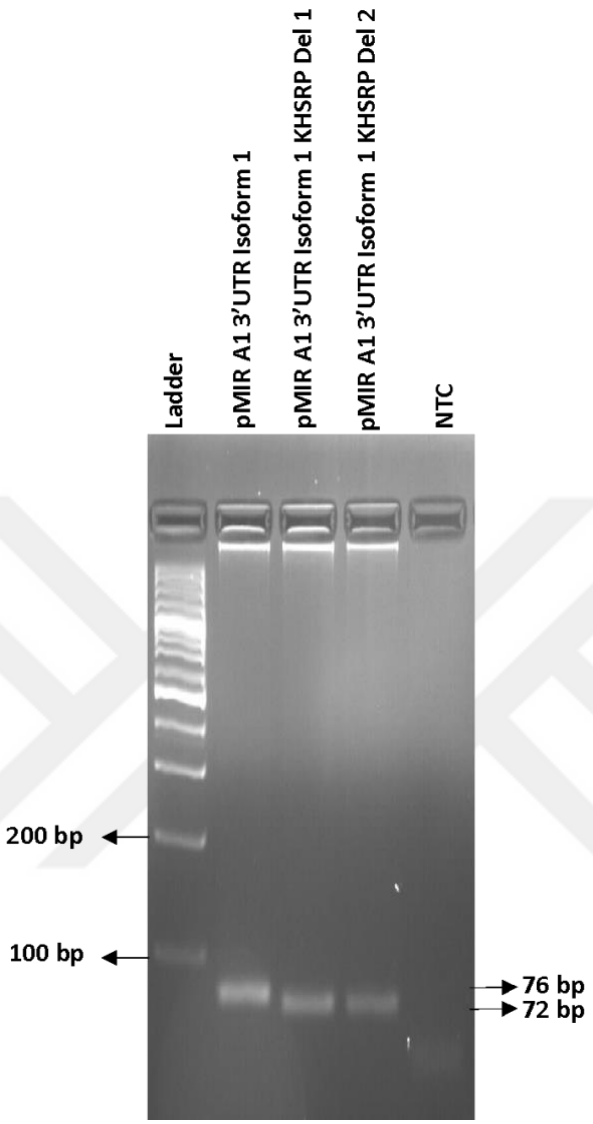

Figure 4.6. Agarose gel of PCR for SDMs of HNRNPA1 isoform 1-3'UTR sequence in pMIR report vector. Wildtype: 76 bp and mutant (deleted KHSRP binding site): 72 bp.

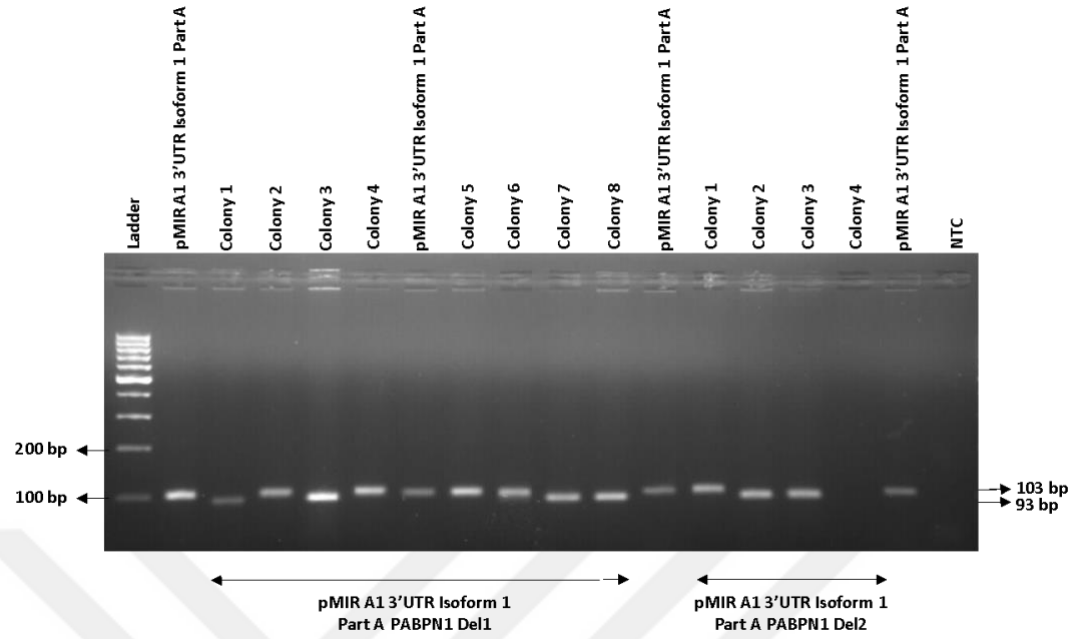

Figure 4.7. Agarose gel of PCR for SDMs of HNRNPA1 isoform 1 Part A-3'UTR sequence in pMIR report vector. Wildtype: 103 bp and mutant (deleted PABPN1 binding site): 93 bp.

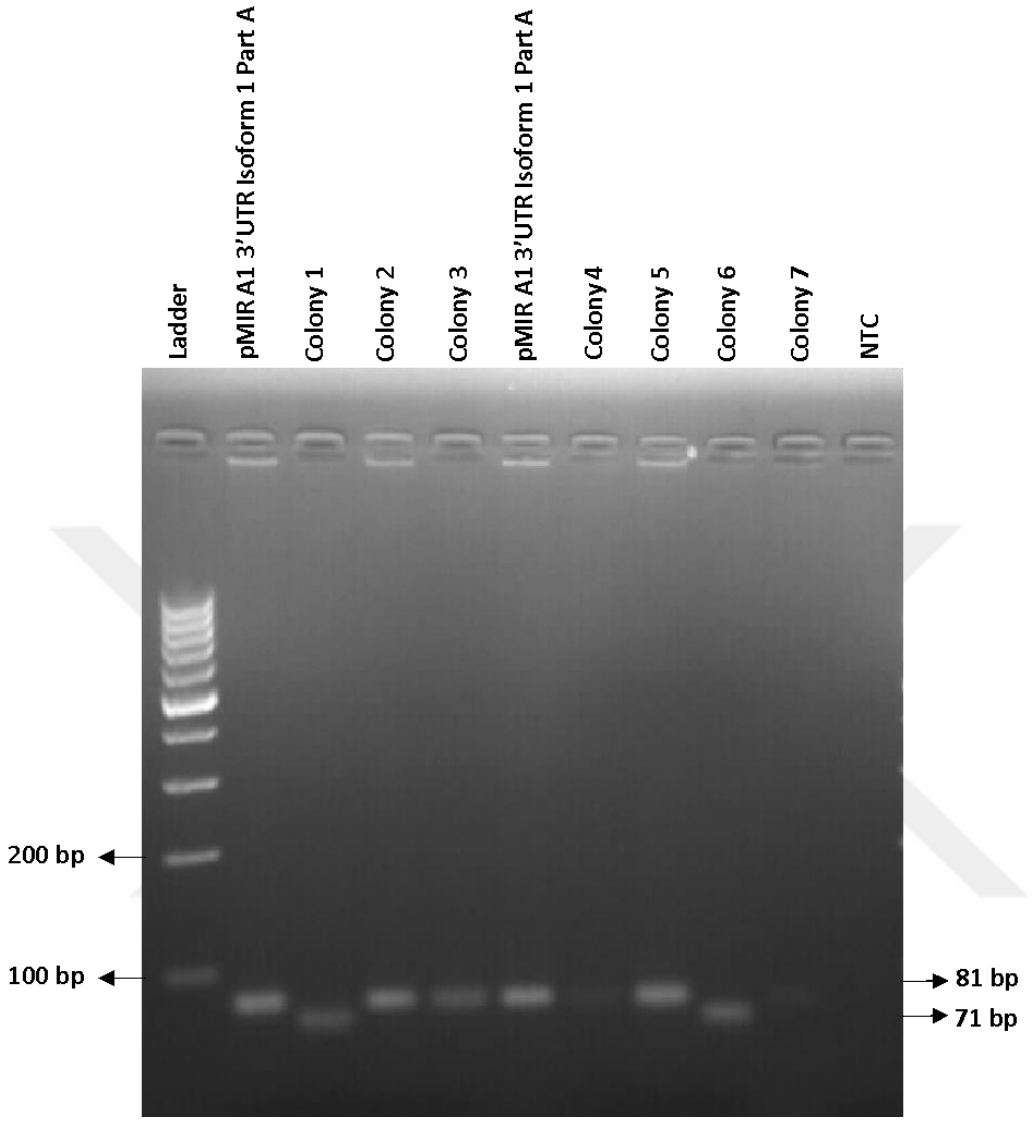

Figure 4.8. Agarose gel of PCR for SDMs of HNRNPA1 isoform 1 Part A-3'UTR sequence in pMIR report vector. Wildtype: 81 bp and mutant (deleted Pum2 binding site): 71 bp.

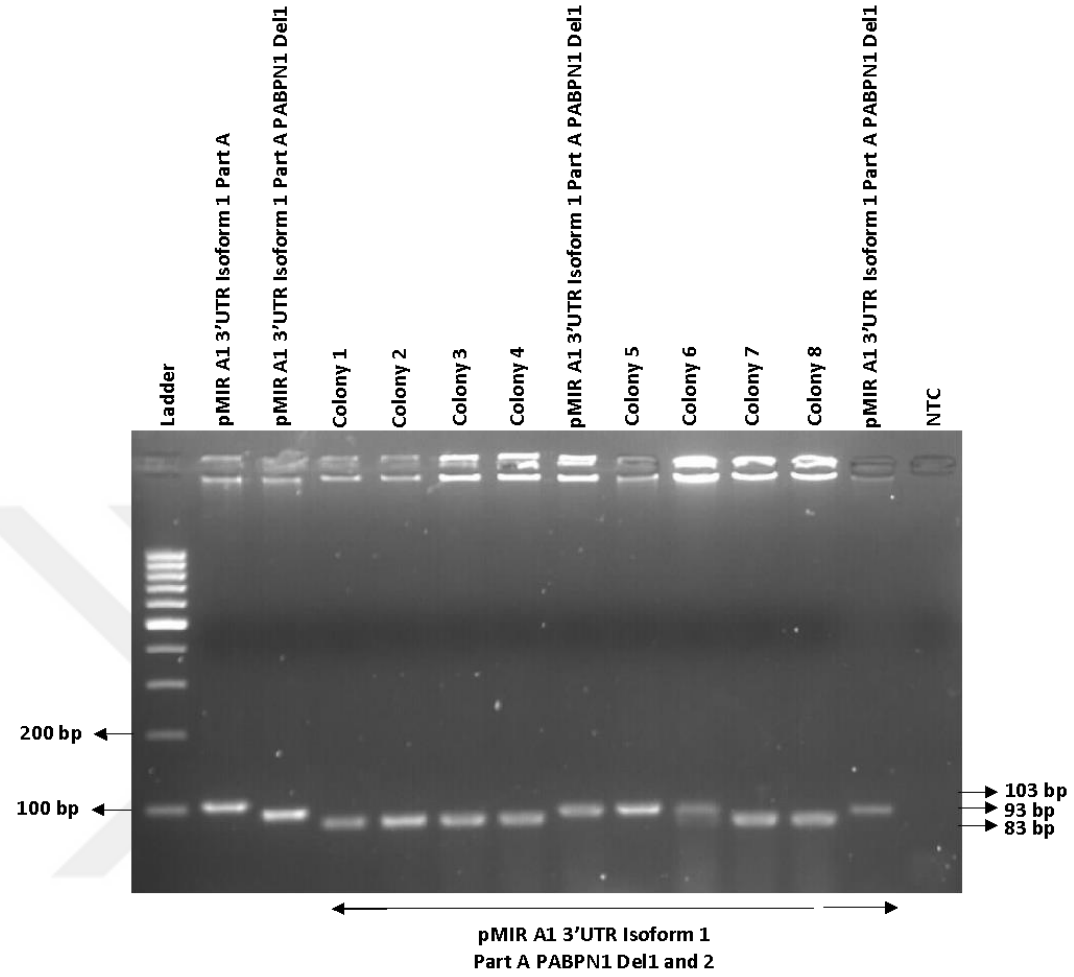

Figure 4.9. Agarose gel of PCR for SDMs of HNRNPA1 isoform 1 Part A-3'UTR sequence in pMIR report vector. Wildtype: 103 bp, single mutant (deletion of one PABPN1 binding site): 93 bp, and double mutant (deletion of both PABPN1 binding sites): 83 bp.

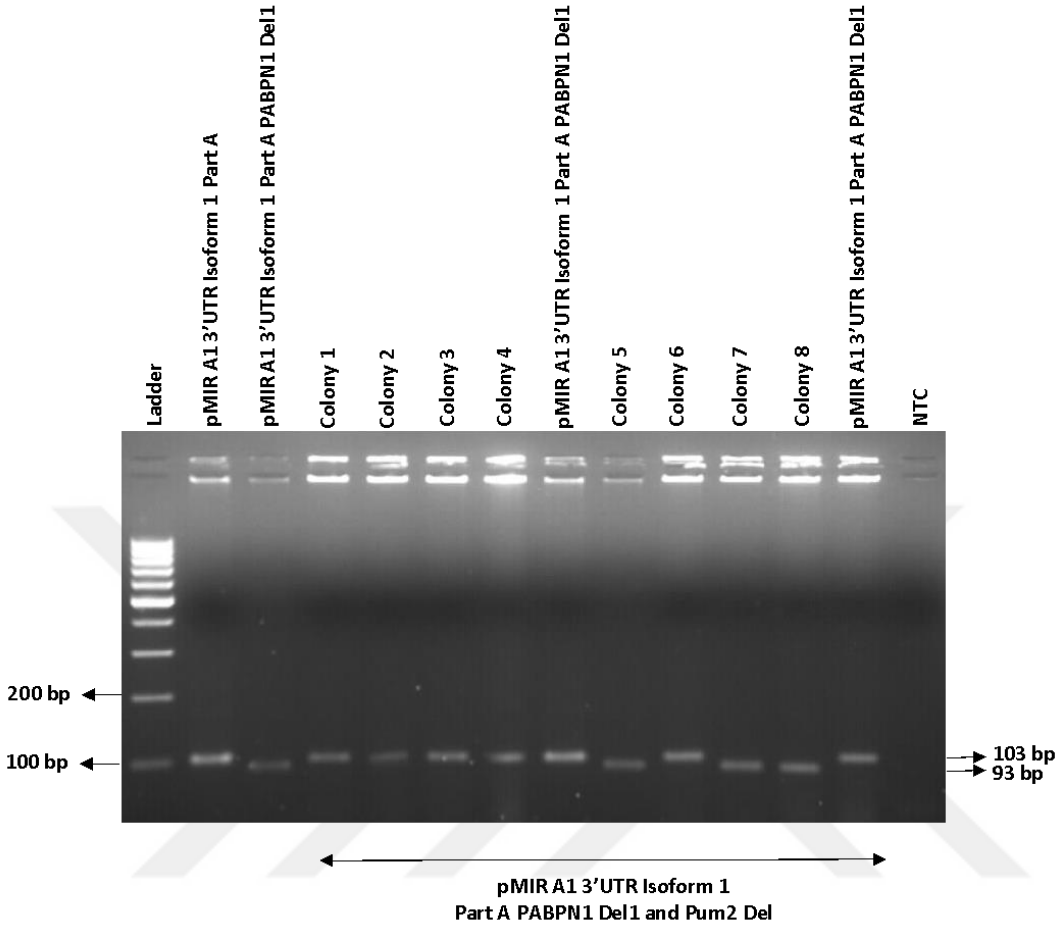

Figure 4.10. Agarose gel of PCR for PABPN1 deletion on Pum2 already deleted HNRNPA1 isoform 1 Part A-3'UTR sequence in pMIR report vector. Wildtype (Pum2 already deleted): 103 bp, single mutant (deletion of one PABPN1 binding site on Pum2 already deleted HNRNPA1 isoform 1 Part A-3'UTR sequence): 93 bp.

D. HNRNPA1 CRISPR/Cas9 Results

A.

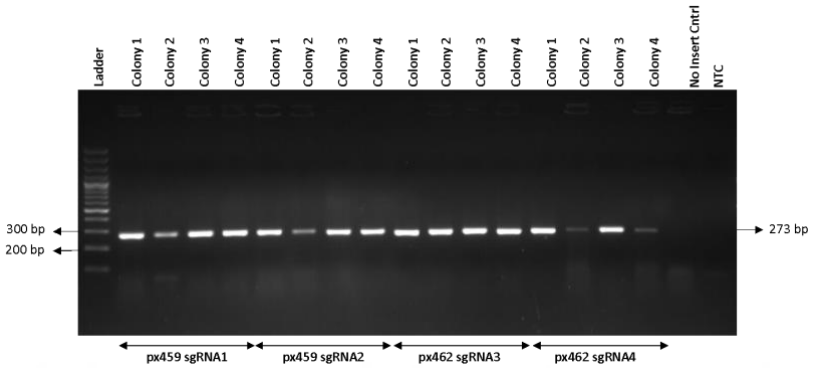

B.

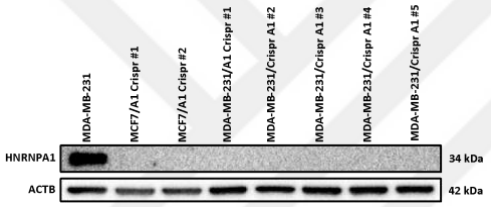

C.

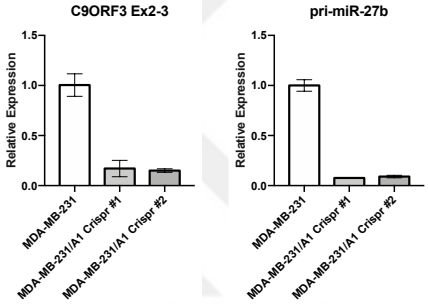

Figure 4.11. *HNRNPA1* knockout in MCF7 and MDA-MB 231 cells via CRISPR/Cas9 system. A. Agarose gel of colony PCR for A1 sgRNAs into px459 vector. B. *HNRNPA1* was deleted in MCF7 and MDA-MB-231 cells using CRISPR/Cas9. ACTB antibody was used as a loading control on the same blot (n=1). C. Relative expression levels of C9ORF3 and pri-miR-27b in MDA-MB-231 cells (*HNRNPA1* knockouts). *RPLP0* was used as a reference gene for other RT-qPCRs. #1 and #2 indicate individual colonies.

CURRICULUM VITAE

Surname, Name: Erdem, Murat

EDUCATION

Degree	Institution	Year of Graduation
MS	METU Biology	2014
BS	METU Molecular Biology and Genetics	2011
High School	Mareşal Fevzi Çakmak Ç.P.L., Mersin	2002

FOREIGN LANGUAGES

Advanced English

PUBLICATIONS

1. Erdem, M., Ozgul, İ., Dioken, D.N. Gurcuoglu I., Guntekin-Ergun S., Cetin-Atalay R., Can T. and Erson-Bensan AE. "Identification of an mRNA isoform switch for HNRNPA1 in breast cancers", Scientific Report, 11(1), 24444 (2021).

2. Erdem M., Yalçın S. and Gündüz U. "Folic acid-conjugated polyethylene glycol-coated magnetic nanoparticles for doxorubicin delivery in cancer chemotherapy: Preparation, characterization, and cytotoxicity on HeLa cell line", Human & Experimental Toxicology, 36(8), 833-845 (2017).

3. Bahrieh G., Ozgur E., Koyuncuoglu A., Erdem. M., Gunduz U. and Kulah H. "Characterization of the distribution of rotational torque on electrorotation chips with 3D electrodes", Electrophoresis, 36(15), 1785- 1794 (2015).

4. Demircan Y., Koyuncuoglu A., Erdem M., Ozgur E., Gunduz U. and Kulah H., "Label-free detection of multidrug resistance in K562 cells through isolated 3D electrode dielectrophoresis", Electrophoresis, 36(9-10), 1149-1157 (2015).

5. Bahrieh G., Erdem M., Ozgur E., Gunduz U., and Kulah H. "Assessment of effects of multi-drug resistance on dielectric properties of K562 leukemic cells using electrorotation", RSC Advances, 4(85), 44879-44887 (2014).